

Politecnico di Torino

Politecnico di Torino

Department of Environmental, Land and Infrastructure Engineering

Master of Science in Georesources and Geoenergy Engineering

A.Y. 2025/2026

LAB TEST-BASED COMPARATIVE ASSESSMENT OF STABILIZERS FOR HIGH-PLASTICITY INORGANIC SOILS

Supervisors:

Prof. Fulvia Chiampo

Prof. Claudio Oggeri

Candidate:

Elie Diab

September, 2026

Abstract

This thesis evaluates and compares four chemical stabilization techniques applied specifically to high plasticity inorganic expansive soils: two traditional binders (lime and cement) and two sustainable, self-cementitious industrial byproducts (Class C fly ash and Cement Kiln Dust). The study is literature-based, drawing on a dataset of published experimental lab studies restricted throughout to soils whose classification was explicitly confirmed or derived from reported Atterberg limit data using the Casagrande A-line criterion. The comparative analysis is structured across three dimensions: quantitative effectiveness at lab scale, qualitative durability, and sustainability. Effectiveness was assessed across four geotechnical criteria: swell reduction, unconfined compressive strength (UCS) gain, compressibility reduction, and plasticity index reduction, with each technique's mean performance on every criterion normalized to a 0–100 scale and combined into an equal-weighted composite Effectiveness Score. This analysis demonstrates that no single technique leads across all three dimensions evaluated. Cement achieved the highest composite Effectiveness Score (72.8/100), and also recorded the highest durability standing of the four techniques; however, it recorded the lowest sustainability rating, reflecting the substantial carbon footprint of Portland cement production. Class C fly ash achieved a composite Effectiveness Score of 48.0, closely matching lime's 47.2, while offering a substantially stronger sustainability profile; given this combination, Class C fly ash emerges as a strong substitute for lime. CKD recorded the highest UCS gain of any technique (1072% mean) and matched cement’s durability standing while sharing Class C fly ash's strong sustainability profile, yet achieved the lowest composite Effectiveness Score of the four (25.5), indicating that strong performance on individual criteria does not guarantee strong performance overall. The central finding is that the traditional-versus-sustainable stabilizer trade-off is not uniform across techniques: Class C fly ash achieves sustainability without sacrificing effectiveness or durability, while cement and CKD each illustrate the opposite pattern, strong performance on some dimensions offset by a clear weakness on another.

Acknowledgment

I would like to express my sincere gratitude to my supervisors, **Prof. Fulvia Chiampo** and **Prof. Claudio Oggeri**, for their guidance, patience, and valuable insights throughout the development of this thesis. Their expertise and constructive feedback were instrumental in shaping both the direction and the quality of this work.

I would also like to extend my thanks to **Politecnico di Torino** and the **Lebanese University** for the opportunity to pursue this thesis within the framework of the double degree program between the two institutions. This experience has broadened my academic and personal horizons, and I am grateful for the knowledge and support I received from both universities throughout my studies.

Finally, I wish to thank everyone who supported me, directly or indirectly, throughout this journey.

Contents

Abstract....2
Acknowledgment....3
List of Tables....6
LIST OF FIGURES....7
Introduction....8
CHAPTER 1 — Fundamentals of Expansive Soils....9
1.1 Introduction to Expansive Soils....9
1.2 Classification of Expansive Soils....9
1.2.1 Methods based on Physical properties....9
1.2.2. Methods based on mineralogical and chemical properties....12
1.3 Mechanisms of Swelling and Shrinkage....17
1.3.1 Isomorphous Substitution and Surface Charges....17
1.3.2 Adsorbed Cations and Cation Hydration....17
1.3.3 Osmotic and crystalline swelling....18
1.3.4 Shrinkage mechanisms....19
1.4 Engineering Problems Associated with Expansive Soils....20
1.4.1 Slope Instability....21
1.4.2 Foundations and Buildings....21
1.4.3 Pavements and Retaining Structures....21
CHAPTER 2 — Classification, Characteristics and Behavior of High-plasticity Inorganic Soils....22
2.1 Unified Classification of Soils....22
2.2 Definition and Characteristics of High-plasticity Inorganic Soils....24
Other General Characteristics....24
2.3 Relationship between fat clays and expansive soils....26
2.4 Factors affecting expansiveness....27
2.4.1 Mineralogical characteristics of fat clays and their effect....27
2.4.2 Mechanical characteristics and their effect....28
2.4.3 Natural water content....29
2.4.4 Dry Density....29
2.4.5 Confining pressure....29
2.4.6 Climate/wet-dry cycles....30
CHAPTER 3 — Traditional Chemical Stabilization Techniques....30
3.1 Lime Stabilization....30
3.1.1 Introduction....30
3.1.2 Stabilization mechanism....31
3.1.3 Effect of lime stabilization on the different properties....34

3.1.4 Performance under Meteorological events....35
3.1.5 Field Applicability of Lime Stabilization....36
3.1.6 Environmental Impact....37
3.2 Cement Stabilization....39
3.2.1 Introduction....39
3.2.2 Stabilization Mechanism....39
3.2.3 Effect of cement stabilization on the different properties....41
3.2.4 Performance under Meteorological events....42
3.2.5 Field Applicability of Cement Stabilization....43
3.2.6 Environmental Impact....44
CHAPTER 4 — Sustainable Chemical Stabilization Techniques....46
4.1 Fly Ash Stabilization....46
4.1.1 Introduction....46
4.1.2 Stabilization mechanism....46
4.1.3 Effect on Engineering Properties....48
4.1.4 Performance Under Meteorological Events....49
4.1.5 Field Applicability of Class C fly ash....50
4.1.6 Environmental Impacts....51
4.2 Cement Kiln Dust (CKD) Stabilization....53
4.2.1 Introduction....53
4.2.2 Stabilization mechanism....53
4.2.3 Effect on Engineering Properties....54
4.2.4 Performance Under Meteorological Events....56
4.2.5 Field Applicability of CKD Stabilization....58
4.2.6 Environmental Impacts....59
CHAPTER 5 — Comparative Analysis of Traditional and Sustainable Chemical Stabilization Techniques....61
5.1 Introduction....61
5.2 Effectiveness Comparison....62
5.2.1 Methodology....62
5.2.2 Results and Discussion....64
5.3 Durability Comparison....68
5.4 Environmental Impact and Sustainability Comparison....70
5.5 Cross-Criteria Synthesis....71
Conclusion....73
REFERENCES....74

List of Tables

TABLE 1 CLASSIFICATION OF SWELLING POTENTIAL BASED ON PLASTICITY INDEX [ADAPTED FROM PECK ET AL. (1974) AND IS 1498] 10
TABLE 2 TYPICAL ACTIVITY VALUES FOR CLAY MINERALS 10
TABLE 3 CLASSIFICATION OF SWELLING POTENTIAL ACCORDING TO THE FREE SWELL INDEX (FSI). 11
TABLE 4 DEGREE OF EXPANSION AS FUNCTION OF SWELLING POTENTIAL AND SWELLING PRESSURE. 12
TABLE 5 SHEET STRUCTURE FOR THE LAYERS OF CLAY MINERALS 13
TABLE 6 TYPICAL VALUES OF CATION EXCHANGE CAPACITY (CEC), SPECIFIC SURFACE AREA (SSA), AND TOTAL POTASSIUM (TP) FOR COMMON CLAY MINERALS. 16
TABLE 7 COMPARISON OF FINE-GRAINED USCS SOIL GROUPS, PLASTICITY-CHART POSITION, AND TYPICAL SWELLING POTENTIAL. 24
TABLE 8 PHYSICAL CHARACTERISTICS OF THE SOIL SAMPLE USED [FROM VUKICEVIC ET AL (2019)]. 27
TABLE 9 PHYSICAL CHARACTERISTICS OF SOILS A AND B [FROM SELVAKUMAR ET AL. (2024)]. 27
TABLE 10 CHEMICAL CONSTITUTIONS OF ORDINARY PORTLAND CEMENT 39
TABLE 11 DOSAGE-RESPONSE PATTERN OF CLASS C FLY ASH ON ATTERBERG LIMITS IN CH EXPANSIVE SOILS 48
TABLE 12 FACTORS INFLUENCING THE DURABILITY OF CKD-STABILIZED EXPANSIVE SOIL UNDER WETTING-DRYING CYCLES 57
TABLE 13 SUMMARY OF THE MAIN SUSTAINABILITY LIMITS FOR CKD STABILIZATION OF CH EXPANSIVE SOILS 60
TABLE 14 NUMBER OF LITERATURE DATA POINTS USED IN THIS STUDY 64
TABLE 15 RESULT MATRIX 65
TABLE 16 NORMALIZED SCORES (0–100) 65
TABLE 17 QUALITATIVE WETTING-DRYING DURABILITY ASSESSMENT. 68
TABLE 18 FREEZE-THAW PERFORMANCE WITH THE CORRESPONDING DOSAGE 69
TABLE 19 SUSTAINABILITY ASSESSMENT. 70
TABLE 20 ASSESSMENT OF THE OVERALL PERFORMANCE BASED ON EFFECTIVENESS, DURABILITY, AND SUSTAINABILITY OF THE SOIL STABILIZATION 71

LIST OF FIGURES

Figure 1 Consolidation-swell oedometer test results. 12
Figure 2 Atomic structures and schematic representations of silicon tetrahedra and alumino–magnesium octahedra: (a) silicon tetrahedron; (b) silica sheet; (c) schematic representation of a silica sheet; (d) alumino–magnesium octahedron; (e) octahedral sheet; and (f) schematic representation of an octahedral sheet. 13
Figure 3 Schematic diagrams of the structure: (a) kaolinite; (b) illite; (c) montmorillonite. 14
Figure 4 Scanning electron micrograph of montmorillonite 15
Figure 5 Conceptual illustration of the influence of cation hydration on the swelling behavior of expansive soils under different hydration conditions: (a) low hydration state, (b) partial hydration state, and (c) full hydration state. 17
Figure 6 Schematic illustration of a clay micelle showing the distribution and concentration of cations surrounding a negatively charged clay particle surface. 18
Figure 7 Schematic illustration of (A) the expansion of a clay particle and (B) the insertion of cations with their relative ionic dimensions. 19
Figure 8 Schematic of a typical shrinkage DiCC curve 20
Figure 9 Plasticity chart for USCS 22
Figure 10 USCS classification procedure- Fine-grained soils. 23
Figure 11 Average values of relative sizes, thicknesses, and specific surfaces of the common clay minerals 25
Figure 12 Plasticity Chart showing the typical ranges of clay minerals 25
Figure 13 Variation of the deviator stress with clay content at failure with clay content [from Dafalla et al. (2020)] 26
Figure 14 The relationship, at three distinct applied pressures between the swelling and the percentage of sand (Fs%) for formed samples according to the standard Proctor [from Alnmr et al. (2024)] 28
Figure 15 Changes in (a) Cc and (b) mv as a function of initial dry unit weight (γd) for various sand percentages at 75 % initial saturation level [from Alnmr et al. (2024)] 28
Figure 16 Comparison of swelling pressures in vertical and lateral directions [from Chi et al. (2023)] 29
Figure 17 quick lime 31
Figure 18 hydrated lime 31
Figure 19 High-resolution TEM images of untreated and lime-treated FoCa clay (a, b) faces section. a: Untreated FoCa clay. b: Treated FoCa clay [from Al-Mukhtar et al. (2012)] 33
Figure 20 Influence of lime content on the Atterberg limits [from Driss et al. (2022)] 34
Figure 21 Stabilization mechanism: (a) cation exchange; (b) flocculation-agglomeration; (c) pozzolanic reaction 41
Figure 22 X-ray computed tomography (CT) grayscale images illustrate expansive soil samples' internal microstructural evolution under cyclic wetting–drying (WD) conditions 43
Figure 23 SEM of a Class C Fly Ash 46
Figure 24 Effect of wet–dry cycles on unconfined compressive strength of the fly ash-stabilized soil [from Bin-Shafique et al. (2010)] 50
Figure 25 Vertical swell of a fly ash-stabilized expansive soil during freeze–thaw cycles [from Bin-Shafique et al. (2010)] 50
Figure 26 Cement Kiln Dust (CKD) 53
Figure 27 Atterberg limits of CKD-soil [from Mohamedzein et al. (2025)] 55
Figure 28 SEM of a soil treated with 15% CKD [from Mohamedzein et al. (2025)] 56
Figure 29 Influence of freeze-thaw cycles and CKD content on unconfined compressive strength of soil [from Ismeik et al. (2021)] 58
Figure 30 Weight loss and volume change vs. percentage of CKD content [from Alhassani et al. (2021)] 58
Figure 31 The energy consumption of cement-stabilized and a CKD-stabilized soil [from Ghavami et al. (2020)]. 60
Figure 32 The e-CO2 emission of cement-stabilized and CKD-stabilized soil [from Ghavami et al. (2020)] 60
Figure 33 Casagrande plasticity chart of all collected soil studies 63
Figure 34 Bar chart of normalized scores 65
Figure 35 Composite Effectiveness Score 67

Introduction

Expansive soils undergo significant volumetric changes in response to moisture variation, generating ground movements that damage foundations, pavements, slopes, and buried infrastructure worldwide. Annual losses attributable to expansive soils in the United States alone are estimated at seven billion dollars, exceeding combined damage from earthquakes, tornadoes, and hurricanes.

Among expansive soils, those classified as highly plastic inorganic clays under the Unified Soil Classification System (USCS) represent a particularly problematic type. Their expansive behavior is rooted in a clay fraction dominated by active 2:1 phyllosilicate minerals, particularly montmorillonite, whose interlamellar structure absorbs water into the clay lattice itself and generates swelling pressures of several hundred kilopascals under confined conditions.

Chemical stabilization has been the dominant practical response to soils for over a century. Lime and Ordinary Portland Cement ( ) are the two traditional stabilizers that have anchored this practice. Both achieve stabilization through a sequence of cation exchange, flocculation, and pozzolanic reaction that reduces plasticity, suppresses swell, and develops long-term compressive strength. Their environmental cost, however, is increasingly recognized as a constraint: lime and OPC production are among the most carbon-intensive inputs, accounting collectively for a substantial share of global CO_2 emissions. This has driven growing research interest in sustainable, waste-derived alternatives, particularly Class C fly ash, a self-cementitious byproduct of coal combustion, and Cement Kiln Dust (CKD), a byproduct of OPC manufacturing, both of which carry sufficient free calcium oxide to initiate the same stabilization reactions as traditional binders without requiring an external activator.

Despite the growing volume of stabilization literature with data achieved in laboratory tests, an important gap persists. No systematic comparative analysis has evaluated traditional and sustainable stabilizers against each other specifically on **verified high-plasticity inorganic soils**, across a consistent set of geotechnical criteria and using a transparent methodological framework.

This thesis tries to cover this gap. Its central aim is to evaluate and compare traditional and sustainable chemical stabilization techniques for high-plasticity inorganic soils, considering data of durability, field applicability, and environmental impact, and to conduct a laboratory data-based comparative analysis of all four techniques on a dataset of experimental measurements.

The thesis is organized into five chapters. Chapter 1 reviews expansive soils broadly: their global distribution, classification, mineralogy, swelling and shrinkage mechanisms, and engineering consequences. Chapter 2 narrows the focus to high-plasticity inorganic soils specifically, examining their USCS classification, physical and mechanical characteristics, relationship to expansiveness, and governing behavioral factors. Chapter 3 reviews lime and OPC stabilization of high-plasticity inorganic soils across mechanism, engineering effects, durability, field applicability, and environmental impact. Chapter 4 applies the same framework to Class C fly ash and CKD. Chapter 5 presents a three-part comparative analysis: quantitative effectiveness, qualitative durability, and sustainability, synthesizing how the four techniques compare against one another.

CHAPTER 1 — Fundamentals of Expansive Soils

1.1 Introduction to Expansive Soils

Expansive soils are fine-grained soils that undergo significant volume changes in response to variations in moisture content. These soils swell when water is absorbed and shrink upon drying, leading to repeated deformation cycles that can adversely affect the stability and performance of engineering structures. The expansive behavior of these soils is primarily associated with the presence of active clay minerals possessing high affinity for water, particularly minerals belonging to the smectite group. Due to their pronounced shrink-swell characteristics, expansive soils are considered among the most problematic geomaterials encountered in geotechnical engineering practice.

The engineering significance of expansive soils arises from their ability to generate swelling pressures and substantial ground movements during wetting and drying cycles. Seasonal moisture fluctuations may cause differential movement, settlement, and cracking in foundations, pavements, retaining structures, and buried utilities. The severity of these problems depends on several factors including mineralogical composition, water content variation, dry density, and environmental conditions.

Expansive soils are found worldwide, particularly in arid and semi-arid regions with alternating wet and dry climates. They are prevalent in countries such as the United States, India, Australia, China, and South Africa, with new deposits continually being identified as construction activities expand. These soils pose significant engineering challenges, causing substantial economic losses through infrastructure damage and maintenance.

1.2 Classification of Expansive Soils

Methods used to determine the swelling potential of expansive soils are generally classified into two main groups. The first group is based on the evaluation of the soil's physical properties, including Atterberg limits and free swell. The second group focuses on the mineralogical and chemical characteristics of the soil, such as clay fraction, cation exchange capacity, and specific surface area.

1.2.1 Methods based on Physical properties

1.2.1.1 Methods Based on Plasticity

Atterberg limits are widely used for soil characterization and play an important role in several methods for identifying expansive soils. One important parameter derived from these limits is the plasticity index (PI).

The Plasticity Index is defined as follows:

$$PI = LL - PL$$

Where:

LL: Liquid limit, which represents the water content at which soil changes from a plastic state to a liquid state.

PL: Plastic limit, which represents the water content at which soil changes from a semi-solid state to a plastic state.

Numerous identification approaches for expansive soils rely on these indices.

For instance, Peck et al. (1991) proposed a general correlation between the plasticity index of a soil and its swelling potential (Table 1).

The swelling potential is defined as the percentage swell of a laterally confined sample which has soaked under a surcharge of 1 pound per square inch after being compacted to a maximum density at optimum moisture content.

Moreover, according to the Indian Standard classification system (IS 1498), the expansiveness of fine-grained soils may be preliminarily assessed as well using index properties such as Plasticity Index (PI) (Table 1).

Table 1 Classification of Swelling Potential based on Plasticity Index [adapted from Peck et al. (1974) and IS 1498]

Swelling Potential	Plasticity Index (%)	
	Peck et al. (1991)	IS 1498
Low	0-15	< 12
Medium	0-35	12-23
High	20-55	23-32
Very High	>35	>32

However, Zapata et al. (2006) demonstrated that the swelling potential of remolded expansive soils is not strongly correlated with the plasticity index alone. Their study indicated that a more reliable correlation can be obtained by relating the expansion potential to the combined effect of the plasticity index and the percentage of soil passing the No. 200 sieve (75 μm). That means soil plasticity may indicate the presence of expansive minerals, but it cannot by itself provide a definitive classification of a soil as expansive. Seed et al. (1964) demonstrated that the plasticity index can nevertheless serve as a preliminary indicator of the swelling behavior of most clay soils.

Although soils with high swelling potential generally exhibit high index properties, the opposite condition is not always valid.

On the other hand, Atterberg limits and clay content can be combined into a parameter called activity, A_c.

$$Activity(Ac) = \frac{Plasticity\ Index\ (\%)}{\%\ by\ weight\ finer\ than\ 2\mu m}$$

Skempton (1953) classified clays into three categories based on their activity values. Clays with an activity lower than 0.75 were described as “inactive,” those with activity values ranging from 0.75 to 1.25 were considered “normal,” and clays with activity values exceeding 1.25 were classified as “active.” Among these categories, active clays exhibit the highest potential for swelling.

Typical values of activities for various clay minerals are shown in Table 2. Sodium montmorillonite has the highest swelling potential, which is reflected by the extraordinarily high value of activity.

Table 2 Typical Activity Values for Clay Minerals

Mineral	Activity
Kaolinite	0.33-0.46
Illite	0.9
Montmorillonite (Ca)	1.5
Montmorillonite (Na)	7.2

1.2.1.2 Free Swell Test

The free swell test consists of placing a known volume of dry soil passing the No. 40 (425 µm) sieve into a graduated cylinder filled with water and measuring the swelled volume after it has completely settled.

The free swell of a soil is defined as the percentage increase in volume when the soil changes from a dry condition to a saturated condition, relative to its initial volume.

Holtz and Gibbs (1956) indicated that soils with free swell values as low as 100% can still undergo significant swelling in the field when subjected to wetting under low surcharge loads. In addition, Dawson (1953) observed that certain clays in Texas with free swell values around 50% were responsible for severe expansion-related damage. This behavior was attributed to harsh climatic conditions combined with the inherent swelling properties of the soils.

However, even for the same type of soil, the results of the test can be influenced significantly by many factors, such as the amount of soil tested, degree of soil grinding, and drop height of the soil sample (Chen et al. 2006).

The Bureau of Indian Standards (1977) IS 2720 Part 40 standard applies the Free Swell Index (FSI) method as an indirect approach for evaluating the swelling potential of expansive soils. The expansion potential of the soil as classified according to the FSI is shown in Table 3.

Table 3 Classification of Swelling potential According to the Free Swell Index (FSI).

Free Swell Index (%)	Swelling potential
< 20	Low
20-35	Medium
35-50	High
>50	Very high

1.2.1.3 Direct measurement of swelling potential and swelling pressure

When Terzaghi first introduced the concept of effective stress, he validated the theory using experimental results obtained from an apparatus known as the oedometer (Terzaghi, 1925; Terzaghi, 1943). This device is also commonly referred to as a consolidometer.

It is a direct measurement method that is considered the most reliable techniques for evaluating the swelling potential of expansive soils because it measures the actual volume change behavior of the soil under controlled laboratory conditions.

The most common type is the consolidation-swell (CS) test, in which the sample is initially subjected to a prescribed vertical stress in the oedometer, and inundated under that vertical stress.

In the CS test, a soil specimen is placed in a consolidation ring and subjected to a prescribed vertical stress, termed the inundation stress, σ''_i

Following the application of the designated inundation stress for a specified duration, typically around 24 hours, the specimen is saturated and permitted to swell while the same vertical stress is maintained. The applied inundation stress may correspond to the natural overburden pressure, the combined effect of overburden and structural loading, or any other selected stress level depending on the objectives of the test.

The vertical strain that occurs due to wetting, termed the percent swell, ε_s%, is measured. After the swelling has been completed the sample may or may not be subjected to additional vertical

load. The stress that would be required to restore the sample to its original height is termed the "consolidation-swell swelling pressure," σ''_{cs}. The test results are shown in Figure 1.

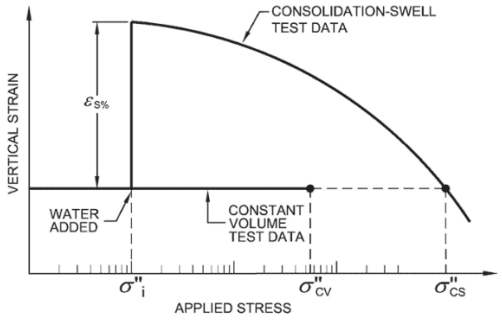


Figure 1 Consolidation-swell oedometer test results.

The oedometer test allows accurate determination of both swelling potential and swelling pressure under various loading conditions. However, the measured swelling behavior is influenced by several factors, including the condition of the sample (undisturbed or remolded), initial moisture content, compaction characteristics, applied surcharge load, and duration of the test. In general, lower initial moisture contents tend to produce greater swelling, whereas increasing the surcharge load reduces the magnitude of expansion.

Consequently, careful control and standardization of testing conditions are essential to obtain reliable and reproducible results. Due to its ability to directly quantify soil expansion, the oedometer swell test is widely regarded as one of the most satisfactory and dependable methods for assessing the expansiveness of clay soils.

So, based on the values of swelling potential and the swelling pressure, Seed et al. (1962) and Chen (1975), respectively, proposed the classification presented in Table 4.

Table 4 Degree of expansion as function of swelling potential and swelling pressure.

Degree of expansion	Swelling Potential (%) [Seed et al. (1962)]	Swelling Pressure (kg/cm^2) [Chen, (1975)]
Low	0-1.5	0-1.5
Medium	1.5-5	1.5-2.5
High	5-25	2.5-9.8
Very High	>25	>9.8

1.2.2. Methods based on mineralogical and chemical properties

The mineralogical composition of expansive soils plays a significant role in determining their swelling behavior. In particular, the presence of montmorillonite is often considered an indicator of a soil's potential for expansion.

1.2.2.1. Mineralogical Composition

Clay Minerals

According to Grim (1959), clay minerals are primarily composed of aluminum, iron, and/or magnesium silicates. Most clay minerals possess a layered or sheet-like crystal structure and may occur in a variety of particle shapes. In expansive soils, a typical clay particle is represented by a microscopic platelet characterized by negatively charged flat surfaces and positively charged edges. The mineralogical structure of clay minerals can be described as a combination of two fundamental structural units.

The fundamental structural components of clay minerals are the silicon tetrahedron and the alumino–magnesium octahedron. The silicon tetrahedron is composed of silicon and oxygen atoms. Due to its positive valence of +4, silicon readily bonds with negatively charged species such as oxygen (O^{2-}) and hydroxyl (OH^{-}) ions, resulting in the tetrahedral arrangement illustrated in Figure 2.a. This geometry arises from the relative sizes and spatial distribution of the silicon and oxygen atoms. The alumino–magnesium octahedron, shown in Figure 2.d, consists of aluminum or magnesium atoms coordinated by hydroxyl groups. The arrangement of these atoms forms an octahedral structure, which serves as another essential building block in the crystal structure of clay minerals.

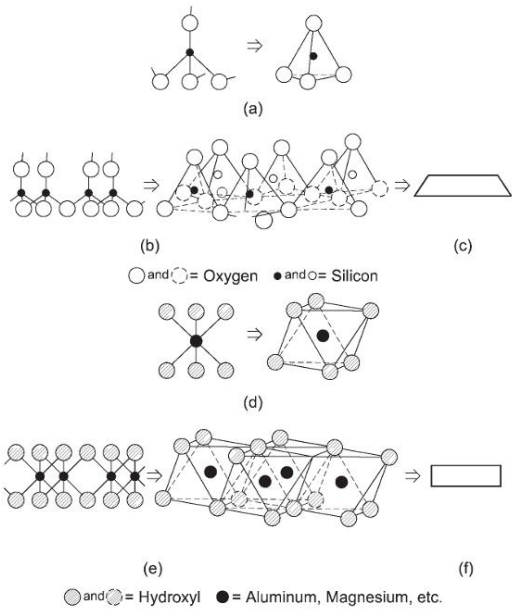


Figure 2 Atomic structures and schematic representations of silicon tetrahedra and alumino–magnesium octahedra: (a) silicon tetrahedron; (b) silica sheet; (c) schematic representation of a silica sheet; (d) alumino–magnesium octahedron; (e) octahedral sheet; and (f) schematic representation of an octahedral sheet.

In the silicon tetrahedral structure illustrated in Figure 2.a, each oxygen atom possesses an unsatisfied chemical bond. The oxygen atoms located at the base of the tetrahedron are shared with neighboring tetrahedra, resulting in the formation of continuous tetrahedral sheets, as shown in Figure 2.b. This sharing process satisfies the bonds of the basal oxygen atoms; however, the oxygen atoms at the tetrahedral apexes remain partially unsatisfied. Consequently, the exposed surface of the silica sheet is capable of attracting and bonding with positively charged cations. Similarly, octahedral units are linked through shared hydroxyl groups to form octahedral sheets, as illustrated in Figure 2.e. In contrast to the silica sheets, the hydroxyl groups within the octahedral sheets have no unsatisfied bonds. The type of cation occupying the central position within the octahedral structure may vary depending on the mineral composition.

Figure 2.c and Figure 2.f present schematic representations of the fundamental structural units used to illustrate the crystalline arrangement of clay minerals. Different types of clay minerals are formed by varying the way these structural units are combined and stacked, mainly Montmorillonite, Kaolinite and Illite.

Table 5 Sheet structure for the layers of clay minerals

Clay mineral group	Layer type
Kaolinite	1:1
Montmorillonite or smectite	2:1

Illite	2:1

The diversity of clay minerals arises from the different arrangements of tetrahedral and octahedral sheets within their crystal structures, as summarized in Table 5. For instance, a 1:1 clay mineral consists of one tetrahedral sheet bonded to one octahedral sheet in each structural layer. In contrast, a 2:1 clay mineral is composed of two tetrahedral sheets enclosing a single octahedral sheet between them.

The size of the mineral particles in a soil is influenced by the nature of the bonds between the silica and octahedral sheets. The structure of the kaolinite as depicted in Figure 3 shows that there is a strong bond between the top of the silica sheet and the octahedral sheet. This is because of the arrangement of the atoms and the fact that the oxygen atoms at the top of the silica tetrahedra can replace some of the hydroxyls in the octahedral sheets. As a result, a strong chemical linkage is formed between the two sheets (Grim, 1959).

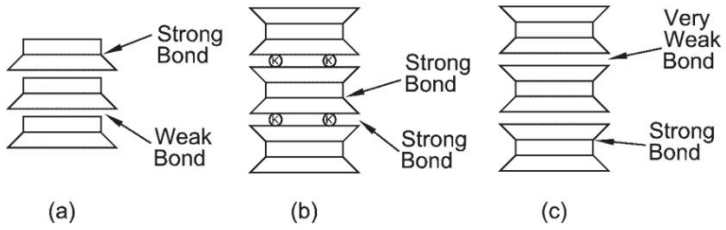


Figure 3 Schematic diagrams of the structure: (a) kaolinite; (b) illite; (c) montmorillonite.

Kaolinite

Since the chemical bonds at the base of the silica sheet are already satisfied, the connection between this surface and the adjacent octahedral sheet is governed mainly by relatively weak hydrogen bonds. Consequently, when mineral cleavage occurs, separation typically takes place along these weaker bonding planes. Despite their relative weakness, these bonds are strong enough to maintain several structural layers within a single clay particle. As a result, kaolinite particles generally possess relatively large lateral dimensions. Owing to its stable crystal structure and limited capacity for interlayer water adsorption, kaolinite typically exhibits a low swelling potential.

Montmorillonite

In montmorillonite, the interaction between adjacent silica sheets is governed primarily by Van der Waals forces, which are considerably weaker than the bonds present in kaolinite. As illustrated in Figure 3.c, these interactions are classified as “very weak.” Consequently, montmorillonite particles are often composed of only one or two structural layers, resulting in extremely thin particles with thicknesses that may be as small as approximately 10 Angstroms.

An important source of montmorillonite in nature is bentonite. It is a rock formed of highly colloidal and plastic clays mainly composed of montmorillonite. In addition to montmorillonite, bentonite may contain some amount of crystalline quartz, cristobalite, and feldspar.

Montmorillonite present in bentonite may occur in either sodium-rich or calcium-rich forms. Sodium montmorillonite generally constitutes the dominant component of bentonite, accompanied by approximately 10–20% of other minerals such as feldspar, calcite, silica, and gypsum. Due to its layered crystal structure, montmorillonite has a remarkable ability to adsorb water within the interlayer spaces. This characteristic leads to substantial volume changes during cycles of wetting and drying, making it one of the most expansive clay minerals. The mechanisms responsible for this behavior are discussed in the following sections.

Illite

The crystal structure of illite is generally similar to that of montmorillonite, as illustrated in Figure 3.b. However, unlike montmorillonite, the adjacent silica sheets in illite are linked by potassium cations that occupy the spaces created by the arrangement of the silica tetrahedra. The size of the potassium ions allows them to fit precisely within these cavities and be shared between neighboring sheets, thereby creating a strong interlayer bond (Grim, 1959). As a result of these stronger interlayer connections, illite exhibits significantly lower swelling potential than montmorillonite, and its expansive behavior is generally comparable to that of kaolinite.

Clay mineralogy can be identified through the examination of crystal structures or by conducting chemical analyses of the soil. Popular mineralogical methods of identification include X-ray diffraction (XRD), and scanning electron microscopy (SEM).

1.2.2.2 Mineralogical Characterization Methods

X-ray diffraction (XRD)

In expansive soil investigations, XRD is primarily used to identify clay minerals belonging to the smectite group, particularly montmorillonite, which is widely recognized as the mineral most responsible for swelling behavior.

Therefore, the presence and relative abundance of these minerals can provide valuable information regarding the potential expansiveness of a soil. Unlike index-property-based methods, which infer swelling potential from physical parameters such as the liquid limit or plasticity index, XRD provides direct information regarding the mineralogical composition of the soil. Since the swelling behavior of expansive soils is largely controlled by the type and abundance of clay minerals present, XRD analysis plays an important role in the assessment of soil expansiveness.

However, most natural clays are mixtures of several clay minerals and a number of accessory minerals. Reflections from clays are usually broad because the crystals are thin and the layer stacking is frequently disordered. This, together with the large number of minerals frequently present, leads to overlapping reflections and few observable reflections from less abundant components. It is therefore usual to examine clay specimens before, and after various treatments that alter the fraction patterns of the components.

Scanning Electron microscopy (SEM)

Electron microscopy enables the direct observation of clay particles and provides valuable information about their morphology.

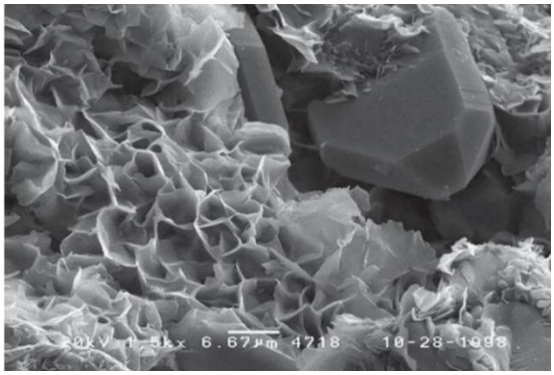


Figure 4 Scanning electron micrograph of montmorillonite

Figure 4 shows the scanning electrons micrograph of montmorillonite, which reveals a characteristic flaky and sheet-like morphology composed of thin, irregularly shaped clay

platelets arranged in loosely packed aggregates. The particles appear highly folded and interconnected, forming an open microstructure with numerous interparticle voids. This morphology is associated with the 2:1 layered crystal structure of montmorillonite and contributes to its high specific surface area and strong affinity for water. The open arrangement of the clay sheets facilitates the penetration of water molecules into the interlayer spaces, resulting in significant swelling and shrinkage behavior. Consequently, the observed microstructure provides a microscopic explanation for the pronounced expansive characteristics commonly exhibited by montmorillonite-rich soils.

1.2.2.3 Chemical Characterization methods

Cation Exchange Capacity (CEC)

The CEC is the total number of exchangeable cations required to balance the negative charge on the surface of the clay particles. Cation exchange capacity (CEC) is expressed in milliequivalents per 100 grams of dry clay and represents the ability of clay particles to retain and exchange cations. During the test, soluble salts are first removed from the soil, and the exchange sites are then saturated with a known cation to replace the naturally adsorbed ions. The quantity of the introduced cation required to achieve saturation depends on the magnitude of the negative surface charge, with higher values indicating a greater charge imbalance. The displaced cations can subsequently be identified through chemical analysis of the extracted solution.

CEC is closely related to clay mineralogy and can be used as an indicator of clay activity. High CEC values generally suggest the presence of highly active clay minerals, such as montmorillonite, whereas low CEC values are typically associated with less active, non-expansive minerals such as kaolinite. Consequently, the swelling potential of a soil generally increases with increasing CEC. Typical CEC values for the three principal clay minerals are summarized in Table 6.

Table 6 Typical Values of Cation Exchange Capacity (CEC), Specific Surface Area (SSA), and Total Potassium (TP) for Common Clay Minerals.

Clay mineral	Cation Exchange Capacity (CEC) (meq/100g)	Specific Surface Area (SSA)(m^2/g)	Total Potassium (TP) (%)
Kaolinite	1-6	5-55	0
Illite	15-50	80-120	6
Montmorillonite	80-150	600-800	0

Specific Surface Area (SSA)

The specific surface area (SSA) of a soil is defined as the total surface area of soil particles in a unit mass of soil. Soils with a high SSA generally exhibit greater water retention capacity and a higher potential for swelling due to the increased surface available for water adsorption [Chittoori and Puppala (2011)]. Nevertheless, a high SSA value alone should not be considered conclusive evidence of expansive behavior.

Typical SSA values for the three principal clay minerals are presented in Table 6. Among these minerals, montmorillonite exhibits SSA values that are approximately an order of magnitude greater than those of kaolinite, which allows it to be distinguished from other clay minerals and often facilitates mineral identification.

Total Potassium (TP)

Illite is the only major clay mineral that contains potassium as an integral component of its crystal structure. Consequently, the concentration of potassium ions in a soil can serve as a direct indicator of the presence of illite [Chittoori and Puppala (2011)]. As shown in Table 6, illite

contains significantly higher amounts of total potassium compared with kaolinite and montmorillonite. Therefore, elevated potassium content in a soil generally suggests a lower swelling and expansion potential.

1.3 Mechanisms of Swelling and Shrinkage

1.3.1 Isomorphous Substitution and Surface Charges

During the natural formation of octahedral sheets, some of the positions typically occupied by Al^{3+} ions may be replaced by other cations. This phenomenon, known as isomorphous substitution, results in changes to the chemical composition and charge characteristics of the clay mineral structure.

Isomorphous substitution involving the replacement of Al^{3+} by cations with lower valence produces two important effects. First, it creates a local charge imbalance due to the reduction in positive charge. Second, the difference in ionic size between the substituting and original cations causes distortion within the crystal lattice. As a consequence of these effects, the surfaces of the structural units, and therefore the clay particles themselves acquire a net negative charge.

1.3.2 Adsorbed Cations and Cation Hydration

The negative surface charges present on clay particles are neutralized by the adsorption of positively charged cations. The type and characteristics of these cations play a significant role in determining the physicochemical behavior and engineering properties of the clay soil.

The cations present in a soil may exist under varying degrees of hydration depending on the moisture conditions. In a completely dry soil, cations are minimally hydrated. As water enters the soil, water molecules become attracted to and surround the cations, particularly sodium ions, through a process known as hydration.

A conceptual representation of the effect of cation hydration on soil swelling is presented in Figure 5. In Figure 5.a, two parallel clay particles are separated by cations with a very low degree of hydration. Figure 5.b illustrates the condition in which the cations have become partially hydrated.

With continued water addition, the cations become fully hydrated, as illustrated in Figure 5.c. Lambe and Whitman (1969) reported that the radius of a sodium ion increases from approximately 0.98 Å in the unhydrated state to about 7.8 Å when fully hydrated. This means that complete hydration can increase the effective ion size by more than seven times. Even so, a relatively small increase in cation diameter, for example 10%, could produce a similar increase in the spacing between clay particles, which may result in significant soil expansion.

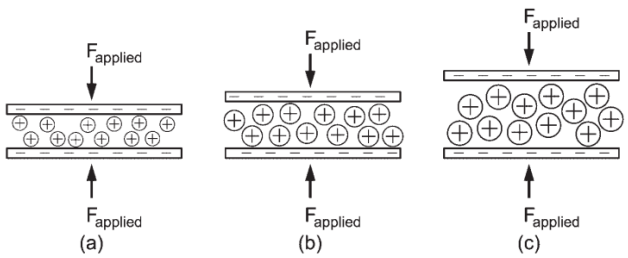


Figure 5 Conceptual illustration of the influence of cation hydration on the swelling behavior of expansive soils under different hydration conditions: (a) low hydration state, (b) partial hydration state, and (c) full hydration state.

1.3.3 Osmotic and crystalline swelling

The clay mineral particles and their associated adsorbed cations behave as a combined physicochemical system. Within a soil–water environment, differences in cation concentration create concentration gradients that drive water molecules toward regions containing higher cation concentrations. This migration of water generates osmotic pressure, which contributes to the expansion and swelling of clay soils. This mechanism is commonly referred to as osmosis.

A portion of the water located near clay particles exists as hydration water, while another portion is attracted toward the particle surfaces and retained by surface forces. Lambe (1958) referred to this surface-bound water as adsorbed water. In contrast, water that migrates toward clay particles due to higher cation concentrations may be described as osmotic water.

To fully understand the behavior of clay soils, three fundamental components must be considered: the clay mineral itself, the associated exchangeable cations, and the water surrounding these particles. For this reason, the concept of the clay micelle is introduced as a useful model for describing the interactions among these components.

A clay micelle, illustrated in Figure 6, may be described as a negatively charged mineral core surrounded by positively charged cations that counterbalance the surface charge of the clay particle. The micelle consists of the clay particle, the adsorbed cations, and the closely associated hydration and osmotic water surrounding the mineral core [Lambe (1958)]. In the absence of these adsorbed cations, the negative charges on the faces of clay particles would generate repulsive forces between individual particles. Therefore, the cations that are strongly adsorbed onto the clay mineral surface play an essential role in neutralizing these electrical surface forces.

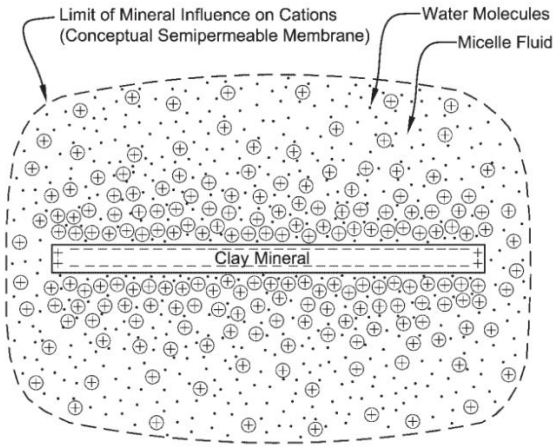


Figure 6 Schematic illustration of a clay micelle showing the distribution and concentration of cations surrounding a negatively charged clay particle surface.

Experimental observations by Norrish (1954) indicated that montmorillonite swelling occurs through two different mechanisms. At small interlayer spacings, typically less than 22 Å, the degree of expansion depends strongly on the type of exchangeable cation present. In this range, the amount of water absorbed is directly associated with the hydration energy of the cation.

Exchangeable cations are attracted toward the negatively charged surfaces of clay particles. Figure 7 illustrates how cation size can influence the migration of cations into the interparticle spaces. In some cases, the spacing between adjacent clay particles is smaller than the dimensions of certain hydrated cations. As these cations migrate into the interlayer region, the weak bonds between clay particles may be disturbed, causing the interlayer spacing to increase. This increase in spacing leads to a rise in volume and, consequently, clay swelling. The process is generally

reversible when the soil water content decreases due to evaporation, evapotranspiration, or water uptake by plant roots.

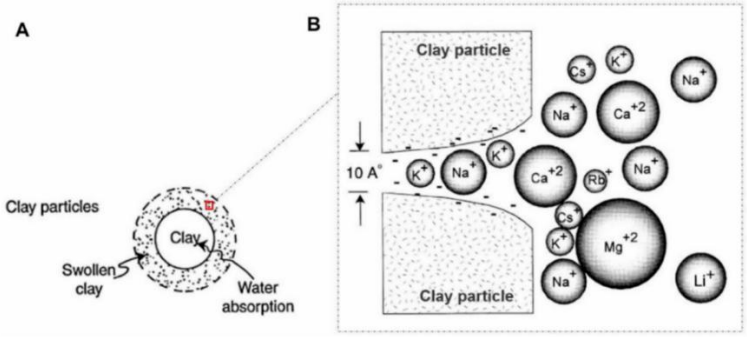


Figure 7 Schematic illustration of (A) the expansion of a clay particle and (B) the insertion of cations with their relative ionic dimensions.

At interparticle spacings greater than approximately 35 Å, montmorillonite swelling is considered to be mainly controlled by the development of micelle fluid, making the swelling process predominantly osmotic. This interpretation helps explain the swelling behavior of expansive soils. When water first enters a dry soil, it is primarily consumed in hydrating the exchangeable cations because of their high hydration energy. Additional water introduced afterward is then drawn into the interparticle spaces in response to osmotic forces.

Accordingly, the initial stage of swelling may be described as crystalline swelling, which is mainly associated with cation hydration, as discussed previously [Slade et al. (1991)]. In the subsequent stage, the high concentration of cations between clay particles attracts water into the interparticle region, producing osmotic swelling. However, these two mechanisms are unlikely to occur as completely separate phases; rather, a transitional zone probably exists between crystalline and osmotic swelling.

1.3.4 Shrinkage mechanisms

As soil dries out from a fully saturated condition, it moves through a transition from saturated to unsaturated states, during which capillary, adsorptive, and osmotic mechanisms come into play. These mechanisms have historically been difficult to capture accurately when modeling how soil shrinks.

The shrinkage response of soil during drying is commonly represented graphically through what is known as a drying-induced compression curve (DiCC), which relates the void ratio (e) to the mean intergranular (or mean effective) stress, p", as shown in Figure 8. Fundamentally, the volume change soil undergoes during drying stems from shifts in this intergranular stress. As a result, plotting the DiCC on an e − ln p" axis effectively produces a compression curve for the soil.

It's important to distinguish this drying-driven compression from conventional consolidation under mechanical loading, even though both processes can be described using intergranular stress as the governing variable. Compression caused by drying results from rising intergranular stress generated as the soil dries and potentially becomes partially saturated. Consolidation, by contrast, arises from increased intergranular stress driven by the dissipation of pore water pressure, with the soil remaining fully saturated throughout. As drying continues and moisture content drops, progressively larger pores empty out, causing the soil to stiffen. This stiffening

causes the DiCC to gradually diverge from the consolidation line associated with fully saturated soil (Figure 8).

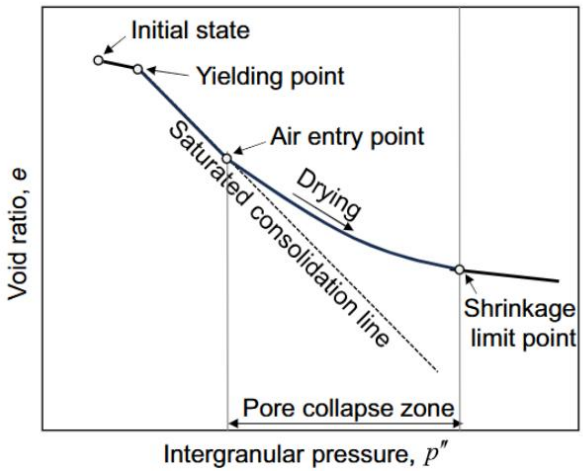


Figure 8 Schematic of a typical shrinkage DiCC curve

At the outset of drying from a saturated state, water leaving the soil boundary causes negative pore pressure to build up throughout the soil, which raises intergranular stress and drives shrinkage. At this early stage, the soil is still fully saturated, and its compression behavior tracks the consolidation line typical of saturated soils. As drying continues, matric suction keeps rising until the air-entry value is crossed, at which point air begins infiltrating the pores and the soil transitions to a partially saturated state. From here on, capillary forces take the lead in driving shrinkage.

As drying progresses further, water in the macropores empties out first, followed later by the release of the more tightly held water within the micropores. As increasing numbers of macropores empty, some collapse under rising intergranular stress, leaving behind a stiffer soil structure. With continued water loss, the intensity of soil-water interaction forces grows, eventually surpassing capillary effects as the primary driver of shrinkage. This process continues until virtually all macropores capable of drying-induced collapse have done so.

1.4 Engineering Problems Associated with Expansive Soils

The main engineering problem groups in expansive soils are: slope instability, damage to foundations and buildings, and distress in pavements and retaining structures. Across them, the common driver is repeated moisture change, which causes swelling, shrinkage, cracking, strength loss, and added pressures on structures.

1.4.1 Slope Instability

Expansive-soil slopes fail because wetting causes volume increase, internal stress redistribution, and crack growth, while drying-wetting cycles progressively weaken the soil mass [Liu et al. (2025); Zhang et al. (2022)].

Cracks are central to the problem because they accelerate rainwater infiltration and reduce structural integrity, which lowers slope stability and promotes shallow landslides or sliding under external loads such as vehicle loads [Zhao et al. (2024)].

Heavy rainfall is especially damaging because expansive minerals absorb water rapidly, shear zones soften, and insufficient shear strength can trigger crack formation and displacement [Liu et al. (2025)].

1.4.2 Foundations and Buildings

For foundations, the main problem is heave and differential movement caused by moisture-driven swelling beneath shallow footings and slabs [Hakro et al. (2026)].

Heave is the vertical expansion or uplift of an expansive-soil profile caused by moisture increase and the accompanying swell of the soil mass. In foundation terms, it is the ground movement that can lift shallow foundations, slabs, or other structural elements as the soil wets and expands.

These movements damage buildings not only by vertical uplift but also by inducing extra bending moments, beam forces, cracking, and uneven support conditions [Mohamed (2024); El-Samea et al. (2022)].

The problem worsens over time and under continued wetting: one numerical study by Hakro et al. (2026) found short-term heave could remain tolerable, but after 100 days vertical movement exceeded tolerable limits due to continuous swelling, and even a shallow expansive layer could cause unacceptable movement.

1.4.3 Pavements and Retaining Structures

Pavements on expansive soils commonly develop fatigue cracking, longitudinal cracking, and edge cracking because seasonal moisture fluctuations cause repeated subgrade swelling and shrinkage [Laporte et al. (2023)]. Water intrusion from pavement edges and surface cracks is a major trigger, and cyclic loading plus repeated swell-shrink degrades shear strength and stiffness over time, leading to larger displacements with more cycles [Pandey et al. (2021); Chabi et al. (2025)]. The damage is often differential rather than uniform, especially near pavement edges where crack networks promote deeper infiltration.

Retaining structures face a different but related problem: lateral swelling pressure develops when expansive soil tries to swell against a restrained wall. That pressure can far exceed ordinary lateral earth pressure, destabilize walls, and contribute to sliding, overturning, settlement, and deformation, especially when groundwater or inundation increases pore pressure [Li et al. (2021); Karunakaran et al. (2025)]. Large-scale and model studies show the pressure evolves with wetting duration and wall mobility, which means both drainage and wall flexibility strongly influence failure risk [Fan et al. (2023)].

CHAPTER 2 — Classification, Characteristics and Behavior of High-plasticity Inorganic Soils

2.1 Unified Classification of Soils

A soil classification system represents, in effect, a language of communication between engineers. It provides a systematic method of categorizing soils according to their probable engineering behavior, and allows engineers access to the accumulated experience of others.

Adopting a classification system doesn't replace the need for thorough property testing. That said, research has shown a strong correlation between measured engineering properties and a soil's index and classification characteristics. This means that once a soil's classification is known, an engineer can already form a reasonably solid expectation of how it will perform under real engineering conditions.

Today, only the Unified Soil Classification System (USCS) and the American Association of State Highway and Transportation Officials (AASHTO) system are commonly used in engineering practice. For this thesis, we will be adopting the USCS classification.

The underlying logic of the USCS is that coarse-grained soils are best classified according to grain size distribution, while for fine-grained soils, engineering behavior is governed primarily by plasticity characteristics. Put differently: soils where "fines" (silt and clay content) have minimal influence on engineering performance are classified based on grain size, whereas soils where fines do control behavior are classified based on plasticity. As a result, classifying a soil under this system requires nothing more than a sieve analysis paired with Atterberg limit testing.

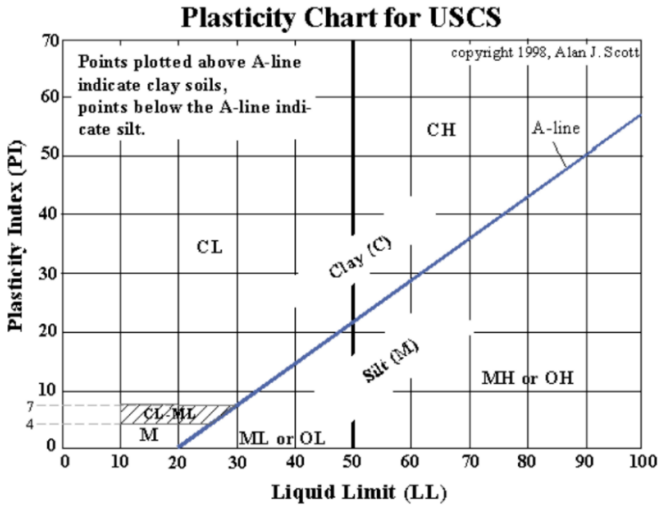


Figure 9 Plasticity chart for USCS

The USCS organizes soils into four principal categories: coarse-grained, fine-grained, organic soils, and peat. Classification applies specifically to material that passes through the 75 mm sieve, with any oversized fraction simply recorded separately on drill logs or data sheets.

Soils qualify as coarse-grained, covering both sands and gravels, when 50% or more of the material is retained on the No. 200 sieve. Conversely, fine-grained soils are defined by having more than 50% of material passing the No. 200 sieve. Highly organic soils and peat, meanwhile, can typically be recognized through visual inspection alone, without requiring lab testing.

The fine-grained soils, are subdivided into silts (M) and clays (C) based on their liquid limit and plasticity index. Within the fine-grained category, soils are classified as silts when their liquid limit and plasticity index values fall below the A-line on Casagrande's (1948) plasticity chart (Figure 9). Conversely, if the LL and PI plot above the A-line, the material is classified as clay.

Broadly speaking, the A-line serves to separate clay-like materials from silty ones, and also distinguishes organic from inorganic soils. One notable exception is organic clays (OL and OH), which actually plot below the A-line despite this, their behavior still aligns more closely with lower-plasticity soils. Beyond this split, the silt, clay, and organic groups are further divided based on whether their liquid limit is relatively low (L) or high (H), with 50 serving as the conventional cutoff point separating the two. The main symbols of fine-grained soil groups are shown in Table 7.

A step-by-step procedure for USCS classification of soils, shows a process of elimination of all the possibilities until only the one left indicates the specific classification (Figure 10).

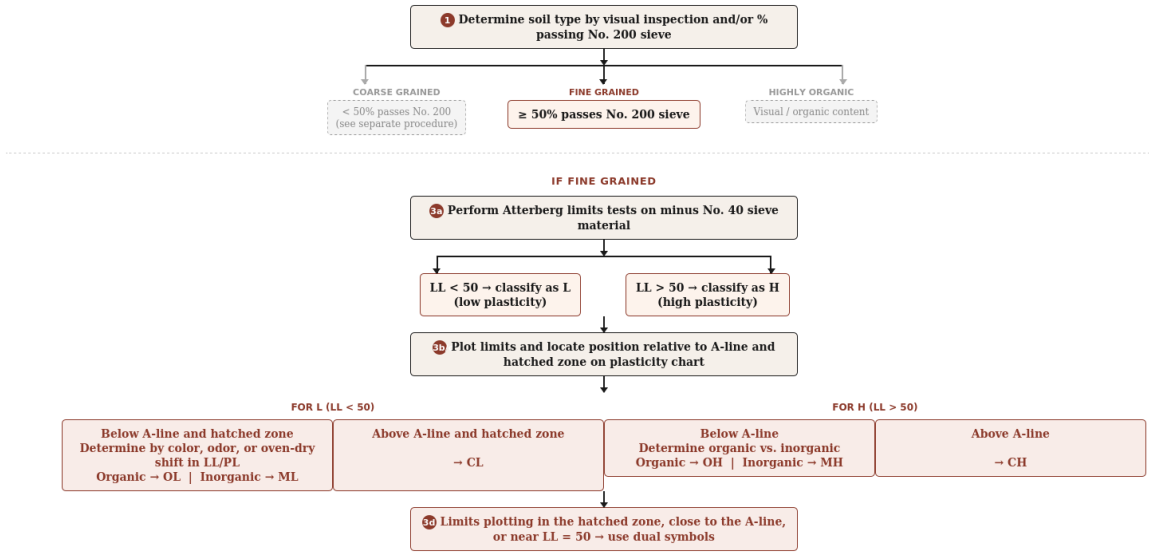


Figure 10 USCS classification procedure- Fine-grained soils.

Table 7 Comparison of fine-grained USCS soil groups, plasticity-chart position, and typical swelling potential.

Symbol	Description	Position on plasticity chart	Typical LL range	Typical swell potential
ML	Inorganic silt, low plasticity	Below A-line	<50%	Low
CL	Inorganic clay, low- to- medium plasticity (lean clay)	Above A-line	20-50%	Low-Medium
MH	Inorganic silt, high plasticity (elastic silt)	Below A-line	≥ 50	Medium
CH	Inorganic clay, high plasticity (fat clay)	Above A-line	Commonly 50-210%	Medium-Very High
OL	Organic silt/clay, low plasticity	Below A-line	< 50%	Low
OH	Organic clay, medium-to-high plasticity	Below A-line	≥ 50	Excluded from expansive-soil studies

In our study, we are going to handle expansive soils classified as CH, as they are amongst the most common types involved in swelling and shrinkage. For that, it is important to know what does a CH classified soil mean and what are its physical characteristics.

2.2 Definition and Characteristics of High-plasticity Inorganic Soils

CH soils are classified in the Unified Soil Classification System as high-plasticity inorganic clays, commonly referred to as fat clays. According to USCS, fat clays have high to very high **Dry Strength**, negligible **dilatancy**, and high **toughness**.

Dry Strength (crushing characteristics): To perform this test, mould a small pat of soil, allow to air dry, then attempt to crush it between thumb and fingers. Soils with high plasticity have high dry strength and vice versa. *CH soils cannot be broken with thumb and hard surface.*

Dilatancy (reaction to shaking): For this procedure, form a pat of soil at or near the liquid limit. Place on the open palm and shake horizontally, then squeeze between fingers. *CH soils show slow or no reaction to the procedure.*

Toughness (consistency near plastic limit): To carry out this test, specimen is hand-rolled on a flat surface (or between the palms) into a thread. This thread is repeatedly folded and re-rolled, gradually losing moisture in the process until it stiffens, loses plasticity, and eventually crumbles, marking the plastic limit. *CH soils show tough thread near the plastic limit.*

Other General Characteristics

Fine-grained soils, especially clay soils, are strongly influenced by the presence of water. The variation of water content gives rise to plasticity and the Atterberg limits are an indication of this influence. *Grain size distribution only rarely is a governing factor in the behavior of fine-grained soils.*

Clay minerals, being relatively small particles, have large specific surfaces, and everything else being equal, you might expect that they would have very active surfaces.

Edge View	Typical Thickness (nm)	Typical Diameter (nm)	Specific Surface (km^2/kg)
Montmorillonite	3	100-1000	0.8
Illite	30	10 000	0.08
Chlorite	30	10 000	0.08
Kaolinite	50-2000	300-4000	0.015

Figure 11 Average values of relative sizes, thicknesses, and specific surfaces of the common clay minerals.

As illustrated in Figure 11, the four primary clay minerals vary significantly in size and specific surface area. Kaolinite represents the largest variety, with edge dimensions averaging around 1 μm, whereas montmorillonite is the smallest, measuring only a few nanometers in thickness. This size discrepancy directly impacts engineering behavior; because montmorillonites are exceptionally small and possess high plasticity indices, they exhibit high activity levels. While sophisticated techniques like differential thermal analysis (DTA) and X-ray diffraction can identify these minerals, Casagrande's plasticity chart offers an equally effective engineering alternative.

As shown in Figure 12, practitioners can identify unknown clay minerals simply by plotting a sample's liquid limit (LL) and plasticity index (PI) and comparing the position against established mineral zones. When a soil sample's Atterberg limits plot well above the A-line and approach the U-line, it typically indicates a high concentration of active clay minerals like montmorillonite. This holds true even for soils classified as sandy clays (CL); if the data points sit near the U-line, montmorillonite remains the dominant mineral within the clay fraction. On Casagrande's plasticity chart, the U-line serves as the empirical upper limit for natural soil plasticity, mathematically defined as:

$$PI = 0.9(LL - 8)$$

Because natural soil data almost always falls below this boundary, any coordinates plotting above the U-line generally signal either highly unusual mineral composition or an error in the laboratory testing process.

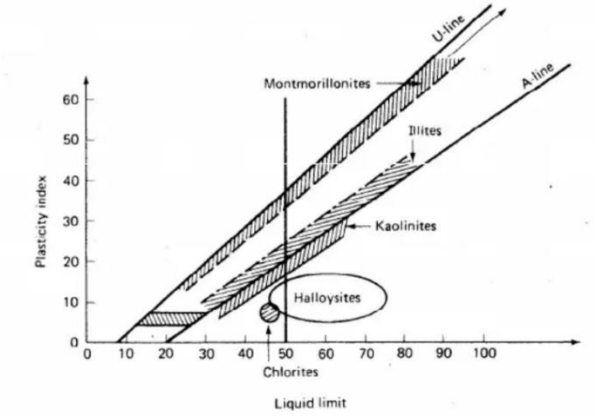


Figure 12 Plasticity Chart showing the typical ranges of clay minerals

Fat clays are cohesive, highly compressible, and their strength behavior is strongly influenced by clay content and confining stress. Dafalla et al. (2020) investigated this directly using a natural high-plasticity, highly expansive clay from the eastern province of Saudi Arabia, mixed with sand at 10%, 20%, and 30% clay content and tested via consolidated-undrained triaxial tests under varying confining pressures. The results showed that increasing the clay content above 10% leads to a decrease in the deviator stress at failure, as shown in Figure 13. However, for the same clay content increasing the confining pressure leads to an increase in the deviator stress at failure.

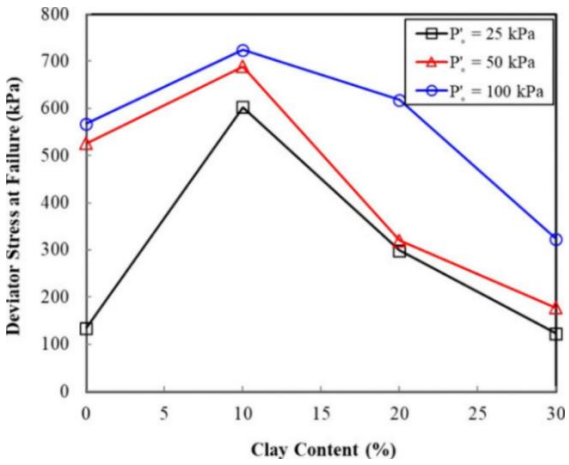


Figure 13 Variation of the deviator stress with clay content at failure with clay content [from Dafalla et al. (2020)]

2.3 Relationship between fat clays and expansive soils

Fat clay refers to a soil classification based on index properties, whereas expansive soil refers to a soil behavior characterized by swelling during wetting and shrinkage during drying. So, what we can say is that CH or fat clay is defined structurally whereas expansiveness is defined on the basis of their behavior.

Therefore, a CH classification does not automatically prove that a soil is expansive, but it indicates that the soil has a higher likelihood of exhibiting expansive behavior compared with low-plasticity soils.

The relationship between fat clays and expansive soils is mainly controlled by clay mineralogy and water sensitivity. CH soils often contain active clay minerals such as smectite or montmorillonite, which have high surface area and strong water adsorption capacity. When these minerals are present in significant amounts, the soil may undergo considerable volume changes as moisture conditions vary. For this reason, many highly expansive soils are classified as CH, especially when they combine high liquid limit, high plasticity index, and active clay mineral content.

Nevertheless, expansiveness should not be evaluated from the CH classification alone. Some fat clays may show moderate or limited swelling if their dominant clay minerals are less active, such as kaolinite or illite, or if moisture and stress conditions limit volume change. Therefore, the classification of a soil as CH should be considered an indicator of possible expansive behavior, while direct swelling tests, mineralogical analysis, and moisture conditions are required to confirm its actual expansiveness as explained in Chapter 1.

Not all fat clays are necessarily highly expansive. CH is necessary-but-not-sufficient for expansiveness.

Vukicevic et al. (2019) proved that, their tested soil was classified as CH under the USCS, yet exhibited only a low-to-moderate swelling potential, with a measured swell deformation of just 2.2% as show in Table 8.

Table 8 Physical characteristics of the soil sample used [from Vukicevic et al (2019)].

LL%	PL%	PI %	Swell %
51	31.5	19.5	2.2

2.4 Factors affecting expansiveness

2.4.1 Mineralogical characteristics of fat clays and their effect

The physical and mechanical properties highlighted previously are fundamentally driven by the mineralogical makeup of fat clays. These soils are primarily composed of 2:1 phyllosilicates, chiefly minerals from the smectite and montmorillonite groups, though illite and kaolinite frequently appear as secondary components.

Quantitative X-ray diffraction (XRD) data reveals that the mineral compositions of fat clays can vary drastically, even when sharing an identical CH classification. For instance, a microstructural analysis by Selvakumar et al. (2024) comparing two distinct expansive soil samples (Sample A and Sample B) revealed that a high volume of smectite is not a strict prerequisite for expansive behavior. Instead, significant swelling can occur with a smaller smectite fraction, provided there is a high enough concentration of clay-sized particles to drive the reaction. The physical characteristics of both samples are shown in Table 9.

The primary distinction between Soil A and Soil B lies in their specific clay mineral assemblages. Soil A is predominantly composed of montmorillonite, which occupies a major portion of its exchange complex, while Soil B is dominated by vermiculite. This mineralogical divergence heavily dictates their respective expansion behaviors and mechanical traits; due to its high montmorillonite content, Soil A exhibits a much greater swelling potential than Soil B. Furthermore, the presence of illite in Soil A enhances its plasticity and water retention capabilities relative to Soil B, which lacks this mineral. For instance, the highly expansive nature of Soil A demands aggressive stabilization to mitigate swelling, whereas the vermiculite-heavy matrix of Soil B requires completely different treatment methodologies.

Table 9 Physical characteristics of soils A and B [from Selvakumar et al. (2024)].

Property	Soil A	Soil B
Specific gravity	2.80	2.66
Free swell index (%)	450	105
Liquid limit (%)	276	74
Plastic limit (%)	33	39
Shrinkage limit (%)	8	10
Plasticity index (%)	243	35
Clay (%)	96	72.5
Silt (%)	4	23.5
Sand (%)	–	4
USCS classification	CH	CH
Maximum dry density (g/cm³)	1.38	1.79
Optimum moisture content (%)	38	19
Mineralogical composition (%)	Montmorillonite: 42–44, Illite: 24–26, Quartz: 14–16, Calcite: 8–10, Feldspar: 2–4	Vermiculite: 46–48, Montmorillonite: 33–34, Quartz: 10–12, Feldspar: 4–6

This supports the conclusion that while smectite/montmorillonite remains the primary driver of expansive behavior in fat clays, the proportion required to produce CH-level plasticity and

swelling is not fixed, and a complete mineralogical characterization is necessary to properly interpret why two fat clays with similar index properties can behave differently.

2.4.2 Mechanical characteristics and their effect

In addition to how confining pressure and clay volume dictate their shear strength, fat clays display high compressibility. Alnmr et al. (2024) investigated this directly through a program of 96 oedometer tests on expansive soil-sand mixtures, examining how sand content, initial degree of saturation, and initial dry unit weight govern compressibility. Higher sand content lowers compressibility, and the reduction becomes more pronounced after 20%. Based on their full test program, they recommend a sand content greater than 30% where reducing the compressibility of a fat clay is the design objective. Figure 14 depicts the effect of different sand percentages on soil swelling under various applied pressures. In general, swelling diminishes as the sand percentage rises to 10 %, with the decrease being more evident at low applied pressure and becoming less noticeable as the stress increases, maintaining nearly constant until 20 %. The lowest swelling can be seen at 30 % sand content, followed by a modest increase in swelling.

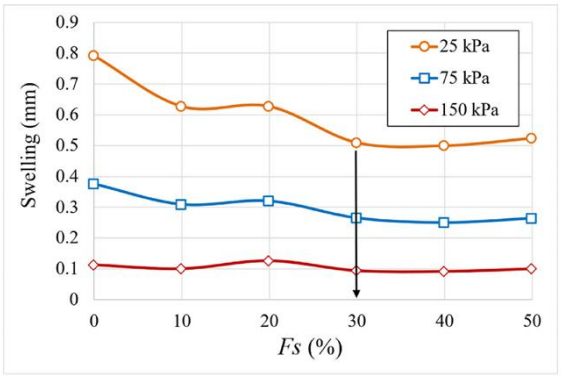


Figure 14 The relationship, at three distinct applied pressures between the swelling and the percentage of sand (Fs%) for formed samples according to the standard Proctor [from Alnmr et al. (2024)]

Furthermore, the findings indicated that elevating the initial dry unit weight simultaneously decreases the permeability and compression index while increasing the recompression index for any fixed sand fraction. This trend is best illustrated by the 50% sand blend in Figure 15; as the dry unit weight rose from 15.3 to 18.4 kN/m³, significant drops occurred in the compression index (Cc) (plummeting by 70%) and the coefficient of volume compressibility (mv) (decreasing by 40%). Consequently, at identical sand concentrations, a denser state restricts both moisture transmission and overall volume change. This behavior stems from tighter particle packing and a minimized void ratio, which collectively restrict the material's susceptibility to deformation when subjected to structural loads.

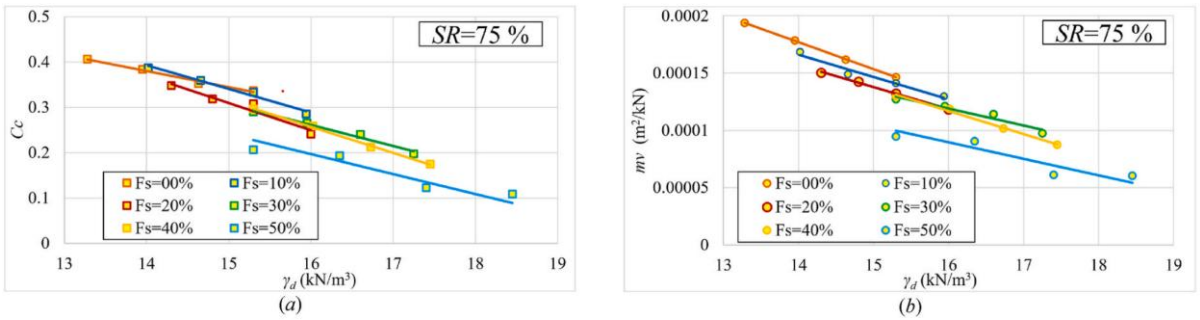


Figure 15 Changes in (a) Cc and (b) mv as a function of initial dry unit weight (γd) for various sand percentages at 75 % initial saturation level [from Alnmr et al. (2024)]

2.4.3 Natural water content

In-situ moisture content is a primary determinant of expansive behavior in fat clays, as it establishes the volume of moisture a soil can still absorb prior to achieving equilibrium. Consequently, this initial state dictates the remaining active swelling potential at any given moment. Rather than being an inherent, static characteristic, natural water content varies continuously. As a result, its impact on soil expansiveness is a dynamic variable rather than a fixed constant.

Irrespective of high swelling potential, if the moisture content of the clay remains unchanged, there will be no volume change; and structures founded on clays with constant moisture content will not be subject to movement. When the moisture content of the clay is changed, volume expansion, will take place. Complete saturation is not necessary to accomplish swelling. Slight changes of moisture content, in the magnitude of only 1 to 2 percent, are sufficient to cause detrimental swelling.

For instance, very dry clays with natural moisture content below 15 percent usually indicate danger. Such clays will easily absorb moisture to as high as 35 percent with resultant damaging expansion to structures. Conversely, clays with moisture contents above 30 percent indicate that most of the expansion has already taken place and further expansion will be small.

2.4.4 Dry Density

Directly related to initial moisture content, the dry density of the clay is another index of expansion. Soils with dry densities in excess of 110 lb/ft^3 generally exhibit high swelling potential. Dry density in soils is the mass or weight of dry soil solids per unit total volume of the soil, meaning the volume includes both solids and voids but excludes the mass of water. On the other hand, initial moisture content is the amount of water present in a material at the start of an experiment, process, or treatment.

Chi et al. (2023) proved that the swelling pressure of a CH soil taken from the Heifei (China) decreases with the increase of the initial moisture content and increases with the increase of the dry density (Figure 16). The average swelling pressure development rate increases with increasing dry density(ρ_d) and decreases with increasing initial moisture content(ω_0).

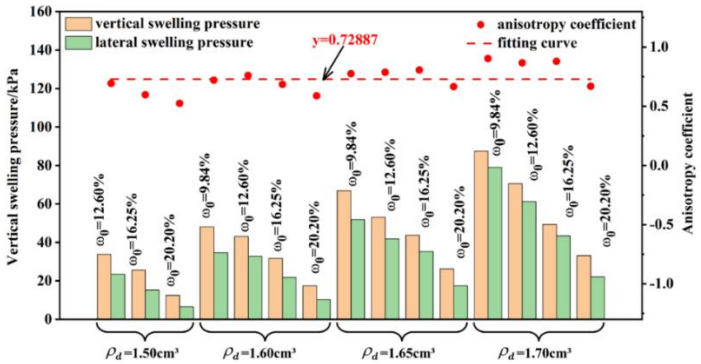


Figure 16 Comparison of swelling pressures in vertical and lateral directions [from Chi et al. (2023)]

2.4.5 Confining pressure

The magnitude of swell-shrink behavior in a fat clay is also strongly governed by the confining pressure (overburden stress or applied surcharge) acting on the soil. This is because swelling and shrinkage are fundamentally a contest between the internal volume-change tendency of the clay and the external pressure resisting it; lower confining pressure allows more of that tendency to manifest as actual deformation, while higher confining pressure suppresses it.

For example, in Cheng et al. (2024), under low confining pressure, specimens showed peak stress followed by stress drop and stabilization, underwent shear shrinkage, and the soil structure was prone to failure. Under high confining pressure, the stress–strain curve became nonlinearly increasing, specimens showed shear dilation, and the soil was less prone to failure.

2.4.6 Climate/wet-dry cycles

Beyond a single measurement of natural water content, the *cyclical* nature of moisture exposure, driven by seasonal climate variation, is itself an independent factor governing fat clay behavior, since repeated wetting and drying progressively alters the soil's structure and mechanical response in ways a single wetting event cannot.

Shafqat et al. (2025) used natural, untreated CH, CL, and ML soils, explicitly stating that natural CH, CL, and ML soils, distinguished by their chemical composition and plasticity, were subjected to a meticulously designed experimental program, with specimens remolded at different compaction states and then subjected to repeated W-D cycles.

Their research indicated that desiccation cracking in both CL and CH soils begins during the first wetting-drying (W-D) cycle, accelerates sharply during the second, and stabilizes into a peak cracking state by the third cycle. Over these sequential cycles, the fractures evolve from superficial surface fissures into deeper structural cracks. Under identical, untreated conditions, the CH soil displayed distinct behavior compared to the other groups. Due to its 2:1-layered clay minerals and intense shrink-swell potential, the CH soil suffered heightened desiccation cracking at elevated initial moisture contents, even when prepared at the same initial dry density. The authors credited this response to the clay's mineralogy and microstructure, which govern the internal stresses generated by moisture fluctuations. Furthermore, the study verified that cyclic environmental exposure alone, without any added chemical stabilizer, directly impairs mechanical performance by reducing soil strength and increasing compressibility as W-D cycles progress.

A separate, earlier study by Tang et al. (2020) working directly and explicitly with a fat clay (CH) examined the role of soil suction in this same degradation process. They found that as the number of W-D cycles increases, the difference in shear strength between drying and wetting paths becomes less significant, attributing this to reduced hydraulic hysteresis with repeated cycling, and confirmed that W-D cycles result in irreversible volume change, with cumulative volumetric strain increasing at a decreasing rate as the number of cycles increases.

Overall, the effect of wet-dry cycling on CH soil is two-stage: suction initially strengthens the soil during drying, but repeated drying leads to crack development that eventually overcomes suction and reduces strength.

CHAPTER 3 — Traditional Chemical Stabilization Techniques

3.1 Lime Stabilization

3.1.1 Introduction

To prevent failures, engineers rely on a few foundational strategies: relocating the project to a safer site, replacing poor soil with superior-quality materials, adapting structural designs to existing ground conditions, or chemically stabilizing the ground. Among these, soil stabilization has emerged as a preferred method. Treating clay with cement or lime has a long history of enhancing soil workability and strength. Lime stabilization specifically refers to blending soil

with burned limestone derivatives, namely calcium oxide or calcium hydroxide [Bell, 1989]. It is widely considered among the most efficient chemical additive for expansive clays because it initiates a series of rapid and long-term reactions such as cation exchange, flocculation, carbonation, and pozzolanic bonds. Although the complex chemistry behind these interactions can be difficult to model, lime stabilization remains a highly successful and widely implemented geotechnical tool.

3.1.2 Stabilization mechanism

3.1.2.1 Types of lime used

Lime used in geotechnical stabilization of expansive CH soils is not a single material but a family of calcium-based products that differ in chemical composition, reactivity, and field application method. The two main traditional types encountered in the literature are **quicklime** and **hydrated lime**.

Quicklime (CaO)

Quicklime (CaO) is a compound of one atom of calcium and one atom of oxygen that is a white or greyish-white solid, produced in large quantities by roasting calcium carbonate so as to drive off carbon dioxide. It is produced by the calcination of limestone at high temperatures, yielding a fine white powder (Figure 17), that is highly reactive upon contact with water. When quicklime is mixed into a wet soil, it undergoes an exothermic hydration reaction ($CaO + H_2O \rightarrow Ca(OH)_2$), releasing significant heat, $\Delta H^0 = -82$ kJ/mol, which simultaneously reduces the soil's natural moisture content making it the preferred lime type when the primary objective is to dry an overly wet soil before further treatment.

Hydrated Lime ($Ca(OH)_2$)

Hydrated lime, or calcium hydroxide, is a soft, white powder (Figure 18) produced commercially by controlled addition of water to quicklime, yielding a stable powder that no longer undergoes the exothermic reaction in the field, making it safer and easier to handle and transport. Because it is already chemically bound with water, it does not provide the immediate drying benefit of quicklime.



Figure 17 quick lime



Figure 18 hydrated lime

3.1.2.2 Mechanism of lime-soil reaction

The stabilization of CH expansive soils with lime is not governed by a single reaction but by a sequence of five interrelated physico-chemical processes: hydration, cation exchange, flocculation and agglomeration, pozzolanic reaction, and also carbonation. These reactions differ in their onset timing, duration, and contribution to soil improvement, and their relative importance depends on lime dosage, soil mineralogy, curing temperature, and time. A broad consensus in the literature attributes improvements in lime-stabilized soils to this four-reaction framework, with the first three classified as short-term modification reactions and the pozzolanic reaction as the long-term stabilization mechanism responsible for permanent strength gain [Al-Mukhtar et al. (2012)].

Hydration

When hydrated lime $Ca(OH)_2$ is introduced into a CH soil, it dissolves in the pore water, releasing calcium ions (Ca^{2+}) and hydroxyl ions (OH^-) into solution. When quicklime (CaO) is used instead, an additional preliminary step occurs: the exothermic hydration reaction $CaO + H_2O \rightarrow Ca(OH)_2$ takes place first, generating heat that simultaneously reduces the soil's natural moisture content, before the dissolved $Ca(OH)_2$ begins interacting with the clay minerals. This initial hydration step, whether pre-formed commercially or generated in-situ, is the prerequisite for all subsequent reactions, since it is the dissolved Ca^{2+} and OH^- ions that drive each downstream process.

Cation Exchange

Almost immediately upon dissolution, the Ca^{2+} ions released by lime begin displacing the monovalent cations (primarily Na^+, K^+, and H^+) that are adsorbed onto the negatively charged surfaces of the CH clay minerals. In fat clays dominated by montmorillonite, this exchange is particularly significant because montmorillonite carries the highest cation exchange capacity (CEC) of the common clay minerals. As Ca^{2+} replaces Na^+ and K^+, the diffuse double layer surrounding each clay particle contracts: the divalent nature of Ca^{2+} allows each ion to neutralize twice the negative surface charge of a monovalent cation. Consequently, fewer cations are needed to balance the clay surface charge, leading to compression of the diffuse double layer and a reduction in the thickness of the surrounding water film. This compression directly reduces the interparticle repulsion that drives osmotic swelling in montmorillonite-rich CH soils. Critically, the effectiveness of cation exchange is itself dependent on the CH soil's clay mineralogy: montmorillonite-rich soils have the highest CEC and therefore respond most strongly to this reaction, while kaolinite-dominant assemblages respond least.

Flocculation and Agglomeration

As Ca^{2+} ions compress the double layer and reduce interparticle repulsion, adjacent clay particles (previously held in a dispersed, face-to-face orientation) begin to approach and aggregate into larger clusters through edge-to-face contacts, a process termed flocculation. These flocs then agglomerate into coarser, more granular assemblages, fundamentally transforming the soil's texture from a cohesive, sticky mass to a more friable, workable material. This microstructural transformation is detectable at the macroscopic level as a shift in compaction behavior: the maximum dry density typically decreases and the optimum moisture content increases as the soil's particle arrangement changes from dispersed to flocculated. For CH soils specifically, this is the reaction responsible for the immediate improvement in workability within hours of lime application, before any pozzolanic reaction has had time to develop. The flocculated fabric also has a lower specific surface area available for water adsorption, further contributing to reduced swell potential in the short term.

A comparative study by Al-Mukhtar et al. (2012) that used the FoCa (soil classified as fat clay and is highly expansive) shows that flocculation is observed on the treated samples; the number of clay layers per particle doubled, and individual layers disappear (rings in Figure 19.a and Figure 19.b). This behavior is explained by the calcium cation exchange in smectite, which reduces the swelling of the inter-lamellar space and facilitates the aggregation of layers. These observations demonstrate and can explain the changes in the geotechnical properties: the flocculation (higher number of layers per particle) induces a reduction in plasticity and an increase in the mechanical resistance of the treated FoCa. Moreover, the behavior of stacked layers is less flexible (plastic) than a single layer.

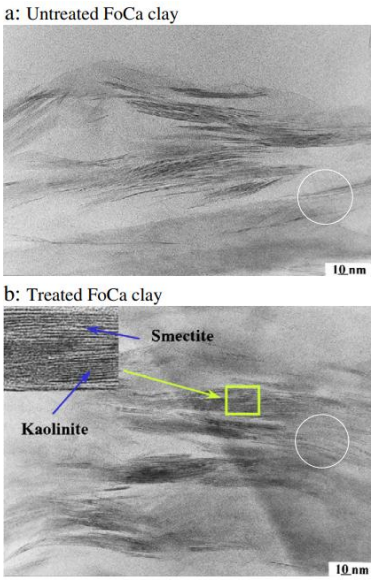


Figure 19 High-resolution TEM images of untreated and lime-treated FoCa clay (a, b) faces section. a: Untreated FoCa clay. b: Treated FoCa clay [from Al-Mukhtar et al. (2012)]

Pozzolanic Reaction

The pozzolanic reaction is the dominant long-term stabilization mechanism and is responsible for the permanent strength gain that distinguishes lime stabilization from simple soil modification. In the highly alkaline environment (pH ≥ 12) created by lime addition, silica (SiO_2) and alumina (Al_2O_3) begin to dissolve from the surfaces and edges of the CH clay minerals, particularly from the silicate tetrahedra and aluminate octahedra of the montmorillonite and illite lattices. These dissolved species then react with the available Ca^{2+} and OH^- ions to form stable cementitious compounds: calcium silicate hydrate and calcium aluminate hydrate, and in some systems calcium aluminate silicate hydrate.

A simplified qualitative view of typical soil-lime reactions is as follows:

$$Ca(OH)_2 \rightarrow Ca^{2+} + 2(OH)^-$$

$$Ca^{2+} + 2(OH)^- + SiO_2(clay\ silica) \rightarrow C-S-H$$

$$Ca^{2+} + 2(OH)^- + Al_2O_3(clay\ alumina) \rightarrow C-A-H$$

Where, C=CaO, A=Al_2O_3, H=H_2O, S= SiO_2

These gel-like reaction products coat and bind the clay particles together, progressively filling inter-aggregate pores and creating a stiffer, less permeable soil matrix.

Unlike cation exchange and flocculation, the pozzolanic reaction is time-dependent and temperature-sensitive: it begins slowly, accelerates with curing time and temperature, and can continue for months or even decades after initial treatment. This is why lime-stabilized CH soils continue gaining strength well beyond the initial 28-day curing period commonly tested in the laboratory. The reaction also consumes lime progressively, meaning an insufficient initial lime dosage below the lime fixation point, can exhaust the available Ca^{2+} before meaningful pozzolanic product formation occurs, leaving only the short-term cation exchange and flocculation benefits.

Carbonation

Carbonation, occurs when atmospheric CO_2 penetrates the lime-treated soil and reacts with the available Ca $(OH)_2$:

$$Ca(OH)_2 + CO_2 \rightarrow CaCO_3 + H_2O$$

The resulting calcium carbonate ($CaCO_3$) precipitates within the soil pores, initially contributing to pore-filling and a denser microstructure. However, carbonation is generally considered a deleterious long-term process in lime-stabilized CH soils, because it competes directly with the

pozzolanic reaction for the available $Ca(OH)_2$, lime consumed by carbonation is lime unavailable for calcium silicate hydrate and calcium aluminate hydrate formation.

3.1.3 Effect of lime stabilization on the different properties

3.1.3.1 Effect on index properties

The most immediate and consistently documented effect of lime addition to CH soils is a systematic modification of the Atterberg limits, specifically a reduction in plasticity index (PI), and a simultaneous increase in plastic limit (PL). These changes reflect the cation exchange and flocculation reactions discussed in the previous section and they occur rapidly often within the first few hours of lime contact, before any pozzolanic reaction has developed. Because the LL, PL, and PI directly govern a soil's classification on the Casagrande plasticity chart, sufficient lime addition can shift a CH-classified soil into a lower-plasticity domain entirely, which is reflected in numerous experimental studies across different regions and lime dosages.

Across three different soil studies by Driss et al. (2022), Nugroho et al. (2021) and Salih & Shafiqu (2024) with samples differing in origin and preparation, but all tested under standard Atterberg-limit procedures on fine fractions and with staged lime addition we can see the effect of lime addition on LL, PL and PI.
Despite differences in sample origin and operative conditions, the effect of lime on the Atterberg limits was directionally similar in the most important way: plastic limit increased and plasticity index decreased in all three studies, while liquid limit was variable. This pattern is consistent with lime-driven flocculation and agglomeration of clay particles since flocculation and agglomeration have an influence on the texture of expansive clay soils by making clay particles clump together to form bigger ones.
For instance, in Driss et al. (2022), LL rose from 52.64% to about 62%, PL rose from 21.18% to 39.41%, and PI fell because PL increased faster than LL (Figure 20).
On the other hand, in Nugroho et al. (2021) and Salih & Shafiqu (2024), LL declined overall, while PL increased, and PI decreased.

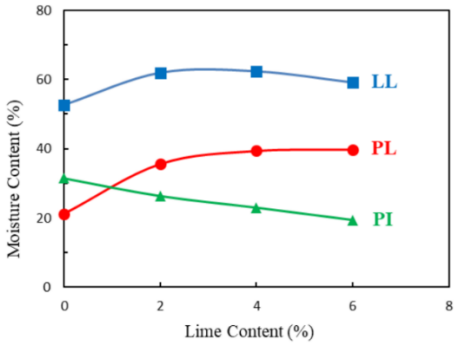


Figure 20 Influence of lime content on the Atterberg limits [from Driss et al. (2022)]

3.1.3.2 Effect on swelling potential and swelling pressure

Adding lime lowers swelling potential and usually swelling pressure in CH Soils. The reduction is attributed to cation exchange, flocculation-agglomeration, and pozzolanic reactions, which replace weaker monovalent cations with calcium, reduce diffuse double-layer effects, and form cementitious products that limit water uptake and expansion [Driss et al. (2022)]. Several studies also report that curing time strengthens this benefit because pozzolanic reactions are time-dependent [Driss et al. (2022); Soltani et al. (2017)].

The main caveat is that swelling pressure does not always decrease monotonically in every test setup. One comparative study found swell potential dropped by 42.5% at 4% lime, but measured

swelling pressure increased from 210 to 320 kPa during inundation, likely because cementitious products stiffened the specimen against compression [Phanikumar et al. (2015)].

Other caveats are that low lime contents can be insufficient in some soils, high-suction/low-stress conditions can still show serious swelling after stabilization, and wetting–drying cycles can erode the initial benefit [Al-Taie et al. (2021); Güney et al. (2007)].
In short, for CH soils, adding lime generally causes a large drop in swelling potential and a usual, but more test-dependent, drop in swelling pressure. The strongest reductions are typically reported around 3–9% lime with adequate curing [Negawo et al. (2019); Salih & Shafiqu (2024)].

3.1.3.3 Effect on strength and compressibility

Across the literature, adding lime to CH expansive soils consistently increases strength and reduces compressibility, with the biggest gains usually appearing after curing and at moderate lime contents rather than unlimited addition [Driss et al. (2022); Jazi et al. (2024)]. The main caveat is that the exact optimum lime content varies by soil and test condition, and some studies report diminishing returns or more brittle behavior at higher dosages [Dhar et al. (2019); Umar et al. (2025); Negawo et al (2019)]

Lime treatment raises unconfined compressive strength in CH expansive clays, and the gain usually increases with curing time because early flocculation is followed by pozzolanic bonding [Nugroho et al. (2021)]. In one CH clay study, UCS rose from 354 to 572 kPa with 6% lime after 1 day, then increased further after curing [Driss et al. (2022)]. In another expansive swelling clay, moving from 5% to 7% lime more than doubled pre-failure stiffness and ultimate strength, indicating that 5% was insufficient for that soil while 7% performed effectively [Negawo et al. (2019)].

However, strength improvement is not unlimited. Several studies report an optimum lime window, after which additional lime gives smaller gains or even reduces UCS [Nugroho et al. (2021); Dhar et al. (2019)]. Recent work on expansive clay also shows cohesion rising with lime content and curing, with 9% lime outperforming 3% and 6% for apparent cohesion [Almuaythir et al. (2025)]. Overall, microstructural explanations are consistent across the literature: lime increases pH, drives cation exchange and flocculation first, then forms CSH/CAH cementitious products that bind particles and strengthen the soil mass.

Lime treatment also reduces compressibility and settlement-related indices in expansive CH soils. Salih & Shafiqu (2024) study reports the compression index falling from 0.581 to 0.193 and the swelling index from 0.070 to 0.030 at 9% lime, alongside a drop in swelling percentage from 18.77% to 6.03%. Jazi et al. (2024) study found that lime percentage had the strongest direct effect on compression index, with decreases of up to 61.4%, while stress history also mattered for the measured response. Another recent study observed that lime alone can initially slow consolidation at low pressures, interpreted as a stiffer, more compression-resistant structure forming during early stabilization [Almuaythir et al. (2025)].

3.1.4 Performance under Meteorological events

Laboratory-measured improvements in strength, compressibility, and swell potential represent the performance of lime-stabilized CH soils under controlled, static conditions. In the field, however, these soils are continuously exposed to meteorological events.

Wetting–Drying Effects

The wetting–drying evidence shows that lime-treated expansive clay usually survives repeated cycling far better than untreated soil. Treated high-plasticity clay retains integrity through all conditioning phases, whereas untreated specimens collapse early. Nabil et al. (2019) showed that

performance under wetting–drying improves once lime dosage reaches a stabilization range rather than a mere modification range, with behavior reported as satisfactory above about 4% lime and many soils resisting all 12 cycles at higher contents.

A recurring nuance is that strength under wetting–drying does not always decline monotonically from the first cycle. An expansive clay treated with 6% lime, showed that strength in the drying state increased with curing time and wetting–drying cycles, consistent with ongoing pozzolanic hardening [Jha & Sharma (2021)]. Another wetting–drying study found compressive strength often rose through the first three cycles, then declined by five cycles in longer-cured specimens as bonds loosened and moisture content rose [Kamaruddin et al. (2020)].

Freeze–Thaw

Freeze–thaw causes the most severe short-term deterioration in lime-stabilized CH-type expansive soils. Chou et al. (2026) reports that freeze–thaw produced the worst damage among the tested durability paths because freezing caused substantial soil swelling. A closely aligned freeze–thaw study by Hotineanu et al. (2015) found that crack formation from ice lenses was more severe in high-plasticity bentonite than in low-plasticity kaolinite, which is directly relevant to CH soils. Freeze–thaw also reduces direct-shear durability mainly by lowering cohesion, even when friction angle changes only slightly. It can cause strength loss in natural soil, but lime substantially reduces this loss.

Resistance improves when the lime-treated matrix is more mature. Longer curing markedly increases UCS before freeze–thaw exposure. For example, in a study by Liu et al. (2019), freeze–thaw reduced UCS by enlarging macropores, but the effect became negligible at more than 9% lime.

3.1.5 Field Applicability of Lime Stabilization

Site Conditions Governing Field Success

The effectiveness of lime stabilization in the field is not guaranteed simply by selecting the dosage defined in the laboratory, but it is governed by a set of site-specific conditions that can either amplify or completely nullify the expected performance.

Success in CH soils starts with **soil suitability**. Lime treatment is very effective in medium- to high-plasticity clays, and CH soils with PI well above 10 and fines above 25% fit the standard suitability envelope [Firoozi et al. (2017); Umar et al. (2025)].

Success also depends on the **right dosage**. The right dosage is the minimum effective lime content that reaches sustained reactivity without excess. The standard starting point is the initial lime consumption or chemical fixation point: the minimum lime content that raises the soil-lime pH to about 12.4, which is needed to dissolve silica and alumina and sustain pozzolanic reactions [Regasa et al. (2023); Cherian & Arnepalli (2015)]. That starting point is only a screening dosage, not the final design dosage. Several studies show that pH-based methods can underestimate the optimum for expansive clays, especially in presence of curing, organics, or unusual mineralogy matter [Babanas et al. (2025); Cherian & Arnepalli (2015); Al-Taie et al. (2018)].

For CH soils, the final “right dosage” is the content that meets the project objective: lowering plasticity, suppressing swell, and delivering strength after curing. Different tests can point to different optima, so dosage should be checked against UCS, swell, shrinkage, and workability rather than pH alone.

Field success further depends on **curing control**. Curing control determines whether lime-treated CH soils gain durable strength or lose it in the field. Curing is the period after mixing when lime reactions continue from rapid flocculation into slower pozzolanic cementation, which is why

strength keeps increasing with time [Driss et al. (2022); Al-Mohammedi (2024)]. For example, a study on an Ethiopian road used a two-day mellowing period after mixing, then tested specimens after 7, 14, and 28 days, reflecting the need to separate short-term mixing effects from later strength gain [Regasa et al. (2023)]. In CH soil specifically, curing time changes the measured performance enough to affect design decisions because strength develops over time, so a 1-day or 7-day test can understate the later in-service capacity [Naveed et al. (2024)].

Curing temperature also matters: higher temperatures accelerate pozzolanic reactions and produce faster strength gain, although the optimum depends on soil and additive system [Nasrizar et al. (2010); Al-Mohammedi (2024)].

For CH expansive clay, compaction at OMC or slightly wet of OMC performed better than dry-side placement during thermal curing. For that compacting expansive clay at OMC or slightly above OMC and curing at elevated temperature is better to obtain maximum benefit from lime stabilization, because the curing response itself depends on that starting moisture state [Nasrizar et al. (2010)].

Limitations of Field Applicability

Carbonation and leaching specifically limit field durability when curing is short or drainage is poor. Carbonation is recognized as deleterious because it consumes lime and carbonates cementitious phases, weakening aggregate bonding and shear strength [Padmaraj & Arnepalli (2023)]. Accelerated studies show carbonation lowers compressive strength and stiffness, while leaching dissolves cementitious gels; short-cured or under-dosed soils are most vulnerable [Padmaraj & Arnepalli (2024)].

Sulfate-bearing sites are the most serious applicability constraint. When sulfate concentrations exceed a certain concentration, lime addition can trigger the formation of ettringite (calcium-aluminate-trisulfate-hydrate), a highly expansive crystalline mineral that forms when Ca^{2+} ions released by lime react with alumina dissolved from the clay minerals and sulfate ions present in the pore water. Ettringite formation causes volumetric expansion that can exceed the original swelling potential of the untreated CH soil, leading to structural failure that is more severe than if no treatment had been applied at all. A practical safe lower limit of about 3,000 ppm soluble sulfate has been validated for some soils, provided additional sulfate does not later migrate into the treated layer [Little et al. (2007)].

Additionally, surface-applied or shallow-incorporated lime does not reliably treat deep CH subgrade because lime effects are usually confined to a thin layer below the application depth. In high-clay field soils, surface-applied lime has often shown significant effects only to about 5–10 cm even after years. Where lime was incorporated into the top 5 cm, its chemical influence extended only about 2.5 cm deeper, for a total affected depth of about 7.5 cm [Nunes et al. (2019)]. The same shallow pattern appears in another profile-monitoring study: residual lime remained in the top 7.5 cm, while soil below stayed acidic, showing limited downward alkalinity movement even after surface treatment [Hume et al. (2023)].
For CH-like expansive subgrades in field trials, stabilization is therefore usually constructed as a mixed layer of specified thickness rather than expecting lime to diffuse deeply on its own [Pokkunuri et al. (2023)].

3.1.6 Environmental Impact

Lime stabilization of CH expansive soils is environmentally dominated by upstream lime manufacture and then partly offset by carbonation during use; the main facets are production burdens, use-phase greenhouse-gas and durability effects.

Production Burdens

For both quicklime and hydrated lime, the largest environmental impact is climate forcing from calcination, not site mixing or haulage [Benghazi et al. (2024); Simoni et al. (2022)]. Quicklime production emits about 1.10-1.18 t CO_2-eq per tonne, with calcination alone contributing about 1134 kg CO_2-eq per tonne on average [Wu et al. (2023)].

In the lime industry, CO_2 emissions from thermal calcination of $CaCO_3$ come from three distinct sources. The largest share, roughly 68%, is process CO_2 (the CO_2 chemically bound in the calcium carbonate itself), released as it thermally decomposes into CaO. Fuel combustion used to reach calcination temperatures accounts for about 30%, and the remaining 2% comes from the electricity consumed during production [Simoni et al. (2022)]. However, for hydrated lime, emissions from the hydration step are negligible relative to calcination.

Benghazi et al. (2024) likewise classify lime among the high-carbon conventional stabilizers, estimating lime at roughly 1.0-1.8 t CO_2 per tonne and energy use at 20-50 kWh per tonne.

Raw-material extraction adds dust, blasting impacts, and transport emissions, but these are smaller than kiln-stage impacts [Benghazi et al. (2024); Wu et al. (2023)].

Use-Phase Effects

In expansive-soil applications, a key environmental benefit is CO_2 reabsorption by carbonation. Moore et al. (2024) shows that accelerated carbonation can achieve 100% lime carbonation with gaseous CO_2, versus mean carbonation of 60% with solid and 40% with aqueous CO_2 sources. Those carbonated lime-treated soils also showed about 50% higher UCS after 7 days and better wetting-drying durability than untreated lime-treated controls, so sequestration and engineering performance can improve together.

However, that benefit has limits. Campo et al. (2021) suggest average use-phase carbonation recovers only 23-33% of calcination emissions across current markets, so carbonation usually partly offsets rather than cancels production emissions.

In lime-stabilized expansive soil specifically, carbonation depth increases with time, temperature, and CO_2 concentration. Carbonation partly restores expansive potential rather than simply improving performance across all metrics. At a given depth, swell recovery increases with carbonation time, and lower pH tracks higher free swell ratio, linking expansive behavior directly to carbonation extent. The mechanism is the conversion of portlandite to calcium carbonate, which consumes available lime; carbonation of calcium silicate hydrate or other secondary products can further weaken the original stabilization chemistry.

Thus, accelerated carbonation is the clearest route in the literature for coupling CO_2 uptake with early mechanical gain, but it is not universally beneficial across all soils or durations. [Moore et al. (2024)].

Field-Scale and Non-CO_2 Impacts

At project scale, environmental burdens are strongly driven by lime dosage and treated volume. In an LCA of consolidation of expansive-soil slopes, lime production contributed 65.22% of total CO_2 emissions for the lime stabilization technique, and increasing lime content by 1% raised total energy use by 8.27% and CO_2 emissions by 13.16% [Zhang et al. (2019)].

Non-CO_2 impacts are less well quantified for CH expansive soils, but the broad literature identifies several. Lime quarrying and processing generate dust and local air pollution [Benghazi et al. (2024)]. Lime production also contributes to broader environmental categories tied to anthropogenic CO_2, including global warming and ocean acidification [Campo et al. (2021)].

Lime stabilization also creates a trade-off between durability and environmental burden. Lime improves plasticity, swell behavior, strength, and modulus of CH soils, which can extend service life and reduce maintenance frequency [Bell (1996)]. But if carbonation progresses unfavorably, some swell-control benefit can erode over time.

3.2 Cement Stabilization

3.2.1 Introduction

Alongside lime, Ordinary Portland Cement (OPC) represents the second pillar of traditional chemical stabilization for expansive soils. Cement stabilization works by mixing cement directly into the soil, where hydration reactions generate cementitious products that bind adjacent soil particles together. The resulting matrix improves the treated soil's strength, stability, and long-term durability. Unlike lime whose long-term stabilization mechanism depends fundamentally on the availability of reactive silica and alumina dissolved from the soil's own clay minerals, cement carries its own cementitious compounds and undergoes hydration largely independently of the host soil's mineralogy. This makes cement a more universally applicable binder in principle, but its interaction with high-plasticity clay soils is more complex and nuanced than its behavior in granular soils for which it was originally developed.

3.2.2 Stabilization Mechanism

3.2.2.1 Type of cement used

OPC cement is the traditional cement used for CH soils. OPC is made from clinker produced by burning limestone, clay or other siliceous materials, and iron- and alumina-bearing materials, then grinding that clinker with a small amount of gypsum to control setting. Its main clinker phases are **tricalcium silicate**, **dicalcium silicate**, **tricalcium aluminate**, and **tetracalcium aluminoferrite**, and their proportions control setting and strength development.

OPC is centered on high CaO, then SiO_2, with smaller Al_2O_3 and Fe_2O_3 fractions as shown in Table 10. The major clinker compounds are the phases that matter most for stabilization behavior: tricalcium silicate hydrates rapidly and drives early strength, dicalcium silicate gives its main contribution after 7 days and longer, tricalcium aluminate hydrates quickly and generates heat with limited strength contribution, and tetracalcium aluminoferrite is comparatively less reactive. Modern characterization papers also note that OPC phases contain minor ions such as Mg, Na, K, and S in solid solution rather than being perfectly pure compounds [Zhao et al. (2021)].

Table 10 Chemical constitutions of ordinary Portland cement

Component	Amount (%)
Lime (CaO)	60-67
Silica (SiO_2)	17-25
Alumina (Al_2O_3)	3-8
Iron oxide (Fe_2O_3)	0.5-6
Magnesia (MgO)	0.1-4
Sulphur trioxide (SO_3)	1-3
Soda and/or Potash (Na_2O+K_2O)	0.5-1.3

In the stabilization techniques, the cement actually used is usually ordinary general-purpose OPC, commonly at about 8–12% of dry soil mass, named ASTM C150 Type I / Grade 42.5 N OPC.

Type II and Type V can also be used but shows up most clearly in studies of sulfate-affected soils, not as a universal cement for all CH expansive soils.

3.2.2.2 Mechanism of cement-soil reaction

The stabilization of CH expansive soils with OPC proceeds through the same four-stage framework as lime: hydration, cation exchange, flocculation and agglomeration, and pozzolanic reaction, but with a fundamental mechanistic difference.

Hydration

Upon mixing OPC with a CH soil, the cement particles come into contact with the available pore water and begin hydrating immediately. The two calcium silicate phases, tricalcium silicate and dicalcium silicate, are the primary drivers of cementitious product formation. Tricalcium silicate hydrates rapidly, producing calcium silicate hydrate, calcium aluminate hydrate gels and calcium hydroxide and this is known as portlandite, within the first hours to days; dicalcium silicate hydrates more slowly, contributing to long-term strength gain over weeks and months. The tricalcium aluminate phase hydrates extremely rapidly, more so than any other clinker compound, and in the presence of gypsum reacts to form ettringite, a needle-like crystalline product that contributes to early stiffening. The tetracalcium aluminoferrite plays a comparatively minor role.

Together, these reactions produce two critical outputs for soil stabilization: calcium silicate hydrate and calcium aluminate hydrate gels that bind soil particles together, and $Ca(OH)_2$ that drives subsequent cation exchange and pozzolanic reactions in the clay matrix.

Critically for CH soils specifically, the hydration reaction consumes a significant portion of the available pore water, which has a direct drying effect on the soil matrix, reducing the natural water content and stiffening the clay even before cementitious bonding develops.

Cation exchange

The $Ca(OH)_2$ produced during hydration of the calcium silicates dissolves in the pore water, releasing Ca^{2+} and OH^- ions into solution, exactly as in lime stabilization. These Ca^{2+} ions displace monovalent cations (Na^+, K^+, H^+) adsorbed on the negatively charged surfaces of the CH clay minerals (Figure 21), compressing the diffuse double layer and immediately reducing the liquid limit, plasticity index, and swell potential of the CH soil. This reaction is rapid occurring within hours of cement addition and is responsible for the immediate workability improvement observed. Although the mechanism is identical to that of lime stabilization, the amount of $Ca(OH)_2$ generated by cement hydration is proportional to the cement's silicates content and is therefore fixed by the cement's composition rather than adjustable by the practitioner, unlike lime, where the practitioner directly controls the $Ca(OH)_2$ dosage.

Flocculation and Agglomeration

As Ca^{2+} ions compress the diffuse double layer surrounding CH clay particles, interparticle repulsion decreases and the particles aggregate into coarser, more granular flocs through edge-to-face contacts (Figure 21.b), identical in mechanism to the flocculation described in lime stabilization (Section 3.1.2.2). This transformation shifts the soil's texture from cohesive and plastic to more friable and workable, reduces maximum dry density, and increases optimum moisture content. For CH fat clays, this flocculation effect is particularly pronounced given the high specific surface area of montmorillonite, which offers more surface sites for Ca^{2+} adsorption and double-layer compression than lower-plasticity clays.

Pozzolanic Reaction

The long-term stabilization mechanism in OPC-treated CH soils is the pozzolanic reaction, which proceeds through the same pathway as in lime stabilization: Ca^{2+} and OH^- ions dissolving silica and alumina mineral surfaces, then forming calcium silicate hydrate and calcium aluminate hydrate gels that progressively cement the clay soil matrix (Figure 21.c). However, in OPC

stabilization, this reaction has two simultaneous sources of Ca^{2+}: the $Ca(OH)_2$ generated by cement hydration (identical to lime's direct supply), and the additional Ca^{2+} released as tricalcium silicate and dicalcium silicate continue hydrating over time. This dual source accelerates both the onset and the intensity of pozzolanic product formation compared to lime alone, which is one reason OPC-stabilized CH soils typically achieve higher early compressive strength than lime-stabilized soils at equivalent dosages. The reaction begins early but matures over time.

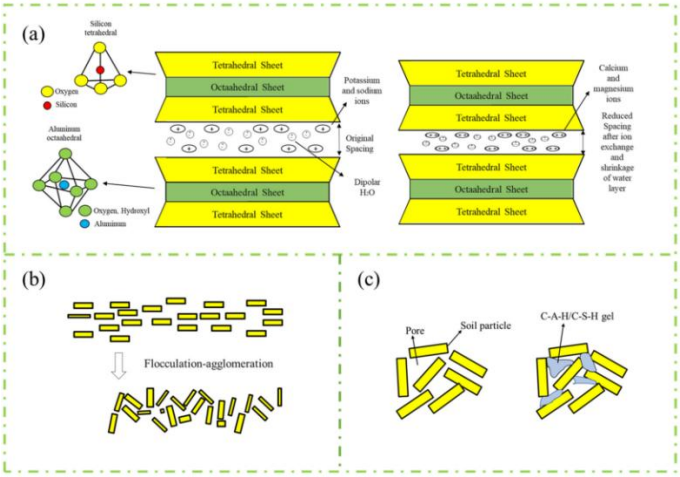


Figure 21 Stabilization mechanism: (a) cation exchange; (b) flocculation-agglomeration; (c) pozzolanic reaction

3.2.3 Effect of cement stabilization on the different properties

3.2.3.1 Effect on index properties

In CH expansive soils, cement treatment usually lowers LL and PI; PL changes less consistently. Alexander et al. (2025) reports the clearest direct pattern for OPC: as cement increased from 0% to 11%, LL fell from 51% to 22%, PL changed only slightly from 16% to 19%, and PI fell from 35% to 3%. Across the CH-soil experiments in the broader set, that same direction is common: cement lowers LL and PI mainly through cation exchange, flocculation-agglomeration, and later cementation, which reduce clay-water affinity. That is why some CH studies show PL rising slightly while others show little change: the soil becomes less deformable and less water-sensitive, but the exact PL shift depends on mineralogy and binder amount [Alexander et al. (2025); Abbey et al. (2019)].

3.2.3.2 Effect on swell potential and swelling pressure

OPC treatment consistently reduces swell potential in CH expansive soils. In one high-plasticity clay study by Mollamahmutoğlu et al. (2017), untreated swell percentage was about 9.82%, while OPC-treated specimens fell to 0.35–0.25% after 28 days. In another cement-only expansive-clay study, 14% OPC reduced swelling potential from 76% to 30% [Sorsa (2022)].

Similarly, in CH expansive soils, OPC-based stabilization generally lowers swelling pressure by reducing the soil's tendency to take up water and expand, and the effect becomes stronger as cement content and curing time increase. In high-plasticity kaolinite–bentonite CH-type mixtures, adding 5% and 8% cement reduced swelling pressure after 7 and 28 days, and the same study linked that reduction to lower plasticity index, flocculated fabric, and cementitious void filling [Abbey et al. (2019)].

However, cement treatment usually lowers swelling pressure in CH expansive soils, often substantially, but the measured outcome depends on curing, binder dosage, sulfate condition, and the test setup; in some strongly cemented specimens, swelling pressure becomes effectively unmeasurable because the soil matrix is too stiff to express conventional swell under load [Phanikumar et al. (2015)].

3.2.3.3 Effect on strength and compressibility

In CH expansive soils, cement treatment raises strength, with larger gains after curing and at moderate-optimal dosages. In Alexander et al. (2025), 28-day UCS increased from 0.294 MPa to 4.547 MPa as OPC rose to 11%, and the study identifies 8–11% OPC as the practical optimum range. Moreover, Sorsa (2022) showed that 14% OPC was the optimum dosage and was reported as very effective for improving expansive-soil strength.

On the other hand, Mumtaz et al. (2021) reports that UCS increased significantly with added OPC and continued to improve with curing time; it recommends 10% cement as sufficient to achieve adequate 1-day UCS.

The effect of OPC treatment on compressibility of CH soils is equally significant but less frequently reported with confirmed-CH verification. However, we can also be based on similar studies to verify the effect of the OPC on the type of soil we are interested in, because strength and compressibility change together since cementation densifies the CH-soil fabric. Umar et al. (2025) found that compressibility parameters explained 46% of UCS variance, making compressibility reduction the dominant causal pathway for strength gain.

The main caveat is that more cement is not always better. Several CH expansive-clay studies place the useful range around 8-15%, depending on soil mineralogy and binder system, and one large program found that higher cement contents can impair expected performance [Alexander et al. (2025); Sorsa (2022)].

3.2.4 Performance under Meteorological events

Wetting–Drying

Under wetting–drying cycles, OPC stabilization usually raises initial strength and reduces visible cracking relative to untreated expansive clay, but repeated cycling progressively weakens the cemented structure. In Oxford clay, OPC-treated specimens kept the highest undrained shear strength at high suction across 1, 5, 10, and 15 cycles, yet the same study reported increasing swelling, higher saturation moisture content, microcracking, and leaching-driven macroporosity with cycling. OPC helps the clay hold loads when relatively dry, but if that same clay goes through seasonal wetting and drying, it can still swell, crack, and progressively lose structural reliability, so high early strength should not be mistaken for equally good long-term volumetric stability. For instance, X-ray computed tomography images showed a denser matrix after one cycle but minor cracking and limited structural deterioration after 10 cycles, indicating that cementitious bonding persists but progressively degrades (Figure 22) [Turrakheil et al. (2025)].

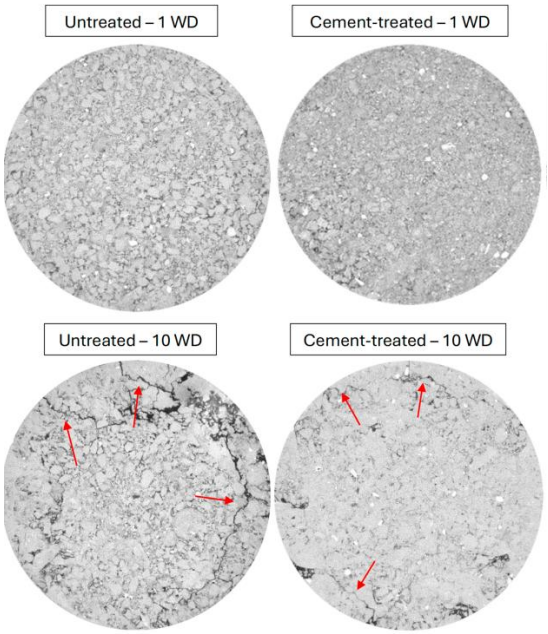


Figure 22 X-ray computed tomography (CT) grayscale images illustrate expansive soil samples' internal microstructural evolution under cyclic wetting–drying (WD) conditions

In expansive soil directly comparing binders, OPC performed better than PPC under normal curing, but PPC outperformed OPC after alternate wetting–drying when binder content was sufficient, suggesting plain OPC is not the most cycle-resistant cement chemistry for repeated moisture attack [James et al. (2021)].

Freeze–Thaw

In cold-climate applications, freeze-thaw cycling represents a secondary but significant stressor for OPC-stabilized CH soils. Ice formation within the pore network of the stabilized matrix generates volumetric expansion during freezing and differential stress during thawing, progressively damaging the calcium silicate hydrate gel network and increasing macro-porosity with each cycle.

OPC cement improves expansive-soil resistance compared with untreated soil, but the first few cycles cause large losses in strength and stiffness. In cement-treated expansive soil with 0% to 7% cement and up to 12 freeze–thaw cycles, cement increased UCS and reduced swelling–shrinkage sensitivity, yet freeze–thaw diluted those gains and even accelerated strength reduction relative to the initial cemented state [Lu et al. (2020)].

Higher cement content and longer curing improve freeze–thaw survival, but they do not eliminate degradation [Wu et al. (2020)]. The first freeze–thaw cycle is often the most damaging, after which volume change and strength degradation tend to level off toward a new residual condition. Mechanistically, freeze-induced cracking lowers water-retention capacity and disrupts cementitious bonds, which explains concurrent drops in modulus, UCS, and reloading stiffness.

3.2.5 Field Applicability of Cement Stabilization

Site Conditions Governing Field Success

Field success on CH soils depends first on water state at treatment and service. High initial water content makes compaction and strength development harder, and untreated wet clays above optimum moisture are difficult to compact to target density [Wonglakorn et al. (2025)].

It also depends on matching OPC dosage and curing to the required performance rather than maximizing cement content. In CH soils, UCS generally rises with OPC content and curing time,

but one study found 10% OPC was sufficient for adequate early UCS in embankment use, while another durability study identified 6% cement as an optimum for strength-plus-durability rather than simply higher dosage [Mumtaz et al. (2021); Reddy et al. (2018)].

Mineralogy and chemistry matter at site scale. Sulfate-bearing expansive soils show reduced strength gain and higher swell under Portland cement treatment, and sulfate-rich calcium-treated soils can later form ettringite and lose strength, so sulfate screening is a key preconstruction condition [Firoozi et al. (2017)]. Same as lime but through a different pathway, OPC stabilization introduces an additional reaction pathway involving the tricalcium aluminate phase, which can react with sulfate ions present in CH soil pore water to form ettringite. At low concentrations, ettringite formation initially creates a needle-like crystal skeleton that contributes to early stiffening and pore-filling. However, when sulfate concentrations in the pore water are elevated, as is common in some CH deposits, particularly in arid and semi-arid regions, ettringite formation becomes expansive and damaging, producing volumetric expansion that creates cracks between particles, reduces calcium silicate hydrate and calcium aluminate hydrate production, and exceeds the swelling behavior of the original untreated CH soil.

Temperature sensitivity is less critical for OPC than for lime because OPC hydration is an exothermic reaction that generates heat; it is somewhat more self-sustaining in cold conditions than lime's temperature-dependent pozzolanic reaction. Nevertheless, cement hydration rates slow significantly below 10°C, and freshly treated CH subgrades must still be protected from freezing during the initial setting period to prevent disruption of the developing calcium silicate hydrate matrix. In cold-climate applications, extended curing periods or heated enclosures may be required to achieve the same 28-day strength that would develop at ambient temperature in temperate conditions.

Limitations of Field Applicability

OPC-stabilized CH soils are mainly limited by organic sensitivity, mixing depth constraints, and more brittle failure.

Organic matter is a real limitation because OPC hydration and cementation weaken as organic content rises [Zhong et al. (2022)]. In CH-classified clay, removing organic matter greatly increased strength, while organic-containing material sharply reduced OPC performance [Chen et al. (2020)].

Organic acids are the most disruptive: when pore-solution pH falls below 9, cementing products barely develop and almost no strength gain occurs [Tremblay et al. (2002)]. Fulvic and humic substances hinder stabilization by coating particles and blocking hydration, crystallization, and particle agglomeration [Shao et al. (2023)].

On the other hand, OPC stabilization tends to trade ductility for strength: cement-treated clays commonly shift from ductile or strain-hardening behavior toward brittle, strain-softening failure. Shear testing likewise found untreated soils failed ductilely, whereas cement-stabilized soils failed brittly.

3.2.6 Environmental Impact

OPC cement in CH stabilization has high production burdens, mixed use-phase benefits, and important non-CO_2 risks. Most environmental burden comes before placement, while use-phase benefits come mainly from durability and reduced swelling rather than low emissions

Production Burdens

OPC production is environmentally intensive because clinker manufacture requires calcination at about 1400-1500°C and is the highest-energy, highest-CO_2 phase of the cement life cycle [Olagunju et al. (2021)]. In general, OPC production emits roughly 1 tonne CO_2 per tonne

cement. An India-based manufacturing study estimates 893-940 kg CO_2/t OPC and finds Indian average energy use and emissions are 15.14% and 12.64% higher than other countries in its comparison set [Bhandari et al. (2023); Karadumpa et al. (2023)].

Other studies places standard OPC around 831-980 kg CO_2-eq/t, and show that partial clinker replacement usually lowers global warming potential substantially [Terán-Cuadrado et al. (2024); Sbahieh et al. (2025)]. Across cement LCAs, clinker production also dominates endpoint damage to human health, ecosystems, and fossil resource depletion, not just climate impact.

Use-Phase Effects

In CH and other expansive clays, OPC-based stabilization improves engineering performance by reducing swell, lowering hydraulic conductivity, and increasing compressive strength through cation exchange, flocculation, and cementitious gel formation, which can extend service life and reduce maintenance frequency [Ijaz et al. (2022); Almuaythir et al. (2024)].

Stabilization can reduce maintenance demand because treated soils are more durable and less erosion-prone over time. However, use-phase gains do not erase production dominance; The LCA study by Govindan et al. (2025) attributes more than 80% of total impact to stabilizer production.

For that, partial replacement strategies can preserve performance while lowering burdens, such as 15% zeolite replacement or industrial by-product blends that still improve UCS and durability [Molaabasi et al. (2022); Mataji et al. (2025)].

Field-Scale and Non-CO_2 Impacts

Soil pH

OPC-based stabilization generally raises soil pH because cement hydration creates a strongly alkaline environment. That alkalinity is often beneficial for stabilization, but excess alkalinity can also alter native soil chemistry and shift contaminant mobility rather than uniformly suppressing it [Almuaythir et al. (2024)].

Heavy-Metal Leaching

OPC and other binders decrease leachability by converting soluble metals into insoluble hydroxides and complexes [Li et al. (2019)]. OPC clinker contains trace amounts of heavy metals including chromium, lead, and vanadium that can be mobilized at low pH conditions.

Cementitious gels and low porosity further immobilize metals through encapsulation and binding [Hu et al. (2024); Negahdar & Amin (2025)]. However, the effect is metal-specific and pH-dependent: OPC performs well for Cd, Mn, and some high-content Ni cases, but not uniformly for Pb, Cu, and Zn [Li et al. (2019)].

Water Quality

Long-term water-quality risk does not come mainly from metals alone. An 841-day leaching study found strong correlations among pH, metals, total nitrogen, ammonium, and Chemical Oxygen Demand (COD), and reported that COD can exceed permissible limits during long-term leaching even when metal stabilization is strong [Hu et al. (2024)].

Stabilization can also improve field water protection indirectly by reducing erosion and sediment delivery to nearby water bodies [Almuaythir et al. (2024)]. However, OPC has relatively high-water demand, with manufacturing-plant water use reported at 0.14-1.28 L/kg cement, while pozzolanic and alkali-activated alternatives tend to require less process water [Benghazi et al. (2024)].

CHAPTER 4 — Sustainable Chemical Stabilization Techniques

4.1 Fly Ash Stabilization

4.1.1 Introduction

The limitations of traditional stabilizers, particularly the high carbon footprint of lime and OPC production, their sensitivity to sulfate-bearing soils, and the documented long-term boundary deterioration revealed by field studies, have driven increasing research interest toward sustainable alternatives that can achieve equivalent or superior geotechnical performance while substantially reducing environmental burden. Among these alternatives, fly ash has emerged as the most extensively studied and widely available industrial byproduct for expansive CH soil stabilization, supported by a growing body of literature that confirms its effectiveness across multiple soil types, climates, and infrastructure applications.

4.1.2 Stabilization mechanism

4.1.2.1 Types of fly ash used

Fly ash used in geotechnical stabilization is classified under ASTM C618 into two primary types, Class C and Class F, based on their chemical composition and reactivity, which directly govern their stabilization mechanism and effectiveness on CH soils. However, across experimental studies, Class C fly ash is the type most often identified as preferred or more effective for stabilizing expansive fat clays.

Class C fly ash is produced from the combustion of lignite or sub-bituminous coal and is classified by a combined silica, alumina, and iron (III) oxide content ($SiO_2 + Al_2O_3 + Fe_2O_3$) of at least 50% by weight, alongside a calcium oxide (CaO) content that typically exceeds 20%. This elevated CaO content endows Class C fly ash with self-cementitious properties. Therefore, it functions simultaneously as a pozzolanic material and a standalone binder.

Physically, Class C fly ash is composed largely of spherical particles with significant glassy/amorphous phase, although some particles are irregular or crystalline as shown in Figure 23 [Ma et al. (2022); Witte & Garg (2024); Turan et al. (2022)]. Its particles are generally in the silt-size range, but the exact size distribution varies substantially by ash source and processing.

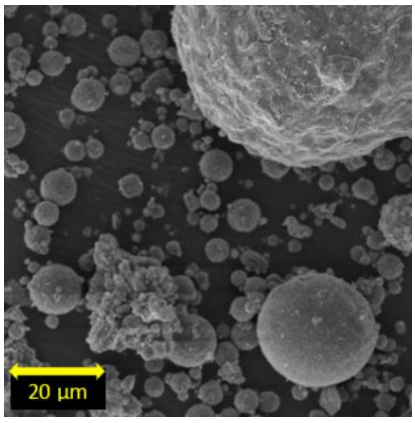


Figure 23 SEM of a Class C Fly Ash

4.1.2.2 Mechanism of Class C Fly Ash-Soil Reaction in CH Expansive Soils

The stabilization of CH expansive soils with Class C fly ash proceeds through four interrelated physico-chemical processes: 1) self-cementitious hydration, 2) cation exchange, 3) flocculation and agglomeration, and 4) pozzolanic reaction. Research confirms that among the four mechanisms, the pozzolanic reaction is the most effective contributor to long-term improvement, while self-cementitious hydration and cation exchange account for the rapid early-stage modifications observed immediately after mixing.

Self-Cementitious Hydration

Upon mixing Class C fly ash with a CH soil, the free CaO present in the ash reacts immediately with the available pore water. This reaction generates $Ca(OH)_2$ in-situ, analogous to the hydration reaction of quicklime, simultaneously releasing heat that reduces the soil's natural moisture content and creating an alkaline pore environment ($pH \geq 12$) that is the prerequisite for all subsequent reactions. Unlike lime, however, the CaO in Class C fly ash is accompanied by reactive calcium aluminate and calcium silicate compounds, analogous to OPC's tricalcium aluminate and dicalcium silicate phases, that hydrate directly to form calcium silicate hydrate and calcium aluminate hydrate gels without requiring dissolution from the soil's own clay minerals.

Cation Exchange

The Ca^{2+} and OH^- ions released by Class C fly ash hydration enter the pore solution, and Ca^{2+} ions immediately begin displacing the monovalent cations (Na^+, K^+) adsorbed on the negatively charged surfaces of the CH clay minerals, the same cation exchange reaction described for lime and OPC in Chapter 3. In montmorillonite-dominant CH soils, they replace Na^+ in the interlamellar spaces, compressing the diffuse double layer and reducing osmotic swelling.

Flocculation and Agglomeration

As double-layer compression reduces interparticle repulsion, the dispersed clay particles of the CH soil aggregate into flocculated clusters through edge-to-face contacts, similar in mechanism to the flocculation described in lime and OPC treatment. In other words, once exchangeable cations are replaced, clay platelets lose some repulsive separation and begin to flocculate into larger aggregates.

The spherical, non-plastic particles of Class C fly ash act simultaneously as physical spacers between clay aggregates, reducing the continuity of the clay fabric and lowering the overall specific surface area available for water adsorption [Lin et al. (2013)].

Pozzolanic Reaction

The dominant long-term stabilization mechanism is the pozzolanic reaction, in which the amorphous reactive silica and alumina present in Class C fly ash dissolve under the high-pH environment created by the self-cementitious hydration step, then react with the available Ca^{2+} ions to form additional calcium silicate hydrate and calcium aluminate hydrate gels. Studies report that these gels fill pores, bind particles into a denser skeleton, and reduce hydraulic conductivity or permeability with curing [Qiu et al. (2025); Prashanth et al. (2001)].

Unlike the self-cementitious hydration products, which form rapidly but consume the fly ash's own reactive calcium phases, the pozzolanic reaction draws on the much larger reservoir of amorphous silica and alumina, meaning it continues developing strength and reducing compressibility for weeks to months beyond the initial treatment. This is the main mechanism behind long-term gains in strength, lower compressibility, and improved volumetric stability.

4.1.3 Effect on Engineering Properties

4.1.3.1 Effect on index properties

The most immediate and measurable effect of Class C fly ash on CH soils is a systematic reduction in liquid limit (LL) and plasticity index (PI), accompanied by a decrease in maximum dry density (MDD) and an increase in optimum moisture content (OMC), the same pattern observed with lime and OPC, but produced through the combined self-cementitious hydration and cation exchange reactions specific to Class C fly ash [Deepak et al. (2020); Seyrek (2018)].

However, in CH expansive soils, the clearest direct study reports that LL and PI keep decreasing up to 25% Class C fly ash, then rise slightly with further addition [Shirkhanloo et al. (2021)]. Other studies compiling Class C datasets also show that LL reduction strengthens as dosage rises from 5% to 30%.

The effect of Class C fly ash on the Atterberg limits of CH soils has been investigated across numerous independent experimental studies, using different soils, different CaO contents, and a wide range of dosages (typically between 5% and 40% by dry weight of soil).

Table 11 synthesizes the dosage-response relationship between Class C fly ash content and Atterberg limit modification in CH soils, compiled across multiple experimental studies. The pattern that emerges is consistent: improvement in LL and PI begins at low dosages (5–10%) [Kumar & Harika (2020)], intensifies through the 15–25% range where most studies report their best results [Rai et al. (2025); Khan et al. (2021)], and plateaus or partially reverses beyond 25% [Seyrek (2018); Shirkhanloo et al. (2021)].

Table 11 Dosage-response pattern of Class C fly ash on Atterberg limits in CH expansive soils

Dosage Range (%)	Atterberg-Limit Effect
5-10	Early reduction in PI and often LL begins
15-20	Strong reductions, often practical optimum
20-25	Largest Atterberg-limit improvement in many CH/Class C studies
>25	Benefits often plateau or slightly reverse

The plateau or reversal effect at higher contents is mainly because ash replaces clay rather than further reacting with it, so the mixture shifts from chemical stabilization toward physical dilution [Jumaa et al. (2026); Seyrek (2018)]. Also, once the main flocculation benefit is achieved, extra ash can contribute to larger silt-sized particles without proportional new bonding.

4.1.3.2 Effect on Swell Potential and Swell Pressure

The reduction of swell potential and swell pressure is a practically significant engineering benefit of Class C fly ash stabilization for CH soils, and the available data confirm substantial reductions achievable at practically applicable dosage levels. This reduction is mainly a calcium-driven microstructural stabilization process: Class C fly ash exchanges cations, flocculates clay, forms cementitious gels, fills pores, lowers water retention, and therefore suppresses both the amount of swell and the pressure generated during wetting.

For example, in Kumar et al. (2022), swell potential was reduced from 10.5% to 0% at 20% fly ash. This direction is reproduced across broader datasets: 20% fly ash gave a significant reduction in swell potential in oedometer testing [Phanikumar (2009)] and Class C fly ash caused substantial decreases in swell percentage as dosage increased [Mollamahmutoğlu et al. (2009)].

Moreover, the experiment by Dayioglu et al. (2017) on an expansive clay showed a reduction of the swelling pressure from 235 kPa to 47 kPa with Class C fly ash. Mixed clay systems also

show large pressure reductions, including up to 64–93% lower maximum swelling pressure with Class C fly ash [Kolay & Ramesh (2016)].

A practical pattern appears across multiple studies: improvements strongly grow up to about 15–25% fly ash, then additional fly ash produces little extra reduction in swell pressure.

However, the main caveats are that the pressure response is less uniform than swell potential, benefits often plateau beyond about 20–25%, and, similarly to lime and OPC, curing time matters because pozzolanic and self-cementing reactions continue after mixing [Zha et al. (2008)].

4.1.3.3 Effect on Strength and Compressibility

Class C fly ash produces progressive, curing-time-dependent improvements in both compressive strength and compressibility of CH soils, driven primarily by the accumulation of pozzolanic reaction products over time.

Strength improvement with Class C fly ash follows a clear dosage-and-time pattern. UCS increases significantly at 20–25% fly ash content, suggesting improved load-bearing capacity and structural integrity, with curing time consistently identified as the most influential factor. Samples cured for 28 days showed markedly higher UCS than 1-day or 7-day samples with the same dosage, confirming that the pozzolanic reaction is the dominant strength-generating mechanism rather than the faster self-cementitious hydration alone [Turan et al. (2022)]. In fact, the self-cementation of Class C fly ash is reflected in the small early strength gain [Nalbantoglu (2004); Shirkhanloo et al. (2021); Turan et al. (2020)].

Compressibility improvements are directly linked to the same pozzolanic product accumulation that drives strength gain. As calcium silicate hydrate and calcium aluminate hydrate gels fill inter-aggregate pores and stiffen the clay matrix, the compression index (Cc) and recompression index (Cs) decrease, that is the same mechanism confirmed for OPC in Chapter 3. For instance, Kolay & Ramesh (2016)'s study using Class C fly ash with sand confirmed this through one-dimensional consolidation tests, finding that both types of expansive clay showed reduced compression behavior with increasing Class C fly ash content, consistent with the progressive pore-filling and particle-binding function of pozzolanic gels reducing the soil's volumetric response to applied stress.

4.1.4 Performance Under Meteorological Events

Wetting-Drying Cycles

In the literature, the most striking finding in the meteorological performance for Class C fly ash-stabilized CH soils is that wetting-drying cycles, the dominant degradation mechanism for both lime and OPC treatments in Chapter 3, appear to have a partial impact on fly ash-stabilized CH soil performance. This advantage stems from the slower, more progressive nature of the pozzolanic reaction in fly ash-treated soils, which produces a distributed cementitious matrix less susceptible to the bond-breaking mechanism that W-D cycling imposes on lime and OPC-stabilized soils.

For example, Turan et al. (2022) conducted cyclic W-D tests on confirmed CH soils stabilized with Class C fly ash at dosages of 0–20%, using both saline water and tap water to simulate different field exposure conditions. Their results showed that the cycles with saline water or tap water did not have a major impact on strength parameters, swelling potential, and plasticity of the fly ash-stabilized CH specimens. The long-term study by Bin-Shafique et al. (2010) included a high-plasticity expansive clay treated with Class C fly ash at 0, 5, 10, and 20%, and the results showed that the effect of 12 wet–dry cycles was essentially insignificant in stabilized soils, with a slight increase in the UCS as shown in Figure 24.

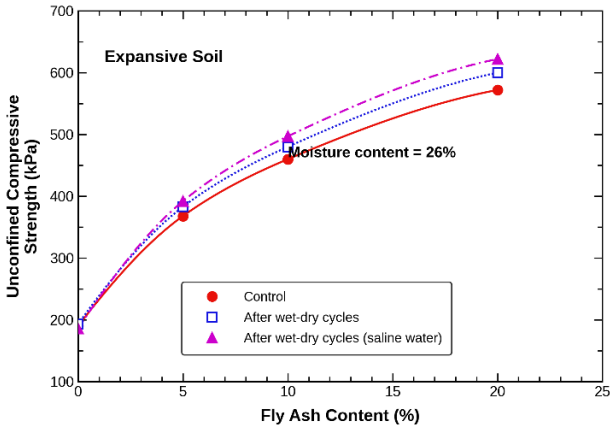


Figure 24 Effect of wet–dry cycles on unconfined compressive strength of the fly ash-stabilized soil [from Bin-Shafique et al. (2010)]

Freeze-Thaw Cycles

Freeze–thaw cycles cause the clearest durability penalty, mainly through strength loss, pore damage, and swelling. In long-term testing, freeze–thaw caused up to 40% strength loss, although stabilized soils remained at least 3 times stronger than untreated soil. Freeze–thaw also raises swell potential in expansive clay, with vertical swell rising rapidly in the first 4–5 cycles and then slowing, as shown in Figure 25 [Bin-Shafique et al. (2010); Bin-Shafique et al. (2011); Solanki & Hauk-Jegen (2016)].

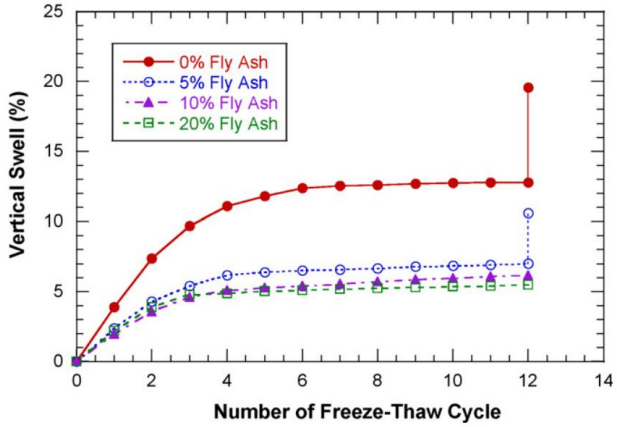


Figure 25 Vertical swell of a fly ash-stabilized expansive soil during freeze–thaw cycles [from Bin-Shafique et al. (2010)]

Damage is strongly tied to microstructure and moisture: thawing increases moisture, ice lenses distort the fabric, and macropores expand as strength falls [Solanki & Hauk-Jegen (2016); Shi et al. (2024)].

4.1.5 Field Applicability of Class C fly ash

Site Conditions Governing Field Success

Success depends first on moisture at compaction. Maximum field strength is reported when clay is compacted about 4–8% below optimum moisture content, while density and strength fall with wetter conditions and with compaction delay [Turan et al. (2022); Edil et al. (2006)].

Moreover, compaction delay is an important construction-management constraint for reactive fly ash stabilization because delay can reduce density and strength, so rapid sequencing is often needed. However, similar delay sensitivity also exists in OPC-treated soils, while lime-treated soils are usually more tolerant and, in some cases, allow controlled mellowing rather than

immediate compaction [Sivapullaiah et al. (1998); Raja & Thyagaraj (2021); Kumar et al. (2021)].

Success also depends on Class C fly ash content being high enough to trigger self-cementing and pozzolanic reactions but not so high that gains plateau or reverse. Class C fly ash gains strength and reduces swell progressively with curing time because pozzolanic and self-cementing products accumulate over days to weeks [Zimar et al. (2022); Zha et al (2008)]. In expansive clay, fly ash-treated soils often show little immediate UCS gain, but become significantly stronger after about 7 days and continue improving toward 28 days [Dayioglu et al. (2017)].

Higher curing temperature accelerates the reactions that bind fly ash-stabilized soil [PaniAparupa & Prasad (2018)]. In fly ash-based systems, raising curing temperature can sharply shorten the time needed to reach a target strength; one study reports that 7-day high-temperature curing can approach 28-day normal-temperature strength [Utkarsh & Jain (2024)].

Additionally, the soil and ash chemistry must be compatible. Higher CaO and unbound lime make Class C fly ash more reactive and generally more effective, while stabilization is strongly controlled by soil mineralogy, pH, and ash type [Utkarsh & Jain (2024)].

Field performance also tends to be lower than laboratory performance because field mixing is less uniform, even though both conditions show improvement with Class C fly ash.

Limitations of Field Applicability

Organic matter content is a major negative site condition, and sulfate-bearing soils are also risky. Studies warn that organics and sulfates can make treated soil perform worse than untreated soil, and organic fine-grained soils showed little benefit from fly ash in one test program [Edil et al. (2006)]. Mainly because organic matter usually suppresses fly ash reactivity and makes strength gain unreliable, while sulfate-bearing soils raise an ettringite-controlled swell risk, whose severity depends on how much reactive calcium the treatment system supplies [Abdullah & Shahin (2023)].

Leaching is a credible limitation because fly ash can contain traces of heavy metals that may enter soil or groundwater under some exposure conditions. However, only a few studies confirm acceptable leachate limits and call for more work on heavy metals and carcinogenic contaminants [Zimar et al. (2022)].

Carbonation is also a limitation because it changes the pH and mineral phases that control immobilization. In stabilized expansive soil, carbonation can decompose hydration products, reduce matrix pH, and increase heavy metals and Ca release under acidic conditions [Zha et al. (2021)].

On the other hand, Class C fly ash's availability is geographically constrained by proximity to coal-fired power plants. Fly ash is only cost-effectively available within a reasonable transport distance from combustion facilities. In regions where coal power generation is being phased out in favour of renewable energy, fly ash supply may decline or become inconsistent over the project's design life, creating long-term supply chain vulnerability for maintenance treatments.

4.1.6 Environmental Impacts

Production Burden and Carbon Footprint

Using fly ash as a stabilizer diverts a coal-combustion waste stream from disposal and reduces reliance on manufactured binders with higher production emissions. Studies consistently frame fly ash reuse as an environmentally friendly substitute because it repurposes an industrial by-product and can lower the carbon footprint of construction relative to cement and lime [Shirkhanloo et al. (2021); Almuaythir et al. (2024)].

Direct field-scale evidence is limited but favorable: in a pavement section using a Class C fly ash layer, construction energy fell by 67% and GHG emissions fell by 59% versus a conventional control section [Joshi & Patel (2022)]. Moreover, a study by Bhandari et al. (2023) stated that the carbon emission intensity for fly ash is approximately 8.70 kg CO_2-eq per tonne, which is extremely low compared to other traditional stabilizers like cement or lime.

Heavy Metal Leaching Concerns

The primary environmental concern specific to coal fly ash soil stabilization is the potential for heavy metal leaching into groundwater from the stabilized matrix. This kind of ash contains trace concentrations of heavy metals including arsenic (As), barium (Ba), cadmium (Cd), chromium (Cr), lead (Pb), and selenium (Se), introduced with coal and concentrated in the ash fraction. There is a recognized relationship between the chemical composition of coal ashes and their leaching behavior, with the mobility of heavy metals in fly ash-stabilized soils governed primarily by pH, pore water chemistry, and the degree of physical encapsulation within cementitious products [Mahedi et al. (2019)].

Critically, the pozzolanic and self-cementitious reactions that produce calcium silicate hydrate and calcium aluminate hydrate gels during Class C fly ash stabilization of CH soils also have an environmental immobilization function: the leaching concentrations of heavy metals in stabilized soil often decreased, sometimes below regulatory limits, under the synergistic effects of physical encapsulation by hydration products and chemical stabilization within the cementitious matrix, meaning the same reactions that improve strength and reduce swell also physically and chemically trap heavy metals within the stabilized matrix, reducing their environmental mobility compared to raw fly ash in an unbound state [Dermatas & Meng (2003); Nag & Shimaoka (2022)].

Main Environmental Benefits

Waste diversion is the clearest benefit because fly ash is produced in large volumes, much of it is landfilled, and reuse in soil stabilization avoids disposal-related pollution [Alqawasmeh (2025)]. Furthermore, it lowers reliance on cement and lime, whose production has high embodied energy and CO_2 emissions, so replacing part of conventional stabilizer demand reduces carbon footprints [Almuaythir et al. (2024)].

Equally, it preserves natural resources because treated soils can be used in place, reducing the need for imported aggregates, borrow materials, and other virgin construction inputs [Renjith et al. (2021)]. Consequently, it supports a circular economy by converting an industrial waste into a useful binder for roadbeds, subgrades, and foundations rather than a landfill burden [Sambre et al. (2024); Zimar et al. (2024)].

Sustainability Limits

The method is considered sustainable **conditionally**, because its benefits depend on using optimum fly ash contents and achieving durable curing rather than simply adding more ash. Long-term wet–dry durability can remain acceptable in well-designed mixtures, but excessive cycling or poor mix design can reduce performance, which would weaken the environmental gains if repairs increase.

Overall, Class C fly ash makes CH expansive soil stabilization sustainable because it combines waste reuse, lower embodied carbon, natural-resource conservation, and longer-lasting ground performance in one treatment strategy. The strongest sustainability case is for projects that can replace cement- or lime-heavy stabilization and keep the treated expansive soil in service longer with less maintenance.

4.2 Cement Kiln Dust (CKD) Stabilization

4.2.1 Introduction

The second sustainable stabilizer examined in this chapter is cement kiln dust (CKD), a fine powdery byproduct generated during the production of Ordinary Portland Cement, the traditional stabilizer examined in Chapter 3. This direct industrial relationship between CKD and OPC gives the material a uniquely coherent sustainability narrative: CKD is literally the waste stream produced by manufacturing the binder it replaces, meaning its use in CH soil stabilization simultaneously addresses the environmental burden of cement production and reduces the need for virgin stabilizer materials.

4.2.2 Stabilization mechanism

4.2.2.1 Types of CKD Used

Cement kiln dust (CKD) (Figure 26) is a fine-grained, highly alkaline particulate byproduct captured from exhaust gases during high-temperature clinker processing in rotary kilns [Barnat-Hunek et al. (2018); Hamadou et al. (2023)]. The physical and chemical characteristics of CKD depend on raw materials, type of kiln operation, dust collection systems and fuel type used in cement clinker production [Marku et al. (2013)].



Figure 26 Cement Kiln Dust (CKD)

CKD is chemically dominated by calcium oxide (CaO) and silicon dioxide (SiO_2), with significant secondary fractions of alkalis, sulfates, and chlorides that limit its recyclability in cement [Hamadou et al. (2023); Al-Bakri et al. (2022); Marku et al. (2013)]. The calcium oxide content in CKD is notably high, typically ranging from 37% to 77% [Adekunle (2024)]. The presence of free lime (CaO) and cementing minerals dictates the material's cementitious value and reactivity for stabilization purposes [Marku et al. (2013)].

The two most practically important distinctions for soil stabilization are **fresh versus aged CKD**.

Fresh CKD is collected directly from the kiln exhaust system before any exposure to atmospheric moisture or CO_2. It retains its full free CaO content and maximum reactivity, making it the most effective type for soil stabilization and the type most commonly referenced in the geotechnical literature.

Aged or landfilled CKD has been exposed to atmospheric moisture and CO_2 before its use, partially hydrating its free CaO to $Ca(OH)_2$ and further converting some to $CaCO_3$ through carbonation, both reactions consuming the reactive lime content and reducing stabilization effectiveness.

4.2.2.2 Mechanism of CKD-Soil Reaction

CKD-soil stabilization proceeds through the same fundamental framework: hydration, cation exchange, flocculation and agglomeration, and pozzolanic reaction, already described in detail for lime (Section 3.1.2), OPC (Section 3.2.2), and Class C fly ash (Section 4.1.2). These mechanisms are triggered identically: CKD's free CaO hydrates upon contact with pore water, releasing Ca^{2+} and OH^- ions, compressing the diffuse double layer of montmorillonite particles, driving flocculation, and creating the high-pH environment needed for calcium silicate hydrate and calcium aluminate hydrate gel formation.

CKD supplies more reactive calcium and alkalis than lime, but lacks the fully pre-formed cementitious phases of OPC, making its performance highly dependent on its specific source composition [Al-Bakri et al. (2023); Lee et al. (2024)]. More **reactive calcium and alkalis** in CKD accelerate early hydration and enhance clay dissolution, but **excessive alkalis** can retard long-term gel formation.

High free-lime CKD generates substantial calcium hydroxide immediately upon mixing with wet soil, promoting rapid cation exchange and flocculation [Peethamparan et al. (2008)]. This immediate release of Ca^{2+} reduces the thickness of the diffuse double layer surrounding clay particles, transforming expansive clay into larger, sand-like aggregates [Almuaythir et al. (2024); Liu et al. (2019)]. CKD with free lime in the 2–5% range is sufficiently reactive for soil stabilization, whereas landfilled CKD with only trace free lime lacks this reactivity and is suitable mainly for drying wet subgrades [Sreekrishnavilasam et al. (2007)].

In alkali-activated or calcium-bearing binders, an excessive concentration of alkali activators (like sodium hydroxide) triggers an overly rapid early-stage reaction. This rapid formation causes early reaction products to quickly adsorb onto the surfaces of unreacted particles. By coating the raw material particles, these early products create a physical barrier that hinders further dissolution of the necessary reactive oxides. The excess alkali ultimately reduces the reaction rate, decreasing the total quantity of calcium aluminosilicate hydrate gel and increasing system porosity [Gebregziabiher et al. (2016)].

4.2.3 Effect on Engineering Properties

4.2.3.1 Effect on Index Properties

The addition of cement kiln dust (CKD) to high-plasticity (CH) expansive soil consistently decreases the liquid limit (LL) and plasticity index (PI), improving overall soil workability [Ogila (2021); Mohamedzein et al. (2025)].

Mohamedzein et al. (2025) showed reductions in the liquid limit dropping from 85% to 75% and the plasticity index falling from 46% to 16% with 6–30% CKD treatment as shown in Figure 27, while broader additive studies report liquid limit reductions up to 37.66% and plasticity index reductions up to 74.76% [Almuaythir et al. (2024)]. Concurrently, the plastic limit (PL) generally increases as CKD dosage rises, a trend attributed to cation exchange, flocculation, and the absorption and evaporation processes caused by the dust [Zemouli et al. (2024)].

This combined effect, lower LL and higher PL, mechanically narrows the plasticity index and transforms the soil texture from plastic to more granular and friable [Zemouli et al. (2024); Mahan & Hussein (2018)]. The underlying mechanism involves the high free lime (CaO) initiating cation exchange and flocculation-agglomeration of fine clay particles, followed by long-term pozzolanic reactions that form calcium silicate hydrates and calcium aluminate hydrates, which bind and densify the soil matrix [Ekpo et al. (2021)].

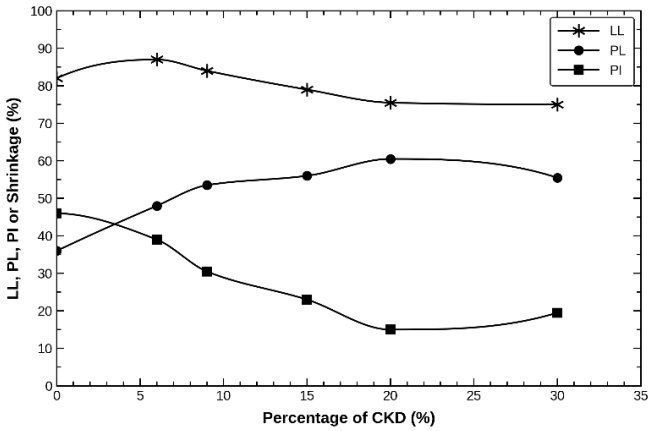


Figure 27 Atterberg limits of CKD-soil [from Mohamedzein et al. (2025)]

4.2.3.2 Effect on Swell Potential and Swell Pressure

The addition of cement kiln dust to high-plasticity (CH) expansive soil consistently reduces both swell potential and swelling pressure, with the magnitude of reduction scaling alongside CKD dosage [Rao & Rajakumar (2020); Almurshedi et al. (2019)].

For example, Mohamedzein et al. (2025) showed that swelling potential drops from 11.2% to 3.4% and swelling pressure decreases from 108 kPa to 17.5 kPa when CKD is added at 6–30% of soil mass.

Similarly, Eid et al. (2024) showed that the free swell index decreases by 50% in CH soil with increasing additive percentage, and the swelling pressure values decrease by 50% for treated expansive soils.

On the other hand, maximum swelling pressures decrease exponentially as CKD content increases [Cui et al. (2018)], while the swelling index drops by 70–75% in some soils mixed with 20% cement dust [Almurshedi et al. (2019)]. In some other cases, free swelling percent is reduced from 80.0% to 0.0% after treatment with CKD and CKD with lime [Ismaiel (2013)].

The underlying mechanism involves calcium ions from CKD interacting with clay silicate sheets to aggregate particles and create a more permeable soil structure, which reduces water absorption [Eid et al. (2024)]. Microstructure analysis reveals that CKD reduces the montmorillonite content of expansive soil, decreases both macro-pore and micro-pore volumes, and forms cementitious phases that improve swelling and shrinkage properties [Cui et al. (2018); Eid et al. (2024)]. XRD patterns confirm a reduction in the intensity of swelling minerals such as montmorillonite, and illite [Mohamedzein et al. (2025)], while SEM micrographs show condensed soil particles with fewer small pores and pozzolanic products filling inter-clay voids for a soil treated with 15% CKD (Figure 28) [Mohamedzein et al. (2025)].

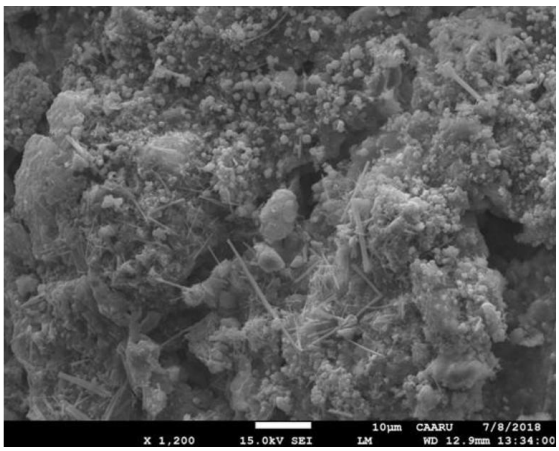


Figure 28 SEM of a soil treated with 15% CKD [from Mohamedzein et al. (2025)]

4.2.3.3 Effect on Strength and Compressibility

The addition of cement kiln dust (CKD) to high-plasticity (CH) expansive soil consistently increases unconfined compressive strength (UCS) and improves compressibility characteristics through pozzolanic reactions and the formation of cementitious compounds [Gilbert (2025); Kumar & Janewoo (2016); Rao & Rajakumar (2020)]

UCS values rise significantly with increasing CKD content and extended curing periods, with one study reporting almost 14 times strength increase from 0.761 kg/cm² to 10.552 kg/cm² at 10% CKD after 28 days [Rimal et al. (2019)]. This strength improvement is attributed to the high free lime (CaO) content in CKD—often up to 60%—which hydrates to form calcium silicate hydrate and calcium aluminate hydrate gels that fill interparticle voids and create a denser, more homogeneous soil structure.

However, the relationship between CKD content and UCS is not purely linear; strength typically peaks at an optimal dosage—often between 10% and 15%—before declining at higher additive levels [Cui et al. (2016); Zemouli et al. (2024); Cui et al. (2018)]. This strength reduction at elevated dosages is attributed to excessive unreacted free calcium oxide, which causes soil structure loosening, heterogeneity, and brittle failure.

Furthermore, CKD can improve the long-term strength of saturated expansive soil, with UCS continuing to increase exponentially up to 28 days and stabilizing thereafter, while the hydration and pozzolanic products restrain the dispersive structural changes normally caused by saturation [Cui et al. (2018)].

CKD also improves compressibility by increasing bearing capacity, which decreases overall settlement potential [Ogila (2021)], while treated soil exhibits a considerable reduction in the compression index [Kumar & Janewoo (2016)]. Compressibility parameters, including the compression index (Cc) and expansion index (Ce), along with settlement and swelling, are significantly enhanced, with noticeable reductions in porosity particularly after 20% CKD addition [Salih (2025)].

4.2.4 Performance Under Meteorological Events

Wetting-Drying Cycles

Cyclic wetting and drying progressively reduces the swelling pressure and deformation of CKD-stabilized CH expansive soil, with values stabilizing in one case after the fourth cycle [Rashed & Mohammad (2019)]. Untreated soil samples collapse during the first wetting-drying cycle, whereas CKD-stabilized mixtures maintain a constant volume with minimal weight loss [Saeed et al. (2024)].

The durability of treated soil improves significantly under wetting-drying conditions, with higher CKD percentages yielding better resistance to volume change and weight loss [Alhassani et al. (2021)].

Soil plasticity declines during the leaching process of wetting-drying cycles, with most CKD-treated soils becoming non-plastic and failing to revert to their initial unstabilized state. The swelling–shrinkage behavior of expansive soil becomes reversible after reaching an equilibrium condition where wetting and drying paths converge [Estabragh et al. (2015)].

Unconfined compressive strength (UCS) in CKD-stabilized soil can paradoxically increase after wetting-drying cycling, with one study showing 20% CKD samples rising from 2.68 MPa to 5.85 MPa post-durability test [Saeed et al. (2024)].

However, prolonged cyclic exposure generally degrades cementitious bonds and increases porosity, a deterioration mechanism observed across various stabilized expansive soils [Hu et al. (2024)].

The main factors influencing durability are shown in Table 12.

Table 12 Factors influencing the durability of CKD-stabilized expansive soil under wetting-drying cycles

Factor	Effect on W/D Performance
CKD Dosage	Higher percentages mitigate strength loss and volume change
Initial Water Content	High initial water content lowers deformation and swelling pressure
Dry Density	High dry density increases deformation and swelling pressure
Microstructure	Cycles increase pores and cracks, diminishing cementitious products

Freeze-Thaw Cycles

Freeze-thaw cycling reduces the unconfined compressive strength (UCS) and resilient modulus (Mr) of CKD-stabilized clayey soils, with the most significant strength loss occurring between zero and one cycle [Solanki & Hauk-Jegen (2016); Khoury & Zaman (2006)]. However, CKD stabilization substantially mitigates this damage; freeze-thaw cycling lowers the UCS of unstabilized clayey soil by 88%, while the reduction for 20% CKD-stabilized soil is only 21% in one study as shown in Figure 29 [Ismeik et al. (2021)]. Soil specimens stabilized with CKD offer maximum resistance toward Freeze-thaw cycles compared to other additives like Class C fly ash [Solanki & Hauk-Jegen (2016)].

Treated samples show reasonable durability for freezing-thawing conditions, surviving up to 12 freeze-thaw cycles with significantly improved weight loss and volume change metrics as shown in Figure 30. Increasing the percentage of CKD leads to greater improvement for the treated soil under freezing-thawing tests [Alhassani et al. (2021)], and a field investigation of a CKD-stabilized pavement subgrade showed retained subgrade strength after six years of service life [Solanki & Hauk-Jegen (2016)].

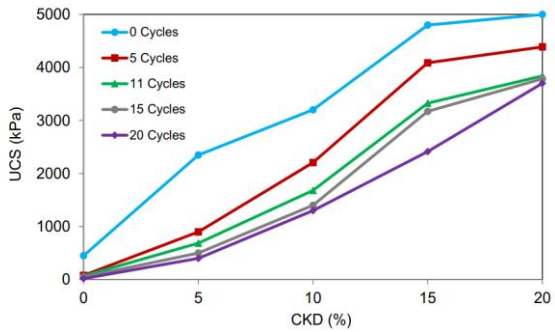


Figure 29 Influence of freeze-thaw cycles and CKD content on unconfined compressive strength of soil [from Ismeik et al. (2021)]

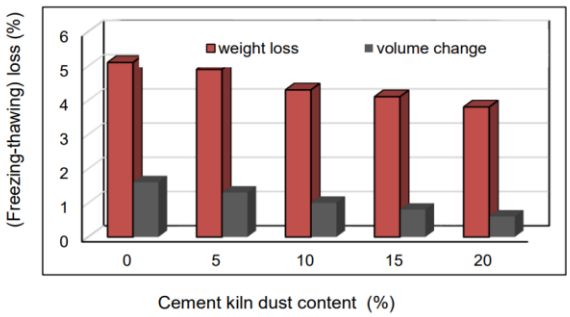


Figure 30 Weight loss and volume change vs. percentage of CKD content [from Alhassani et al. (2021)]

The Mr values of CKD-stabilized specimens decrease with increasing freeze-thaw cycles up to 30, a reduction attributed to increased moisture content during thawing and the formation of ice lenses within pores during freezing [Khoury & Zaman (2006)].

Moreover, Rothhämel et al. (2021) showed that after twelve freeze-thaw cycles, the strength of stabilized samples is reduced compared to without freeze-thaw cycles, but it remains higher than without stabilization.

4.2.5 Field Applicability of CKD Stabilization

Site Conditions Governing Field Success

Successful field stabilization of high-plasticity CH expansive soils with CKD is strongly governed by the soil's initial plasticity index (PI), as unconfined compressive strength gains are inversely proportional to the untreated PI [Miller & Azad (2000); Alhassani et al. (2021)]. CKD treatment is highly effective for CH soils because it reduces liquid limit and plasticity index via cation exchange and flocculation, while simultaneously increasing optimum moisture content (OMC) and decreasing maximum dry density (MDD) to improve workability [Almuaythir & Abbas (2023); Kumar & Janewoo (2016); Mohamedzein et al. (2025)].

The degree of stabilization is further controlled by soil mineralogy, molding water content, curing temperature, and the pH of the soil matrix [Adeyanju & Okeke (2019)]. CKD can stabilize and improve the engineering properties of weak subgrade soils with adequate reactive SiO_2 and Al_2O_3 so that in presence of water the two react with CaO to form cementitious properties [Gilbert (2025)].

Curing duration exerts a significant influence on stress-strain behavior, with UCS values from 1.25 to 5.25 times higher than freshly prepared specimens as curing time increases. The strain at failure decreases by 30–50% with longer curing, indicating that field stabilized layers become stiffer and require time before opening to construction traffic [Peethamparan et al. (2008)].

The effectiveness of CKD in soil stabilization is dependent on both its physical and chemical characteristics, with particle distribution, percentage of CaO, SiO_2, alkali and sulfate content affecting the stabilization effectiveness. CKD's effect on strength depends heavily on the balance between its free CaO and alkali content. When free CaO exceeds roughly 15% while alkalis stay below about 4% K_2O and 3% Na_2O, treated clayey soils gain strength; the reverse composition (low free CaO paired with elevated alkali levels) tends to reduce compressive strength instead [Adeyanju & Okeke (2019)].

High free-lime content CKDs, when reacted with water, produced significant amounts of calcium hydroxide, ettringite and syngenite, and also developed higher unconfined compressive strength

compared to CKDs with lower amounts of free-lime [Peethamparan et al. (2008)]. The active montmorillonite clay flakes adsorbed the soluble calcium cation and sulfate anion on their surfaces that are rich in silica and alumina and then the cation exchange and flocculation–agglomeration processes began [Ogila (2021)].

Field implementation introduces variables difficult to control in the laboratory, including degree of mixing, weather, and subgrade variation [Miller et al. (2003)]. Also, the stress-strain behavior of CKD-treated soil is more brittle than that of lime-treated soil, so the potential for cracking under load must be considered [Miller & Azad (2000)].

Limitations of Field Applicability

A primary limitation of CKD stabilization is that CKD contains significant amounts of alkali, free lime, chloride, and sulfate as native chemical constituents [Mohamedzein et al. (2025); Al-Bakri et al. (2022)]. Because of this sulfate content, CKD acts as a major sulfate source introduced into the ground when used as a soil stabilizer. Whether CKD addition causes a sulfate-induced soil problem depends on the amount of CKD and the existing sulfate concentration in the native soil [Salih et al. (2022)]. Sulfate should not be a significant concern if CKD is added to a base that previously had no or a low content of sulfate, but it could be a problem if large amounts of CKD were added to a base that already contained a high sulfate content [Zemouli et al. (2024)]. The presence of deleterious compounds such as sulfates or organic matter can render CKD-treated soils unfavorable, occasionally performing worse than unstabilized soil [Adeyanju & Okeke (2019)].

As with other calcium-based stabilizers, the potential for adverse reactions in sulfate-bearing soils should be considered. The high free lime and sulfate contents in CKD lower the rate of strength increase in stabilized mixtures compared to cement mixtures [Zemouli et al. (2024)]. Because of the nature of variation in the chemical and mineralogic composition of CKD, sulfate tests should be performed before application of CKD for soil stabilization [Yan et al. (2025)].

The quality of CKD can vary significantly from plant to plant, which can pose a major problem for adopting a state highway specification for general use of CKD. Because of the variation in effectiveness between different CKD sources, the use of CKD should be evaluated on a job-specific basis [Miller & Azad (2000); Miller et al. (2003)].

CKD was also found to have a negative role; it decreased the values of UCS of stabilized soil for sub-base and base materials in the pavement [Salih et al. (2022)]. Increased cement kiln dust content heterogeneously reduces the strength of the clay + CKD mixture beyond an optimal threshold [Zemouli et al. (2024)].

4.2.6 Environmental Impacts

Waste Diversion and Carbon Footprint Reduction

Utilizing industrial waste like CKD as soil stabilizers, decreases pollution and diminishes environmental hazards [Almuaythir et al. (2024); Almuaythir & Abbas (2023)]. The global mass of CKD generated in the World is estimated at 2.4 to 2.8 billion metric tons yearly, making its beneficial use in ground improvement critical to mitigating a massive solid waste problem [Adeyanju & Okeke (2019); Rimal et al. (2019)].

CKD industrial utilization is highly recommended from economic, environmental, and sustainability perspectives because the generated dust quantity equals 15–20% of produced cement [Al-Bakri et al. (2022)]. Accumulation of factory waste like CKD is a serious issue, and its removal and use for soil stabilization provide positive environmental features, solving disposal and soil stability problems simultaneously [Salih (2025); Rimal et al. (2019)].

Using CKD as an additive, cuts down on the need for traditional stabilizers such as cement and lime, which have high carbon emissions during production, thereby lowering the carbon footprint of construction projects [Almuaythir et al. (2024); Almuaythir & Abbas (2023)]. For instance, a stabilized clayey soil with 15% CKD as an environment-friendly method significantly reduces energy consumption (Figure 31) and e-CO_2 emission (Figure 32) compared to a soil stabilized with 9% cement [Ghavami et al. (2020)].

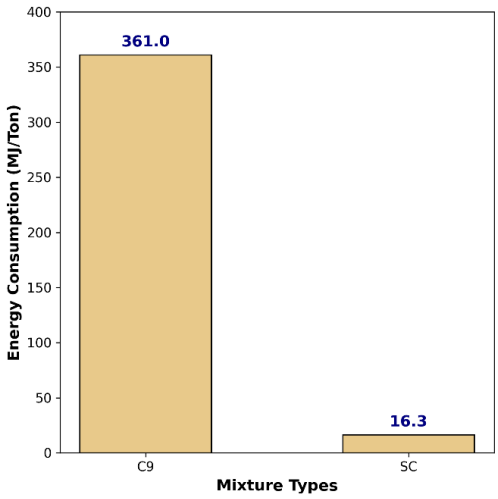


Figure 31 The energy consumption of cement-stabilized and a CKD-stabilized soil [from Ghavami et al. (2020)].

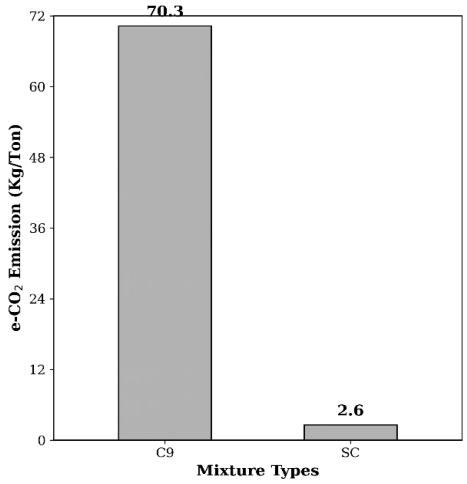


Figure 32 The e-CO2 emission of cement-stabilized and CKD-stabilized soil [from Ghavami et al. (2020)]

'C9' represents the treated soil with 9% of cement and 'SC' represents the treated soil with 15% of CKD.

CKD does not need any further processing or treatment, making it a cheap and readily available waste product that can be utilized in dust form directly from cement production [Adeyanju & Okeke (2019)].

Remediation Benefits

Beyond waste diversion, CKD stabilization actively remediates contaminated soils and reduces the structural damage caused by expansive clays. Utilizing industrial waste like CKD to stabilize expansive soils is of importance in reducing the environmental impact of waste and in alleviating the expansive soil-induced structural damage to infrastructure [Mohamedzein et al. (2025); Ogila (2021)].

CKD exhibits strength in inactivating contaminated soil's toxic elements, such as arsenic and cadmium, introducing it as a low-cost solution in the soil stabilization field. Specifically, the Toxicity Characteristic Leaching Procedure (TCLP) test has shown that CKD stabilization inactivated 80.70% of the cadmium in treated soil [Al-Bakri et al. (2022)].

The use of CKD at 10% was found to be more economical and environmentally beneficial, aligning with sustainable waste management practices in the construction industry [Adeyanju & Okeke (2019)].

Sustainability limits

Table 13 Summary of the main sustainability limits for CKD stabilization of CH expansive soils

Limiting Factor	Why It Reduces Sustainability in CH Expansive Soils

Variable CKD composition	CKD performance depends on particle distribution and CaO, SiO_2, alkali, and sulfate contents, so results are not transferable across dust sources.
Source-dependent reactivity	Fresh CKD appears more effective than generic or mixed-source dust, so stabilization reliability depends on how the dust was produced and collected.
High alkali, sulfate, and chloride loads	Elevated soluble salts can create chemically undesirable treated soils and can restrict safe reuse of some CKD streams.
Performance drops in highly plastic soils	Strength gain is inversely related to untreated plasticity index, so the most problematic CH soils can show smaller proportional improvement.
Negative effect at some dosages	CKD can reduce UCS in some pavement-related applications, so adding more CKD does not always improve sustainability or performance.
Non-unique optimum content	Reported optimum CKD contents range from about 5% to 15% or higher, which makes field design less robust and increases overuse risk.
Higher moisture demand	Several studies report increased optimum moisture content with CKD, which can raise water demand and complicate construction logistics.
Possible compaction penalty	CKD can require higher compactive energy or reduce maximum dry density, which adds construction effort even when other properties improve.
Environmental benefit depends on replacement case	CKD is more sustainable than other stabilizers mainly when it displaces cementitious ones or landfill disposal.

CHAPTER 5 — Comparative Analysis of Traditional and Sustainable Chemical Stabilization Techniques

5.1 Introduction

Building on the traditional stabilization techniques examined in Chapter 3 and the sustainable alternatives described in Chapter 4, this chapter presents a systematic comparative analysis of the four chemical stabilization techniques applied to CH expansive soils: two traditional binders, lime and cement, and two sustainable alternatives, Class C fly ash and cement kiln dust (CKD).

The latter two were selected specifically for their inherent self-cementing properties, which allow them to stabilize expansive soils without requiring a supplementary activator.

As the literature specifically addressing sustainable stabilization of CH-classified soils remains comparatively limited, this chapter also serves to consolidate and critically evaluate the available evidence base.

The comparison is structured into three separate parts, reflecting the different nature of the evidence available for each:

Part I: Effectiveness Comparison evaluates the four techniques quantitatively across four geotechnical performance criteria at lab scale: swell potential reduction, strength gain (unconfined compressive strength), compressibility reduction, and plasticity index reduction.

Part II: Durability Comparison evaluates the four techniques qualitatively, based on reported resistance to degradation mechanisms such as wetting-drying and freeze-thaw cycling.

Part III: Environmental Impact and Sustainability Comparison evaluates the four techniques qualitatively with respect to their sustainability profile.

5.2 Effectiveness Comparison

5.2.1 Methodology

Literature Synthesis Approach

As this thesis is literature-based rather than experimental, the comparative analysis in this chapter relies entirely on the synthesis of previously published laboratory studies. Each labscale study was collected in an **Excel dataset** and is considered a data point.

Where multiple samples were tested within a single study (for instance, soils blended at varying proportions to achieve a range of plasticity values), each sample was treated as an independent data point, since each represents a distinct combination of soil properties and treatment outcome.

Soil Classification Verification

A Python code was designed to confirm that each data point collected falls within the CH classification by plotting LL and PI of every collected sample against the Casagrande A-line, defined as: $PI = 0.73(LL - 20)$.

A soil is classified as CH where $LL \geq 50\%$ and its PI plots above the A-line.

This verification step was considered necessary given that many studies in the sustainable-stabilization literature specifically do not state soil classification explicitly, despite reporting the underlying index properties required to determine it.

Figure 33 presents the outcome after running the code. All data points fall within the CH classification zone, confirming the consistency of the underlying dataset with the scope of this thesis.

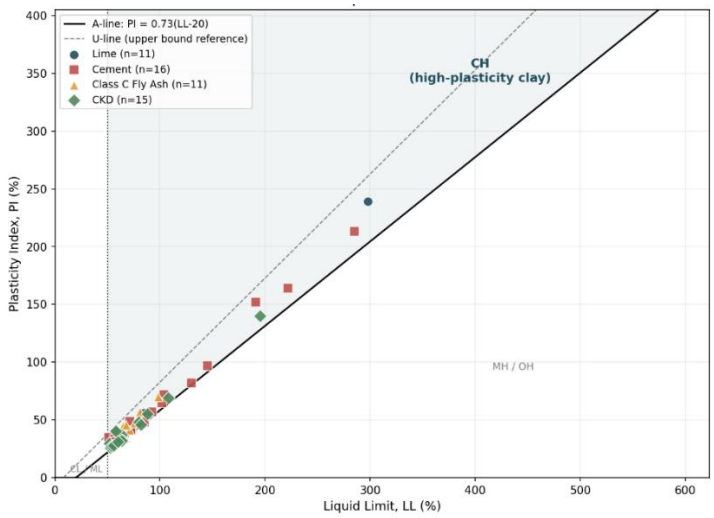


Figure 33 Casagrande plasticity chart of all collected soil studies

Data Extraction and Evidence Thresholds

Data extraction followed a standardized template capturing, for each sample: soil index properties, optimum dosage, curing time, optimum moisture content of the untreated soil, and Plasticity Index (PI), swell potential, UCS, Compressibility, before and after treatment.

A minimum threshold of two independent data points was applied for a technique–criterion combination to be treated as quantitatively comparable. A target of three to five data points per combination was established as providing reasonably stable comparison.

Testing Basis

Four criteria were selected for the quantitative comparison: swell potential reduction, unconfined compressive strength gain (UCS), compressibility reduction, and plasticity index reduction.

All four criteria examined in this chapter are derived exclusively from **laboratory testing** reported in the source literature; no field or in-situ data informs any part of this comparison. The specific laboratory basis for each criterion is described below.

Swell Reduction: swell data were drawn from confined, one-dimensional laboratory swell tests, most commonly following the ASTM D4546 standard, in which a compacted, additive-treated specimen at optimum dosage is inundated under a fixed surcharge pressure (mainly between 1-5 kPa).

UCS Gain: Unconfined compressive strength was determined via the standard unconfined compression test (ASTM D2166), performed on cylindrical, additive-treated specimens compacted at optimum dosage and optimum moisture content, then cured for 28 days.

Compressibility Reduction: Compressibility was assessed through laboratory one-dimensional consolidation (oedometer) testing, following the standard test ASTM D2435, in which a treated specimen at optimum dosage is subjected to incremental vertical loading in a confined ring, and the resulting compression index (Cc) or coefficient of volume compressibility (mv) is derived.

PI Reduction: Plasticity index was determined from the standard Atterberg limits testing (ASTM D4318), measuring the liquid and plastic limits of the soil immediately after mixing with the additive at the optimum dosage, without an intervening curing period.

Normalization and Composite Scoring

For each criterion, outcome values were normalized to percentage change relative to each study's own untreated baseline, rather than compared as absolute values, to account for differing initial soil conditions across studies. Reported ranges are presented as minimum, maximum, and mean values alongside the number of supporting data points (n).

To enable cross-technique comparison, each criterion's mean value per technique was further normalized to a 0–100 scale using min-max normalization across the four techniques, such that the highest-performing technique on a given criterion scores 100 and the lowest scores 0. The normalization equation used is:

$$N_{i,j} = \frac{\bar{x}_{i,j} - \min(\bar{x}_j)}{max(\bar{x}_j) - \min(\bar{x}_j)} \times 100$$

Where:

- i∈ {Lime, Cement, Fly Ash C, CKD} and j∈ {Swell Reduction, UCS Gain, Compressibility Reduction, PI Reduction}
- $\bar{x}_{i,j}$= the mean value of criterion j for technique i
- $\min(\bar{x}_j)$, $\max(\bar{x}_j)$= the minimum and maximum mean values for criterion j across all four techniques.
- $N_{i,j}$= the resulting normalized score (0–100) for technique i on criterion j.

Then, an equal-weighted composite Effectiveness Score was computed using this formula:

$$E_i = \frac{1}{4}\sum_{j=1}^{4} N_{i,j} = \frac{N_{i,Swell} + N_{i,UCS} + N_{i,Comp} + N_{i,PI}}{4}$$

5.2.2 Results and Discussion

Literature Coverage

Error! Reference source not found. summarizes the number of independent data points (n) supporting each technique–criterion combination. All combinations meet the minimum evidentiary threshold of two data points established in Section 5.2.1.

Table 14 Number of literature data points used in this study

Criterion	Lime	Cement	Fly Ash C	CKD
Swell Reduction	5	8	7	6
UCS Gain	6	7	7	8
Compressibility Reduction	4	4	3	2
PI Reduction	9	11	8	12

Summary Matrix and normalized comparison

Error! Reference source not found. presents the outcome of the calculation, which is the range and mean for each technique across all four criteria, expressed as percentage improvement relative to each study's own untreated baseline.

Table 15 Result matrix

Criterion	Lime	Cement	Fly Ash C	CKD
Swell Reduction	67.9–95.4% (mean 85.7%)	70.0–99.5% (mean 92.7%)	32.7–86.5% (mean 71.3%)	63.8–85.0% (mean 71.7%)
UCS Gain	137.6–469.3% (mean 298.2%)	225.0–1503.9% (mean 668.0%)	58.3–450.0% (mean 286.1%)	118.2–2383.8% (mean 1072.0%)
Compressibility Reduction	12.7–90.0% (mean 63.8%)	15.4–92.6% (mean 64.3%)	58.3–66.0% (mean 61.8%)	28.6–38.5% (mean 33.5%)
PI Reduction	23.8–73.0% (mean 46.7%)	3.0–91.4% (mean 50.8%)	8.0–92.5% (mean 62.2%)	23.1–65.5% (mean 42.4%)

Each criterion's mean value normalized to a 0–100 scale across the four techniques is shown in **Error! Reference source not found.**, with Figure 34 (grouped bar chart) presenting the same data visually.

Table 16 Normalized scores (0–100)

Criterion	Lime	Cement	Fly Ash C	CKD
Swell Reduction	67.3	100	0	1.9
UCS Gain	1.5	48.6	0	100
Compressibility Reduction	98.4	100	91.9	0
PI Reduction	21.7	42.4	100	0

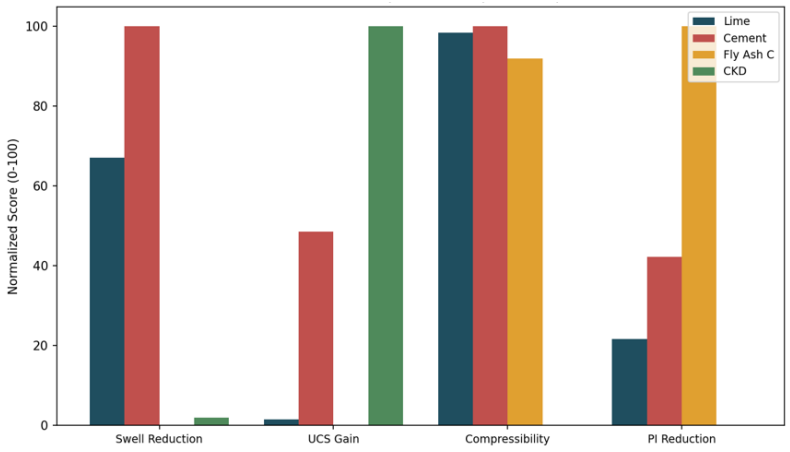


Figure 34 Bar chart of normalized scores

Swell reduction

Based on the mean values, cement recorded the highest mean swell reduction (92.7%), followed by Lime (85.7%), with CKD (71.7%) and Fly Ash C (71.3%) trailing closely behind each other at the bottom of the ranking. Cement leads this criterion with a normalized score of 100, followed by Lime (67.3), with CKD (1.9) and Fly Ash C (0) essentially tied well behind both.

Cement's strong performance here is nonetheless mechanistically explicable. OPC undergoes immediate hydraulic hydration upon contact with water, producing calcium silicate hydrate and calcium aluminate hydrate gels that fill interparticle voids and rigidly bind clay particles together within hours, whereas lime, Class C fly ash, and CKD rely primarily on cation exchange and flocculation in the short term and develop cementitious bonds only through slower pozzolanic reactions that require sustained high-pH conditions and longer curing periods [Ijaz et al. (2022); Yan et al. (2025); Ogila (2021)].

Lime treatment depends on dissolution of clay silica and alumina at high pH before pozzolanic products form, a process that is inherently slower and more sensitive to ambient temperature and moisture than cement hydration [Ogila (2021); Utkarsh & Jain (2024)].

Class C fly ash possesses some self-cementing properties, but its pozzolanic reactivity is lower than OPC's hydraulic reactivity [Utkarsh & Jain (2024)].

CKD contributes soluble calcium for cation exchange and produces pozzolanic compounds with curing, but its variable composition and lower free-lime content compared with OPC limit the rate and quantity of hydration products formed [Ogila (2021); Yan et al. (2025)].

UCS Gain

Based on the mean values, CKD recorded the highest UCS gain (1072.0%), followed by Cement (668.0%), Lime (298.2%), and Fly Ash C (286.1%), with Lime and Fly Ash C close and at the bottom of the ranking. CKD and Cement with a normalized score of 100 and 48.6, respectively, lead this criterion by a wide margin over Lime and Fly Ash C with a normalized score of 1.5 and 0, respectively, which is broadly consistent with the underlying stabilization mechanisms.

CKD-stabilized specimens exhibit higher unconfined compressive strength (UCS) than lime and Class C fly ash-treated specimens because CKD supplies both free lime for immediate cation exchange and reactive silica/alumina for sustained pozzolanic cementation [Solanki et al. (2009); Almuaythir et al. (2024); Gilbert (2025)]. Upon contact with water, CKD rapidly raises the pH, Electrical Conductivity, and Total Dissolved Solids of the clay system, creating favorable conditions for dissolution of clay particle edges and surfaces, which accelerates pozzolanic product formation compared with the slower dissolution-dependent mechanisms of lime alone [Ogila, (2021)].

While ordinary Portland cement (OPC) achieves rapid hydration, CKD's combination of hydraulic and pozzolanic reactivity yields comparable and even higher long-term strength, with 13% CKD matching the strength of 10% OPC at extended curing [Yoobanpot et al. (2017); Yan et al. (2025)].

Compressibility reduction

This criterion shows a distinctly different pattern from swell reduction and UCS gain: rather than a spread across, all three techniques cluster tightly together with a normalized score of 100

(mean of 64.3%), 98.4 (mean of 63.8%) and 91.9 (mean of 61.8%) respectively, while CKD sits well apart with a normalized score of 0 (mean of 33.5%), at roughly half their performance.

CKD-stabilized specimens showed the lowest increments in optimum moisture content and only slight reductions in maximum dry density, indicating less pore-filling, double-layer suppression and particle bonding than the other stabilizers achieve [Almuaythir et al. (2024)].

The higher calcium oxide content in cement, lime, and Class C fly ash drives more complete pozzolanic reactions, producing a denser soil structure that yields greater compressibility reduction than CKD can achieve at equivalent dosages [Utkarsh & Jain (2024); Almuaythir et al. (2024); Almuaythir et al. (2025)].

PI reduction

Class C Fly Ash leads this criterion by a clear margin with a normalized score of 100 and a mean of 62.2, with Cement, Lime, and CKD clustered more closely together beneath it with a normalized score of 42.4 (mean of 50.8%), 21.7 (mean of 46.7%) and 0 (mean of 42.4%), respectively.

The main reason is that fly ash itself possesses no plasticity; therefore, its direct addition, dilutes the soil's clay fraction and lowers the PI proportionally to the replacement ratio [Deepak et al. (2020)]. Cement and lime primarily rely on hydraulic hydration or slow pozzolanic dissolution, respectively, which modify interparticle bonding but do not physically dilute the clay fraction to the same extent [Deepak et al. (2020); Rai et al. (2021)].

Composite Effectiveness Score

After applying an equal-weighted composite Effectiveness Score, we obtained that cement achieves the highest composite score by a clear margin (72.7), followed by Fly Ash C and Lime that closely matched in second and third place (48 and 47.2 respectively), while CKD ranked last by a substantial margin (25.5).

The composite Effectiveness Scores across the four techniques are shown in Figure 35.

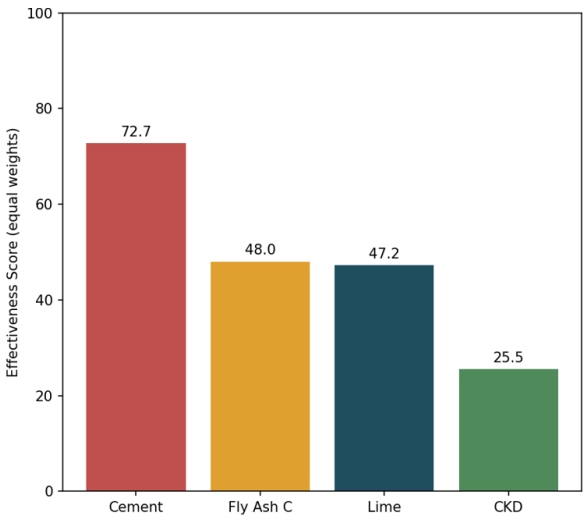


Figure 35 Composite Effectiveness Score

Taken together, the results of this section point to a clear overall conclusion: **Cement is the most effective technique for stabilizing CH expansive soils at lab scale** among the four evaluated in this thesis.

A notable secondary finding is that Fly Ash C and Lime achieved closely matched effectiveness, indicating that a sustainable, self-cementing byproduct can perform at a level of overall effectiveness comparable to an established traditional binder, rather than trailing behind it as a lesser alternative. This is a meaningful result for the sustainability motivation of this thesis: it demonstrates that adopting a lower-carbon industrial byproduct in place of lime did not come at the cost of reduced geotechnical effectiveness.

CKD, by contrast, ranks lowest of the four overall, despite recording the single highest score of any technique on UCS gain that outperformed all others by a wide margin. This apparent contradiction illustrates an important point: strong performance on one criterion does not guarantee strong performance overall, and CKD's comparatively weak results on the remaining three criteria were sufficient to outweigh its standout strength gain in the composite ranking.

5.3 Durability Comparison

5.3.1 Wetting-drying durability assessment

Error! Reference source not found. presents a qualitative assessment of wetting-drying durability performance across the four stabilization techniques.

Table 17 Qualitative wetting-drying durability assessment.

Stabilizer	Qualitative Assessment	Wetting-drying Performance	Key Dosage Finding	Citations
Cement	High	Survived 12 wetting-drying cycles in several cases with limited mass loss.	≥10% cement needed to meet Portland Cement Association durability specifications.	Zhang et al. (2019); Eskişar et al. (2015); Liu et al. (2021)
Lime	Low	5%, 7%, and 9% lime-treated CH failed after 3, 4, and 6 wetting-drying cycles.	> 6% lime required for satisfactory wetting-drying resistance.	Ismeik & Shaqour (2018); Nguyen et al. (2019); Akhtar & Li (2025)
Class C Fly Ash	Medium	Class C fly ash-stabilized clay survived 12 wetting-drying cycles but with progressive mass loss.	15–20% Class C fly ash optimal for pozzolanic durability.	Zhang et al. (2019); Shibi & Kamei (2014)
CKD	High	CKD-treated soils survived 12 wetting-drying cycles; durability improved proportionally with CKD content.	10–15% CKD provides maximum wetting-drying resistance.	Solanki et al. (2013)

Cement-treated CH soil specimens remain intact for more wetting-drying cycles than lime-treated soil at the same dosage, demonstrating insusceptibility to moisture fluctuations [Kumar et al. (2024)]. High cement content enhances stability by strengthening cementation bonds and reducing the weight loss of soil samples during cyclic wetting-drying exposure [Yangsukkasem et al. (2024)]. On the other hand, CKD represents an effective alternative to traditional stabilization agents, indicating robust pozzolanic and cementitious bonding under wetting-drying cycling [Parsons & Kneebone (2004); Khoury & Zaman (2007)]

Lime-treated CH soil is not durable against wetting-drying cycles, as surface cracks induced during the first drying cycle propagate into open cracks, allowing water infiltration and complete specimen failure [Kumar et al. (2024)]. The initial beneficial effect of lime stabilization on swelling behavior is usually lost after the first wetting-drying cycle, with swelling potential increasing in subsequent cycles [Güney et al. (2007)]. Consequently, Class C Fly ash underperforms compared to robust stabilizers like cement, earning it a medium qualitative assessment.

5.3.2 Comparative freeze-thaw durability assessment

Error! Reference source not found. presents a qualitative comparison between the four stabilizers based on the durability under freeze-thaw cycling. The ranking is driven mainly by how each stabilizer holds strength after repeated freeze-thaw exposure in high-plasticity clay. CKD stays at the top because direct fat clay comparisons found it provided the maximum resistance [Solanki et al. (2013); Solanki & Hauk-Jegen (2016)]. OPC remains strong, but not perfectly damage-proof. Lime sits in the middle because it clearly improves durability versus untreated clay, whereas Class C fly ash is best treated as low-medium to medium rather than high.

Table 18 Freeze-thaw performance with the corresponding dosage

Stabilizer	Qualitative Assessment	Freeze-thaw Performance	Key Dosage Finding
OPC	Medium-High to High	Cement-treated fat clays retain much higher strength than untreated soil under freeze-thaw cycling, but strength still drops with increasing cycles, especially in the first few cycles [Eskişar et al. (2015); Ding et al. (2018); Zhang et al. (2026)]. Some OPC-treated clay mixtures survive 12 cycles and satisfy Portland Cement Association durability criteria based on percentage loss [Aryal & Kolay (2020)].	5–10% OPC is the most supported range in clay soils, with clear gains from higher cement content [Sagidullina et al. (2022); Eskişar et al. (2015)]

Lime	Medium	Lime improves freeze-thaw resistance relative to untreated cohesive soils, but freeze-thaw cycles still reduce strength and cause cracking, with worse damage in highly plastic or bentonitic soils [Ismeik & Shaqour (2018); Nguyen et al. (2019); Hotineanu et al. (2015); Soğancı et al. (2012)]. Lime-treated soils can retain integrity better with longer curing, but performance is less reliable in very active CH soils [Hotineanu et al. (2015); Nguyen et al. (2019); Orazi et al. (2022)].	4–8% lime is the most consistent effective range, with durability improving as lime content rises, though soil mineralogy strongly controls the outcome [Ismeik & Shaqour (2018); Dağlı et al. (2026); Shirmohammadi et al. (2021); Soğancı et al. (2012)].
Class C Fly Ash	Low-Medium to Medium	Class C fly ash improves post-freeze-thaw strength relative to untreated CH soils, but repeated cycles still cause substantial strength loss and higher swell in expansive clays [Bin-Shafique et al. (2010); Bin-Shafique et al. (2011)]. Direct CH comparisons show Class C fly ash underperforms CKD under freeze-thaw cycling. [Solanki & Hauk-Jegen (2016)].	10–20% Class C fly ash is the most supported range, with 10% often practical and 20% often giving stronger stabilization, though durability remains cycle-sensitive [Bin-Shafique et al. (2010); Bin-Shafique et al. (2011); Sengul et al. (2023); Arslan et al. (2025)].
CKD	High	CKD shows the most consistent high freeze-thaw durability in fat clay comparisons, with higher post-cycle UCS than Class C fly ash and major reductions in freeze-thaw damage relative to untreated soil [Solanki & Hauk-Jegen (2016); Ismeik et al. (2021); Alhassani et al. (2021)]. Treated specimens commonly survive full test programs, and durability improves as CKD content increases [Alhassani et al. (2021); Al-Hassani et al. (2015)].	10–20% CKD is the clearest durability-oriented range, with 20% giving the strongest freeze-thaw improvement in some clayey-soil studies [Ismeik et al. (2021); Alhassani et al. (2021)].

5.4 Environmental Impact and Sustainability Comparison

Table 19 shows the assessment of the sustainability of each stabilizer, considering its environmental impacts and sustainability profile.

Ordinary Portland cement (OPC) and lime carry high carbon footprints, while Class C fly ash and cement kiln dust (CKD) offer substantial sustainability advantages as industrial wastes. The production of traditional stabilizers is energy-intensive and emissions-heavy, driving a transition toward waste-derived alternatives. In short, the literature strongly agrees that replacing traditional binders with industrial wastes reduces environmental impacts.

Table 19 Sustainability assessment.

Stabilizer	Qualitative Assessment	CO_2 Emissions & Energy	Sustainability Profile

OPC	Low	Manufacturing 1 tonne of OPC consumes 1.5 tonnes of raw materials, requires 5.6 GJ/tonne of energy, and emits ~0.9 tonnes of CO_2 [Hm (2021)]. Cement production accounts for 7–8% of global CO_2 emissions [Pankaja et al. (2023)]	High environmental burden from calcination and raw material extraction [Wang et al. (2021)].
Lime	Low to Medium	Lime production emits approximately 1.281 tonnes of CO_2 per tonne, exceeding cement per unit mass [Wang et al. (2021)]. Production is highly energy-intensive.	High emissions but lower than OPC; often blended with pozzolans to reduce footprint [Wang et al. (2021)].
Class C Fly Ash	High	Global warming potential is 0.00526–0.027 kg CO_2 eq/kg, drastically lower than OPC and lime. Requires no calcination energy as a waste by-product [Pankaja et al. (2023)]	Decrease of waste landfilling; pozzolanic reactions provide self-cementing properties, conserving natural resources [Pankaja et al. (2023)].
CKD	High	Bypasses energy-intensive clinker production; upcycling CKD cuts landfill disposal impacts [El-Attar et al. (2017)] CKD can cut CO_2 emissions by up to 89% versus OPC [Mousa et al. (2025)].	Reuses industrial waste; reduces reliance on traditional binders, aligning with circular economy goals [Akbulut et al. (2024); El-Attar et al. (2017)].

5.5 Cross-Criteria Synthesis

The three assessment criteria described in this chapter evaluated Lime, Cement, Class C Fly Ash, and CKD along dimensions that do not necessarily point toward the same conclusion. This section draws the three parts together to assess whether a consistent recommendation emerges. Table 20 represents a summary of the results of the three parts.

Technique	Effectiveness (composite)	Durability (wetting-drying / freeze-thaw)	Sustainability profile
Cement	1st (72.8)	High / Medium-High–High	Low
Fly Ash C	2nd (48.0)	Medium / Low-Medium–Medium	High
Lime	3rd (47.2)	Low / Medium	Low–Medium
CKD	4th (25.5)	High / High	High

Table 20 Assessment of the overall performance based on effectiveness, durability, and sustainability of the soil stabilization

Cement leads decisively on effectiveness at lab scale and matches CKD for the strongest durability standing of the four techniques, performing reliably under both wetting-drying and freeze-thaw cycling compared to the other techniques. Its environmental profile, however, is the weakest of the four: the lowest sustainability rating of any technique evaluated, driven by the substantial CO_2 emissions and energy intensity inherent to Portland cement production. This

combination illustrates a clear trade-off: cement's leading performance and durability come at a distinct environmental cost, making it the least favorable of the four techniques on sustainability grounds specifically.

Fly Ash C and Lime present a closely comparable profile on the two performance dimensions, but diverge sharply on sustainability. Their composite effectiveness scores are nearly identical, and both occupy the same lower durability tier relative to Cement and CKD: Fly Ash C performs somewhat better under wetting-drying cycling, while their freeze-thaw performance is broadly similar. Where the two techniques clearly separate is sustainability: Fly Ash C carries a high rating, reflecting its status as a waste, requiring no calcination energy, whereas Lime's production remains energy-intensive and carbon-heavy despite being less severe than Cement's. Given that Fly Ash C matches Lime's effectiveness, is not meaningfully behind it on durability, and offers a substantially better environmental profile, Fly Ash C stands as a strong substitute for Lime in CH soil stabilization, an interesting finding in this comparison where a shift toward sustainability does not require sacrificing geotechnical performance.

Finally, **CKD** shares the strongest durability, alongside cement, and shares the strongest sustainability standing, alongside Fly Ash C. Its effectiveness ranking, however, is the weakest of the four by a substantial margin. CKD therefore presents an unusual profile among the four techniques: strong on durability and sustainability, but held back on overall effectiveness by weakness in one specific criterion rather than a broadly weaker stabilization mechanism.

Conclusion

This thesis set out to examine chemical stabilization of CH expansive soils, motivated by the absence of a standardized framework for comparing these techniques directly against one another on CH-classified soils specifically. Chapters 3 and 4 established the individual performance characteristics of two traditional binders, lime and cement, and two sustainable, self-cementing industrial wastes, Class C fly ash and cement kiln dust (CKD), drawing on published literature spanning swell suppression, strength development, compressibility, and plasticity behavior. Chapter 5 then undertook a systematic comparison of all four techniques across three dimensions: quantitative effectiveness, qualitative durability, and sustainability, synthesizing data points across a verified CH-classified soil dataset.

The comparative analysis in Chapter 5 demonstrated that no single technique leads across all three dimensions evaluated.

1. Cement achieved the highest composite effectiveness score and the strongest durability standing of the four techniques, but recorded the lowest sustainability rating, reflecting the substantial carbon footprint associated with Portland cement production.
2. Fly Ash C and Lime achieved closely matched results on both effectiveness and durability, but diverged sharply on sustainability, given that Fly Ash C does not require calcination energy. Seen its performance and durability alongside this environmental advantage, Fly Ash C emerges as a strong substitute for Lime.
3. CKD presented the most distinctive profile of the four: it matched Cement's durability standing and Fly Ash C's sustainability standing, but it recorded the weakest overall effectiveness score despite achieving the highest score for UCS gain, indicating that strong performance on one property does not guarantee strong performance overall.

This finding constitutes the central contribution of the thesis: rather than identifying a universal replacement for traditional binders, the comparison demonstrates that the traditional-versus-sustainable trade-off is not uniform across techniques. In the case of Fly Ash C and Lime, sustainability was achieved without a corresponding loss in effectiveness or durability, showing that a shift toward a lower-carbon alternative did not come at the cost of geotechnical performance. Cement and CKD, by contrast, illustrate the opposite pattern: strong performance on some dimensions paired with a clear weakness on another.

It should be emphasized that all findings presented in this thesis, including the comparative rankings established in Chapter 5, are derived exclusively from laboratory-scale data. No field-scale testing or long-term in-situ monitoring informs any part of this comparison. Consequently, the relative performance differences identified in this thesis should be regarded as indicative rather than conclusive for field-scale application, and field trials with long-term monitoring are recommended to consolidate these findings.

REFERENCES

Abbey, S., Eyo, E., & Ng'ambi, S. (2019). Swell and microstructural characteristics of high-plasticity clay blended with cement. *Bulletin of Engineering Geology and the Environment, 79*, 2119-2130. https://doi.org/10.1007/s10064-019-01621-z

Abdullah, H. H., & Shahin, M. A. (2023). Geomechanical Properties of Clay Stabilised with Fly Ash-Based Geopolymer Subjected to Long-Term Sulfate Attack. *International Journal of Geosynthetics and Ground Engineering, 9*, 1-11. https://doi.org/10.1007/s40891-023-00493-4

Adekunle, S. (2024). Carbon sequestration potential of cement kiln dust: Mechanisms, methodologies, and applications. *Journal of Cleaner Production*. https://doi.org/10.1016/j.jclepro.2024.141283

Adeyanju, E., & Okeke, C. (2019). Clay soil stabilization using cement kiln dust. *IOP Conference Series: Materials Science and Engineering, 640*. https://doi.org/10.1088/1757-899x/640/1/012080

Akbulut, Z., Yavuz, D., Tawfik, T. A., Smarzewski, P., & Guler, S. (2024). Enhancing Concrete Performance through Sustainable Utilization of Class-C and Class-F Fly Ash: A Comprehensive Review. *Sustainability*. https://doi.org/10.3390/su16124905

Akhtar, S., & Li, B. (2025). Experimental study of mechanical behaviours of lime-treated Quebec silty clay soils under freeze–thaw cycles. *Environmental Geotechnics*. https://doi.org/10.1680/jenge.24.00118

Al-Bakri, A. Y., Ahmed, H. M., & Hefni, M. (2022). Cement Kiln Dust (CKD): Potential Beneficial Applications and Eco-Sustainable Solutions. *Sustainability*. https://doi.org/10.3390/su14127022

Al-Bakri, A. Y., Ahmed, H. M., & Hefni, M. (2023). Eco-Sustainable Recycling of Cement Kiln Dust (CKD) and Copper Tailings (CT) in the Cemented Paste Backfill. *Sustainability*. https://doi.org/10.3390/su15043229

Alexander, D. V., Wilson-Ollivierre, Y., Herreira, X., & Mohammed, A. Cement Stabilization of a Tropical Expansive Clay: Effect on Plasticity and Shear Strength.

Al-Hassani, A. M. J., Kadhim, S. M., & Fattah, A. (2015). Characteristics of Cohesive Soils Stabilized by Cement Kiln Dust.

Alhassani, A. M. J., Kadhim, S. M., & Fattah, A. (2021). Stabilization of Clayey Soil Using Cement Kiln Dust as Sustainable Material. *IOP Conference Series: Earth and Environmental Science, 856*. https://doi.org/10.1088/1755-1315/856/1/012038

Al-Mohammedi, A. A. S. (2024). Analysis of the Effects of Temperature and Treatment Duration on the Resistance of Expansive Soil Improved with Lime in Baghdad, Iraq. *Engineering, Technology & Applied Science Research*. https://doi.org/10.48084/etasr.8850

Almuaythir, S., & Abbas, M. F. (2023). EXPANSIVE SOIL REMEDIATION USING CEMENT KILN DUST AS STABILIZER. *Case Studies in Construction Materials*. https://doi.org/10.1016/j.cscm.2023.e01983

Almuaythir, S., Zaini, M. S. I., & Hasan, M. (2025). Shear strength, compressibility, and consolidation behaviour of expansive clay soil stabilized with lime and silica fume. *Scientific Reports, 15*. https://doi.org/10.1038/s41598-025-10642-6

Almuaythir, S., Zaini, M. S. I., Hasan, M., & Hoque, M. I. (2024). Sustainable soil stabilization using industrial waste ash: Enhancing expansive clay properties. *Heliyon, 10*. https://doi.org/10.1016/j.heliyon.2024.e39124

Al-Mukhtar, M., Khattab, S., & Alcover, J. F. (2012). Microstructure and geotechnical properties of lime-treated expansive clayey soil. *Engineering geology*, *139*, 17-27. https://doi.org/10.1016/j.enggeo.2012.04.004

Almurshedi, A. D., Thajeel, J. K., & Dekhn, H. (2019). Swelling Control of Expansive Soils Using Cement Dust. *IOP Conference Series: Materials Science and Engineering, 584*. https://doi.org/10.1088/1757-899x/584/1/012021

Alnmr, A., Alsirawan, R., Ray, R., & Alzawi, M. O. (2024). Compressibility of expansive soil mixed with sand and its correlation to index properties. *Heliyon*, *10*(15). https://doi.org/10.1016/j.heliyon.2024.e35711

Alqawasmeh, H. (2025). Enhancing the sustainability of geotechnical engineering with utilization of fly Ash. *Discover Materials, 5*. https://doi.org/10.1007/s43939-025-00183-0

Al-Taie, A., Disfani, M., Evans, R., Arulrajah, A., & Horpibulsuk, S. (2018). Impact of curing on behaviour of basaltic expansive clay. *Road Materials and Pavement Design, 19*, 624 - 645. https://doi.org/10.1080/14680629.2016.1267660

Al-Taie, A., Disfani, M., Evans, R., Arulrajah, A., & Yaghoubi, E. (2021). Impact of Lime Stabilization on Swelling and Soil Water Retention Behavior of Expansive Subgrade. *Lecture Notes in Civil Engineering*. https://doi.org/10.1007/978-3-030-77230-7_58

Altmeyer, W. T. (1955, March). Discussion of engineering properties of expansive clays. In *Proc. ASCE* (Vol. 81, No. 658, pp. 17-19).

Arslan, E., Develioglu, I., & Pulat, H. F. (2025). A Comparative Study on the Performance of Freeze-Thaw Cycled Alluvial Soils Stabilized with Lime and Fly Ash. *Karadeniz Fen Bilimleri Dergisi*. https://doi.org/10.31466/kfbd.1609555

Aryal, S., & Kolay, P. (2020). Long-Term Durability of Ordinary Portland Cement and Polypropylene Fibre Stabilized Kaolin Soil Using Wetting–Drying and Freezing–Thawing Test. *International Journal of Geosynthetics and Ground Engineering, 6*, 1-15. https://doi.org/10.1007/s40891-020-0191-9

ASTM, D. (1988). Standard test method for expansion index of soils. *Annual Book of ASTM Standards*, 4-8.
ASTM, D. (2004). 427, Test Method for shrinkage factors of soils by the mercury method. *Annual Book of ASTM Standards*, *4*.
ASTM, D. (2017). 4318-17e1. *Standard Test Methods for Liquid Limit, Plastic Limit, and Plasticity Index of Soils, ASTM International, West Conshohocken, PA*.
Babanas, H., & Courcelles, B. (2025). Enhancing Lime Dosage Determination for Lean Clay Soil Improvement: Significance of Plasticity Limit and Interpretation Approach. *Geotechnics*. https://doi.org/10.3390/geotechnics5010009
Barnat-Hunek, D., Góra, J., Suchorab, Z., & Łagód, G. (2018). Cement kiln dust. 149-180. https://doi.org/10.1016/b978-0-08-102156-9.00005-5
Bell, F. (1996). LIME STABILIZATION OF CLAY MINERALS AND SOILS. *Engineering Geology, 42*, 223-237. https://doi.org/10.1016/0013-7952(96)00028-2
Bell, F.G. Lime stabilization of clay soils. *Bulletin of the International Association of Engineering Geology* **39**, 67–74 (1989). https://doi.org/10.1007/BF02592537
Benghazi, Z., Tobal, R., & Djellali, A. (2024). Life Cycle Analysis Comparison of Stabilizing Materials for Expansive Soils. *ARCHive-SR*. https://doi.org/10.21625/archive-sr.v8i2.1086
Bhandari, I., Kumar, R., Sofi, A., & Nighot, N. (2023). A systematic study on sustainable low carbon cement – Superplasticizer interaction: Fresh, mechanical, microstructural and durability characteristics. *Heliyon, 9*. https://doi.org/10.1016/j.heliyon.2023.e19176
Bin-Shafique, S., Rahman, K., & Azfar, I. (2011). The Effect of Freezing-Thawing Cycles on Performance of Fly Ash Stabilized Expansive Soil Subbases. 697-706. https://doi.org/10.1061/41165(397)72
Bin-Shafique, S., Rahman, K., Yaykiran, M., & Azfar, I. (2010). The long-term performance of two fly ash stabilized fine-grained soil subbases. *Resources Conservation and Recycling, 54*, 666-672. https://doi.org/10.1016/j.resconrec.2009.11.007
BIS, I. (1970). 1498 Classification and identification of soils for general engineering purposes. *Methods test soils*.
BIS, I. (1977). 2720 Methods of test for soils: part 40 determination of free swell index of soils. *Bureau of Indian Standards, New Delhi, India: BIS*.
Campo, F., Tua, C., Biganzoli, L., Pantini, S., & Grosso, M. (2021). Natural and enhanced carbonation of lime in its different applications: a review. *Environmental Technology Reviews, 10*, 224 - 237. https://doi.org/10.1080/21622515.2021.1982023
Casagrande, A. (1948). Classification and identification of soils. *Transactions of the American Society of Civil Engineers*, *113*(1), 901-930. https://doi.org/10.1061/TACEAT.0006109
Chabi, E., Adéoti, G. O., Ahlinhan, M., & Agassoussi, L. M. (2025). Evaluating Pavement Performance on Expansive Clay Soils Subjected to Cyclic Shrinkage and Swelling. *Open Journal of Applied Sciences*. https://doi.org/10.4236/ojapps.2025.151006
Chen, F. (1975). Foundations on expansive soils.
Chen, S. X., S. Song, Yu, Z. G. Liu, F. Yu, and X. C. Xu. 2006. "Effect of Soil Sample Preparation on Free Swelling Ratio and Its Improved Measures." Rock and Soil Mechanics 27(8): 1327–1330.
Chen, Y., He, X., Zhang, S., Tan, X., & Wan, Y. (2020). Strength and microstructure properties of solidified sewage sludge with two types of cement-based binders. *Scientific Reports, 10*. https://doi.org/10.1038/s41598-020-77701-y
Cheng, X., Li, Q., Hai, R., Li, S., & He, X. (2024). Research on mechanical properties of weak expansive soil under conditions of different confining pressures and moisture contents based on triaxial test. *PLOS ONE, 19*. https://doi.org/10.1371/journal.pone.0308364
Cherian, C., & Arnepalli, D. N. (2015). A Critical Appraisal of the Role of Clay Mineralogy in Lime Stabilization. *International Journal of Geosynthetics and Ground Engineering, 1*, 1-20. https://doi.org/10.1007/s40891-015-0009-3
Chi, ZC., Dai, ZJ., Chen, SX. *et al.* Effect of hydration on mechanical properties and microstructure of expansive soil. *Environ Earth Sci* **82**, 133 (2023). https://doi.org/10.1007/s12665-023-10837-y
Chittoori, B., & Puppala, A. J. (2011). Quantitative estimation of clay mineralogy in fine-grained soils. *Journal of Geotechnical and Geoenvironmental engineering*, *137*(11), 997-1008. https://ascelibrary.org/doi/abs/10.1061/(ASCE)GT.1943-5606.0000521
Chou, S., Huang, J., Lakkimsetti, B., Parr, K., Puppala, A., & Cetin, B. (2026). Experimental study on engineering and microstructural behavior of lime sludge stabilized expansive soils under cyclic environmental stressors. *Engineering Geology*. https://doi.org/10.1016/j.enggeo.2026.108690
Cui, S., Du, Y., Tian, M., & Wang, X.-P. (2016). Effect of Cement Kiln Dust on unconfined compressive strength property of expansive soil. https://doi.org/10.2991/iccahe-16.2016.10
Cui, S., Wang, J. D., Wang, X., Du, Y., & Wang, X. (2018). Mechanical behavior and micro-structure of cement kiln dust-stabilized expensive soil. *Arabian Journal of Geosciences, 11*, 1-8. https://doi.org/10.1007/s12517-018-3864-0
Dafalla, M., Shaker, A., Elkady, T., Almajed, A., & Al-Shamrani, M. (2020). Shear strength characteristics of a sand clay liner. *Scientific reports*, *10*(1), 18226. https://doi.org/10.1038/s41598-020-75188-1

Dağlı, E., Çapar, Ö., & Sert, S. (2026). Lime–fly ash binder composition controls freeze–thaw durability of stabilized clays. *Scientific Reports, 16*. https://doi.org/10.1038/s41598-026-52479-7
Dawson, B. (1953). The structure of the 9(18)-heteropoly anion in potassium 9(18)-tungstophosphate, K6(P2W18O62).14H2O. *Acta Crystallographica, 6*, 113-126. https://doi.org/10.1107/s0365110x53000466
Dayioglu, M., Cetin, B., & Nam, S. (2017). Stabilization of expansive Belle Fourche shale clay with different chemical additives. *Applied Clay Science, 146*, 56-69. https://doi.org/10.1016/j.clay.2017.05.033
Deepak, M., Rohini, S., Harini, B., & Ananthi, G. B. G. (2020). Influence of fly-ash on the engineering characteristics of stabilised clay soil. *Materials Today: Proceedings*. https://doi.org/10.1016/j.matpr.2020.07.497
Dermatas, D., & Meng, X. (2003). UTILIZATION OF FLY ASH FOR STABILIZATION/SOLIDIFICATION OF HEAVY METAL CONTAMINATED SOILS. *Engineering Geology, 70*, 377-394. https://doi.org/10.1016/s0013-7952(03)00105-4
Dhar, S., & Hussain, M. (2019). The strength and microstructural behavior of lime stabilized subgrade soil in road construction. *International Journal of Geotechnical Engineering, 15*, 471 - 483. https://doi.org/10.1080/19386362.2019.1598623
Ding, M., Zhang, F., Ling, X., & Lin, B. (2018). Effects of freeze-thaw cycles on mechanical properties of polypropylene Fiber and cement stabilized clay. *Cold Regions Science and Technology*. https://doi.org/10.1016/j.coldregions.2018.07.004
Driss, A., Harichane, K., & Ghrici, M. (2022). Effect of lime on the stabilization of an expansive clay soil in Algeria. *Journal of Geomechanics and Geoengineering*. https://doi.org/10.38208/jgg.v1i1.413
Edil, T., Acosta, H. A., & Benson, C. (2006). Stabilizing Soft Fine-Grained Soils with Fly Ash. *Journal of Materials in Civil Engineering, 18*, 283-294. https://doi.org/10.1061/(asce)0899-1561(2006)18:2(283)
Eid, M., Gomaa, Y., & Galal, S. (2024). Effectiveness of lime kiln dust on swelling of subgrade expansive soil. *Beni-Suef University Journal of Basic and Applied Sciences, 13*. https://doi.org/10.1186/s43088-024-00501-0
Ekpo, D. U., Fajobi, A., Ayodele, A. L., & Etim, R. K. (2021). Potentials of Cement Kiln Dust-Periwinkle Shell Ash Blends on Plasticity Properties of Two Selected Tropical Soils for use as Sustainable Construction Materials. *IOP Conference Series: Materials Science and Engineering, 1036*. https://doi.org/10.1088/1757-899x/1036/1/012033
El-Attar, M. M., Sadek, D., & Salah, A. M. (2017). Recycling of high volumes of cement kiln dust in bricks industry. *Journal of Cleaner Production, 143*, 506-515. https://doi.org/10.1016/j.jclepro.2016.12.082
El-Samea, W. A., Mowafy, Y., El-Naiem, M. A., & Towfeek, A. (2022). NUMERICAL ANALYSIS OF SHALLOW FOUNDATION ON EXPANSIVE SOIL. *Journal of Al-Azhar University Engineering Sector*. https://doi.org/10.21608/auej.2022.233745
Eskişar, T., Altun, S., & Kalıpcılar, İ. (2015). Assessment of strength development and freeze–thaw performance of cement treated clays at different water contents. *Cold Regions Science and Technology, 111*, 50-59. https://doi.org/10.1016/j.coldregions.2014.12.008
Estabragh, A. R., Parsaei, B., & Javadi, A. (2015). Laboratory investigation of the effect of cyclic wetting and drying on the behaviour of an expansive soil. *Soils and Foundations, 55*, 304-314. https://doi.org/10.1016/j.sandf.2015.02.007
Fan, K., Zou, W., Zhang, P., Wang, X., & Shen, Y. (2023). Laboratory investigation and theoretical analysis of lateral pressure exerted by expansive soils on retaining walls with expanded polystyrene geofoam block upon water infiltration. *Geotextiles and Geomembranes*. https://doi.org/10.1016/j.geotexmem.2023.11.005
Firoozi, A. A., Olgun, G. C., Firoozi, A., & Baghini, M. S. (2017). Fundamentals of soil stabilization. *International Journal of Geo-Engineering, 8*, 1-16. https://doi.org/10.1186/s40703-017-0064-9
Frank, H. S., & Wen, W. Y. (1957). Ion-solvent interaction. Structural aspects of ion-solvent interaction in aqueous solutions: a suggested picture of water structure. *Discussions of the Faraday Society*, *24*, 133-140. https://doi.org/10.1039/DF9572400133
Gebregziabiher, B. S., Thomas, R., & Peethamparan, S. (2016). Temperature and activator effect on early-age reaction kinetics of alkali-activated slag binders. *Construction and Building Materials, 113*, 783-793. https://doi.org/10.1016/j.conbuildmat.2016.03.098
Ghavami, S., Jahanbakhsh, H., Azizkandi, A. S., & Nejad, M. F. (2020). Influence of sodium chloride on cement kiln dust-treated clayey soil: strength properties, cost analysis, and environmental impact. *Environment, Development and Sustainability, 23*, 683-702. https://doi.org/10.1007/s10668-020-00603-6
Gilbert, A. (2025). Investigating the Effectiveness of Cement Kiln Dust as an Expansive Soil Stabilizer in Road Construction. *International Journal of Research and Innovation in Social Science*. https://doi.org/10.47772/ijriss.2025.9010117
Govindan, S. A., Mudavath, H., & Vaddemani, G. P. R. (2025). Evaluating the sustainability of using calcium carbide residue for clay stabilization: integrating mechanical behaviour and life cycle assessment. *Environmental Science and Pollution Research, 32*, 15772 - 15789. https://doi.org/10.1007/s11356-025-36608-9
Grim, R. E. (1959). Physico-chemical properties of soils: Clay minerals. Journal of the Soil Mechanics and Foundations Division, 85(2), 1-17. https://ascelibrary.org/doi/abs/10.1061/JSFEAQ.0000179

Güney, Y., Sari, D., Çetin, M., & Tuncan, M. (2007). Impact of cyclic wetting–drying on swelling behavior of lime-stabilized soil. *Building and Environment, 42*, 681-688. https://doi.org/10.1016/j.buildenv.2005.10.035

Hakro, M. R., Channa, M. A., & Hakro, I. (2026). The Numerical Modelling of Shallow Foundation of Expansive Soil under Wet and Dry Cycles. *IEM Journal*. https://doi.org/10.54552/v87i1.277

Hamadou, T., Kanouo, N. S., Dikwa, J., Tchamba, A. B., & Duna, L. L. (2023). Cement kiln dust in CIMENCAM Figuil (North Cameroon): characteristics and recycling as additives for blended cement production. *SN Applied Sciences, 5*. https://doi.org/10.1007/s42452-023-05401-z

Hm, S. (2021). A Review on Cement Kiln Dust (CKD), Improvement and Green Sustainable Applications. *International Journal of Nuclear Medicine & Radioactive Substances*. https://doi.org/10.23880/ijnmrs-16000141

Holtz, W. G., & Gibbs, H. J. (1956). Engineering properties of expansive clays. *Transactions of the American Society of Civil Engineers*, *121*(1), 641-663. https://ascelibrary.org/doi/abs/10.1061/TACEAT.0007325

Hotineanu, A., Bouasker, M., Aldaood, A., & Al-Mukhtar, M. (2015). Effect of freeze–thaw cycling on the mechanical properties of lime-stabilized expansive clays. *Cold Regions Science and Technology, 119*, 151-157. https://doi.org/10.1016/j.coldregions.2015.08.008

Hu, N., Chen, G., Chen, Y., Lin, M., Tang, P., Zhang, W., & Ye, Z. (2024). Cement and zeolite stabilization/solidification of heavy metal-contaminated sediments: 841-Day leaching characteristics, mechanisms, and microstructure. *Waste management, 190*, 306-317. https://doi.org/10.1016/j.wasman.2024.09.025

Hume, R., Marschner, P., Mason, S., Schilling, R., Hughes, B. T., & Mosley, L. (2023). Measurement of lime movement and dissolution in acidic soils using mid-infrared spectroscopy. *Soil and Tillage Research*. https://doi.org/10.1016/j.still.2023.105807

IBC, I. International Code Council (2012): International Building Code.

Ijaz, N., Ye, W., Rehman, Z., & Ijaz, Z. (2022). Novel application of low carbon limestone calcined clay cement (LC3) in expansive soil stabilization: An eco-efficient approach. *Journal of Cleaner Production*. https://doi.org/10.1016/j.jclepro.2022.133492

Internasional, A. S. T. M. (2007). Standard Test Method for Particle-Size Analysis of Soils (ASTM D 422). *ASTM Internasional, United State*.

Ismaiel, H. A. H. (2013). Cement Kiln Dust Chemical Stabilization of Expansive Soil Exposed at El-Kawther Quarter, Sohag Region, Egypt. *International Journal of Geosciences, 2013*, 1416-1424. https://doi.org/10.4236/ijg.2013.410139

Ismeik, M., & Shaqour, F. (2018). Effectiveness of lime in stabilising subgrade soils subjected to freeze–thaw cycles. *Road Materials and Pavement Design, 21*, 42 - 60. https://doi.org/10.1080/14680629.2018.1479289

Ismeik, M., Shaqour, F., & Hasan, S. (2021). Geotechnical evaluation of clayey soils amended with cement kiln dust during freeze-thaw cycling. *Arabian Journal of Geosciences, 14*. https://doi.org/10.1007/s12517-021-08144-6

James, J., Natesan, A., Manohar, A., & Subramanian, V. (2021). Potential of Portland pozzolana cement in the stabilization of an expansive soil subjected to alternate cycles of wetting and drying. https://doi.org/10.5937/grmk2102081j

Jazi, F. N., Mir, S., Hosseini, M., Ghasemi-Fare, O., & Rockaway, T. D. (2024). Experimental evaluation of stress history effect on compressibility characteristics of lime-stabilized expansive soils. *Geomechanics and Geoengineering, 20*, 21 - 34. https://doi.org/10.1080/17486025.2024.2354873

Jha, A., & Sharma, M. (2021). Effect of Wetting–Drying Cycles on Strength Behavior of Lime Stabilized Expansive Soil. 23-33. https://doi.org/10.1007/978-981-33-6466-0_3

Joshi, A. R., & Patel, S. (2022). Investigation Into Sustainable Application of Class C Fly Ash Layer in Flexible Pavement. *Journal of Hazardous, Toxic, and Radioactive Waste*. https://doi.org/10.1061/(asce)hz.2153-5515.0000727

Jumaa, R. M., Saeed, K., & Al-Jaberi, L. A. (2026). Effect of Fly Ash and Nano-Silica Fume on Soft Clay: Atterberg Limits, MDD, and OMC. *Civil Engineering Journal*. https://doi.org/10.28991/cej-2026-012-02-012

Kamaruddin, F. A., Anggraini, V., Huat, B. K., & Nahazanan, H. (2020). Wetting/Drying Behavior of Lime and Alkaline Activation Stabilized Marine Clay Reinforced with Modified Coir Fiber. *Materials, 13*. https://doi.org/10.3390/ma13122753

Karadumpa, C. S., & Pancharathi, R. K. (2023). Study on energy use and carbon emission from manufacturing of OPC and blended cements in India. *Environmental Science and Pollution Research*, 1-20. https://doi.org/10.1007/s11356-023-31593-3

Karunakaran, P., & Tan, J. (2025). EXPERIMENTAL INVESTIGATION ON THE INFLUENCE OF LATERAL EARTH PRESSURES ON RETAINING WALLS. *Journal of Engineering & Technological Advances*. https://doi.org/10.35934/segi.v10i2.106

Khan, F., Das, B., & Dewangan, N. (2021). Determination of Geotechnical Properties and Stability of Expansive Soil using Fly Ash. *Walailak Journal of Science and Technology (WJST)*. https://doi.org/10.48048/wjst.2021.22783

Khoury, N., & Zaman, M. (2006). Environmental Effects on Durability of Aggregates Stabilized with Cementitious Materials. *Journal of Materials in Civil Engineering, 19*, 41-48. https://doi.org/10.1061/(asce)0899-1561(2007)19:1(41)

Khoury, N., & Zaman, M. M. (2007). Durability of stabilized base courses subjected to wet–dry cycles. *International Journal of Pavement Engineering, 8*, 265 - 276. https://doi.org/10.1080/10298430701342874
Kolay, P., & Ramesh, K. (2016). Reduction of Expansive Index, Swelling and Compression Behavior of Kaolinite and Bentonite Clay with Sand and Class C Fly Ash. *Geotechnical and Geological Engineering, 34*, 87-101. https://doi.org/10.1007/s10706-015-9930-4
Kumar, A. T., Thyagaraj, T., & Robinson, R. (2022). Swell–shrink behaviour of fly ash-stabilised expansive soils. *Proceedings of the Institution of Civil Engineers - Ground Improvement*. https://doi.org/10.1680/jgrim.21.00024
Kumar, B. S., Sreenivasulu, C., & Singh, S. (2021). Effects of Delay Time on Compaction and Strength Properties of Stabilized Granular Soil. *Lecture Notes in Civil Engineering*. https://doi.org/10.1007/978-981-33-6444-8_66
Kumar, P. G., & Harika, S. (2020). Stabilization of expansive subgrade soil by using fly ash. *Materials Today: Proceedings*. https://doi.org/10.1016/j.matpr.2020.11.469
Kumar, P., Puppala, A. J., Biswas, N., Congress, S., Tingle, J., & Little, D. (2024). Assessment of Durability of Chemically Stabilized Soils Using Different Moisture-Susceptible Methods. *Transportation Research Record, 2678*, 1454 - 1467. https://doi.org/10.1177/03611981241244795
Kumar, S. J., & Janewoo, U. (2016). Stabilization of Expansive Soil with Cement Kiln Dust and RBI Grade 81 at Subgrade Level. *Geotechnical and Geological Engineering, 34*, 1037-1046. https://doi.org/10.1007/s10706-016-0024-8
Lambe, T. w. & Whitman, R. V. (1969). Soil mechanics. New York: Wiley.
Lambe, T. W. (1958). The engineering behavior of compacted clay. *Journal of the Soil Mechanics and Foundations Division*, *84*(2), 1655-1. https://doi.org/10.1061/JSFEAQ.0000115
Lambe, T. W. (1960). The character and identification of expansive soils, soil PVC meter. *Federal housing administration, technical studies program, FHA*, *701*.
Laporte, S., Eichhorn, G., Kingswood, J., Siemens, G., & Beddoe, R. (2023). Physical modelling of Climate-Soil-InfraStructure Interactions of Paved roadways constructed in expansive soil. *Transportation Geotechnics*. https://doi.org/10.1016/j.trgeo.2023.101126
Lee, W.-S., & Choi, Y. (2024). Hydration and Mechanical Properties of Cement Kiln Dust-Blended Cement Composite. *Materials, 17*. https://doi.org/10.3390/ma17194841
Li, M., Wei, Y., Liu, Y., & Jin, J. (2021). A Framework for Interpreting Lateral Swelling Pressure in Unsaturated Expansive Soils. *Advances in Civil Engineering*. https://doi.org/10.1155/2021/6626835
Li, W., Ni, P., & Yi, Y. (2019). Comparison of reactive magnesia, quick lime, and ordinary Portland cement for stabilization/solidification of heavy metal-contaminated soils. *The Science of the total environment, 671*, 741-753. https://doi.org/10.1016/j.scitotenv.2019.03.270
Lin, B., Cerato, A., Madden, A. S., & Madden, M. (2013). Effect of Fly Ash on the Behavior of Expansive Soils: Microscopic Analysis. *Environmental & Engineering Geoscience, 19*, 85-94. https://doi.org/10.2113/gseegeosci.19.1.85
Little, D., & Nair, S. (2007). Sensitivity of Selected Colorado Soils to Form Ettringite/Thaumasite When Treated with Calcium-Based Stabilizers and When Soluble Sulfates Are Available.
Liu, H.-B., Sun, S., Wei, H.-B., & Li, W.-J. (2021). Effect of freeze-thaw cycles on static properties of cement stabilised subgrade silty soil. *International Journal of Pavement Engineering, 23*, 3770 - 3782. https://doi.org/10.1080/10298436.2021.1919306
Liu, Y. (2025). Stability analysis of an expansive soil slope under heavy rainfall conditions with different anchor reinforcements. *Scientific Reports, 15*. https://doi.org/10.1038/s41598-024-84799-x
Liu, Y., Wang, Q., Liu, S., Shangguan, Y., Fu, H., B., Chen, H., & Yuan, X. (2019). Experimental investigation of the geotechnical properties and microstructure of lime-stabilized saline soils under freeze-thaw cycling. *Cold Regions Science and Technology*. https://doi.org/10.1016/j.coldregions.2019.03.003
Lu, Y., Liu, S.-H., Li, Z., & Lei, X. (2020). Freeze-thaw performance of a cement-treated expansive soil. *Cold Regions Science and Technology, 170*, 102926. https://doi.org/10.1016/j.coldregions.2019.102926
Ma J., Zhang, H., Wang, D., Wang, H., & Chen, G. (2022). Rheological Properties of Cement Paste Containing Ground Fly Ash Based on Particle Morphology Analysis. *Crystals*. https://doi.org/10.3390/cryst12040524
Mahan, E. J., & Hussein, A. (2018). Effect of Additive Type and Percent on Soil Plasticity.
Mahedi, M., Cetin, B., & Dayioglu, A. Y. (2019). Leaching behavior of aluminum, copper, iron and zinc from cement activated fly ash and slag stabilized soils.. *Waste management, 95*, 334-355. https://doi.org/10.1016/j.wasman.2019.06.018
Marku, J., Dumi, I., & Liço, E. (2013). The charachterization and the utilization of cement kiln dust (CKD) as partial replacement of portland cement in mortar and concrete production.
Mataji, S., Choobbasti, A., & Kutanaei, S. S. (2025). The effect of construction moisture content on the mechanical, shear and environmental characteristics of clay stabilized with cement and CS: a micro and macro study. *Case Studies in Construction Materials*. https://doi.org/10.1016/j.cscm.2025.e04818
Miller, G., & Azad, S. (2000). INFLUENCE OF SOIL TYPE ON STABILIZATION WITH CEMENT KILN DUST. *Construction and Building Materials, 14*, 89-97. https://doi.org/10.1016/s0950-0618(00)00007-6

Miller, G., Zaman, M., Rahman, J., & Tan, N. K. (2003). Laboratory and field evaluation of soil stabilization using cement kiln dust.
Mohamed, W. (2024). Assessing the effects of different foundation base shapes on settlement and heaving in expansive clay: numerical analysis. *Journal of Umm Al-Qura University for Engineering and Architecture, 15*, 517 - 528. https://doi.org/10.1007/s43995-024-00073-1
Mohamedzein, Y., Al-Aghbari, M., & Kindi, A. Z. (2025). CEMENT KILN DUST (CKD) AS A POTENTIAL STABILIZER TO MITIGATE THE SWELLING OF CLAYS. *Jurnal Teknologi (Sciences & Engineering)*. https://doi.org/10.11113/jurnalteknologi.v87.23243
Molaabasi, H., Kharazmi, P., Khajeh, A., Saberian, M., Chenari, R. J., Harandi, M., & Li, J. (2022). Low plasticity clay stabilized with cement and zeolite: An experimental and environmental impact study. *Resources, Conservation and Recycling*. https://doi.org/10.1016/j.resconrec.2022.106408
Mollamahmutoğlu, M., Avci, E., & Erdem, A. (2017). Volume Change Control of High Plasticity Clay by the Stabilization of Fine-grained Cements. https://doi.org/10.11159/icgre17.178
Mollamahmutoğlu, M., Yilmaz, Y., & Güngör, A. (2009). Effect of a Class C Fly Ash on the Geotechnical Properties of an Expansive Soil. 1-6.
Moore, J., Akula, P., Ray, S., Bastola, A., Noell, P. J., & Rimsza, J. (2024). Carbon sequestration into lime-stabilized soils: Engineering and mineralogical characterization. *Journal of Cleaner Production*. https://doi.org/10.1016/j.jclepro.2024.144613
Mousa, E., Fouad, M., El-Naga, I. A., El-Sekelly, E.-M. A., & El-Ashwah, A. (2025). Utilising cement kiln dust as a sustainable cementitious alternative for recycled asphalt pavement materials: a mechanical, economic, and environmental study. *International Journal of Pavement Engineering, 26*. https://doi.org/10.1080/10298436.2025.2544904
Mumtaz, M., Shahriar, K., & Barua, S. (2021). Characterization of High Plastic Clay Under Varying Proportion Ordinary Portland Cement for Soil-cement Stabilization. *Daffodil International University Journal of Science and Technology*. https://doi.org/10.36481/diujst.v16i1.jjwxg495
Nabil, M., Mustapha, A., & Rios, S. (2019). Impact of wetting—drying cycles on the mechanical properties of lime-stabilized soils. International Journal of Pavement Research and Technology, 13, 83 - 92. https://doi.org/10.1007/s42947-019-0088-y
Nag, M., & Shimaoka, T. (2022). A novel and sustainable technique to immobilize lead and zinc in MSW incineration fly ash by using pozzolanic bottom ash.. *Journal of environmental management, 329*, 117036. https://doi.org/10.1016/j.jenvman.2022.117036
Nalbantoglu, Z. (2004). Effectiveness of Class C fly ash as an expansive soil stabilizer. *Construction and Building Materials, 18*, 377-381. https://doi.org/10.1016/j.conbuildmat.2004.03.011
Nasrizar, A. A., Muttharam, M., & Ilamparuthi, K. (2010). Effect of Placement Water Content on Strength of Temperature Cured Lime Treated Expansive Soil. 174-180. https://doi.org/10.1061/41108(381)23
Naveed, M., Ahmed, S., Ullah, A., & Zia, M. D. (2024). Mechanism of improvement and best-fit models for the prediction of geotechnical properties of lime stabilized expansive soil used in pavement subgrade. *Mehran University Research Journal of Engineering and Technology*. https://doi.org/10.22581/muet1982.2977
Negahdar, H., and Amin Tohidi. "Assessment of geopolymer and cement stabilizers on geotechnical properties of heavy metal-contaminated clay." *Scientific Reports*, vol. 15, 2025, https://doi.org/10.1038/s41598-025-04514-2.
Negawo, W. J., Di Emidio, G., Bezuijen, A., Flores, R. V. D., & François, B. (2019). Lime-stabilisation of high plasticity swelling clay from Ethiopia. *European Journal of Environmental and Civil Engineering, 23*, 504 - 514. https://doi.org/10.1080/19648189.2017.1304272
Nguyen, T.-T.-H., Cui, Y.-J., Ferber, V., Herrier, G., Ozturk, T., Plier, F., Puiatti, D., Salager, S., & Tang, A. (2019). Effect of freeze-thaw cycles on mechanical strength of lime-treated fine-grained soils. *Transportation Geotechnics*. https://doi.org/10.1016/j.trgeo.2019.100281
Norrish, K. (1954). The swelling of montmorillonite. *Discussions of the Faraday society*, *18*, 120-134. https://doi.org/10.1039/DF9541800120
Nugroho, S., Wibisono, G., Ongko, A., & Mauliza, A. (2021). Effects of High Plasticity and Expansive Clay Stabilization with Lime on UCS Testing in Several Conditions. https://doi.org/10.22146/jcef.59438
Nunes, M. R., Denardin, J. E., Vaz, C., Karlen, D., & Cambardella, C. (2019). Lime movement through highly weathered soil profiles. *Environmental Research Communications, 1*. https://doi.org/10.1088/2515-7620/ab4eba
Ogila, W. (2021). Effectiveness of fresh cement kiln dust as a soil stabilizer and stabilization mechanism of high swelling clays. *Environmental Earth Sciences, 80*, 1-24. https://doi.org/10.1007/s12665-021-09589-4
Olagunju, B. D., & Olanrewaju, O. (2021). Life Cycle Assessment of Ordinary Portland Cement (OPC) using Damage Oriented (Endpoint) Approach. *Proceedings of the International Conference on Industrial Engineering and Operations Management*. https://doi.org/10.46254/an11.20210031
Orazi, M., Orazi, U. S., Romeo, E., Van Rompaey, G., & Tebaldi, G. (2022). Mechanical recovery of lime-stabilised clays subjected to freeze–thaw damage. *Road Materials and Pavement Design, 24*, 2104 - 2112. https://doi.org/10.1080/14680629.2022.2117070.

Padmaraj, D., & Arnepalli, D. N. (2023). Carbonation in lime-stabilized clays: mechanism, effects, and future prospects. *Bulletin of Engineering Geology and the Environment, 82*, 1-24. https://doi.org/10.1007/s10064-023-03273-6
Padmaraj, D., & Arnepalli, D. N. (2024). Comprehensive evaluation of carbonation and leaching reactions in lime stabilised soils. *Environmental Geotechnics*. https://doi.org/10.1680/jenge.24.00011
Pandey, P., Hossain, M., & Ahmed, A. (2021). Performance evaluation of modified moisture barrier in mitigating expansive soil associated pavement distresses. *Transportation Geotechnics*. https://doi.org/10.1016/j.trgeo.2021.100667
PaniAparupa, and S. Prasad. "Effect of temperature on the strength of lime-stabilised fly ash." *Environmental geotechnics*, 2018, https://doi.org/10.1680/jenge.17.00050.
Pankaja, B. S., Ranjita, N. H., Ramesh, H., Kho, J. C., & Raghunandan, M. (2023). Suitability of Fly Ash-Cement Kiln Dust Columns for Stabilizing Expansive (Black Cotton) Soils. *Archives of Advanced Engineering Science*. https://doi.org/10.47852/bonviewaaes32021451
Parsons, R., & Kneebone, E. (2004). Use of Cement Kiln Dust for the Stabilization of Soils. *Geotechnical special publication*, 1124-1131. https://doi.org/10.1061/40744(154)101
Peck, R. B., Hanson, W. E., & Thornburn, T. H. (1991). *Foundation engineering*. John Wiley & Sons.
Peethamparan, S., Olek, J., & Lovell, J. (2008). Influence of chemical and physical characteristics of cement kiln dusts (CKDs) on their hydration behavior and potential suitability for soil stabilization. *Cement and Concrete Research, 38*, 803-815. https://doi.org/10.1016/j.cemconres.2008.01.011
Phanikumar, B. (2009). Effect of lime and fly ash on swell, consolidation and shear strength characteristics of expansive clays: a comparative study. *Geomechanics and Geoengineering, 4*, 175 - 181. https://doi.org/10.1080/17486020902856983
Phanikumar, B., Sreedharan, R., & Aniruddh, C. (2015). Swell-compressibility characteristics of lime-blended and cement-blended expansive clays – A comparative study. *Geomechanics and Geoengineering, 10*, 153 - 162. https://doi.org/10.1080/17486025.2014.902120
Pokkunuri, G. R., Sinha, R. K., & Verma, A. (2023). Field Studies on Expansive Soil Stabilization with Nanomaterials and Lime for Flexible Pavement. *Sustainability*. https://doi.org/10.3390/su152115291
Prashanth, J., Sivapullaiah, P., & Sridharan, A. (2001). Pozzolanic fly ash as a hydraulic barrier in land fills. *Engineering Geology, 60*, 245-252. https://doi.org/10.1016/s0013-7952(00)00105-8
Qiu, X., Lai, Z., Zuo, J., & Li, W. (2025). Synergistic stabilization of expansive soil using ultrafine high-reactivity fly ash and calcium carbide slag: performance optimization and microstructural insights. *Frontiers in Materials*. https://doi.org/10.3389/fmats.2025.1710809
Rai, A., Sahu, N., Kumar, A., Kumar, D., & P. (2025). Stabilization of Expansive Soil using Industrial Solid Waste. *Communications on Applied Nonlinear Analysis*. https://doi.org/10.52783/cana.v32.5451
Rai, P., Qiu, W., Pei, H., Chen, J., Ai, X., Liu, Y., & Ahmad, M. (2021). Effect of Fly Ash and Cement on the Engineering Characteristic of Stabilized Subgrade Soil: An Experimental Study. *Geofluids*. https://doi.org/10.1155/2021/1368194
Raja, S. P., & Thyagaraj, T. (2021). Significance of compaction time delay on compaction and strength characteristics of sulfate resistant cement-treated expansive soil. *Journal of rock mechanics and geotechnical engineering*. https://doi.org/10.1016/j.jrmge.2021.03.003
Rao, P. K. R., & Rajakumar, C. (2020). Green Stabilization of Clay Soil Using Cement Kiln Dust. *International Journal of PharmTech Research, 13*, 109-115. https://doi.org/10.20902/ijptr.2019.130113
Rashed, K., & Mohammad, P. H. (2019). Effect of Wetting and Drying Cycles on Expansive Soils Using Cement Kiln Dust. 435-443. https://doi.org/10.24271/
Reddy, D. K. "Durability of Cement Stabilized Expansive Clay." *Journal of emerging technologies and innovative research*, 2018.
Regasa, H., Jothimani, M., & Oyda, Y. (2023). Subgrade soil stabilization using the Quicklime: a case study from Modjo- Hawassa highway, Central Ethiopia. *International Journal of Geo-Engineering, 14*, 1-12. https://doi.org/10.1186/s40703-023-00197-8
Renjith, R., Robert, D., Setunge, S., Costa, S., & Mohajerani, A. (2021). Optimization of fly ash based soil stabilization using secondary admixtures for sustainable road construction. *Journal of Cleaner Production, 294*, 126264. https://doi.org/10.1016/j.jclepro.2021.126264
Rimal, S., Poudel, R., & Gautam, D. (2019). Experimental study on properties of natural soils treated with cement kiln dust. *Case Studies in Construction Materials*. https://doi.org/10.1016/j.cscm.2019.e00223
Rothhämel, M., Al-Jabban, W., & Laue, J. (2021). Influence factors for using hydraulic binders for soil stabilisation of fine-grained soils in cold environment. *IOP Conference Series: Earth and Environmental Science, 710*. https://doi.org/10.1088/1755-1315/710/1/012050
Saeed, S., Abdulkareem, A., & Abd, D. (2024). Improvement durability of cohesive soil using CKD and RAP. *2ND INTERNATIONAL CONFERENCE FOR ENGINEERING SCIENCES AND INFORMATION TECHNOLOGY (ESIT 2022): ESIT2022 Conference Proceedings*. https://doi.org/10.1063/5.0190551

Sagidullina, N., Abdialim, S., Kim, J. R., Satyanaga, A., & Moon, S.-W. (2022). Influence of Freeze–Thaw Cycles on Physical and Mechanical Properties of Cement-Treated Silty Sand. *Sustainability*. https://doi.org/10.3390/su14127000
Salih, N. B. (2025). Cement Kiln Dust for Improving Properties of Soil. *Jordan Journal of Civil Engineering*. https://doi.org/10.14525/jjce.v19i2.09
Salih, N., Rashed, K. A., & Abdulwahab, K. (2022). Experimental Study on Using Cement Kiln Dust and Plastic Bottle Waste to Improve the Geotechnical Characteristics of Expansive Soils in Sulaimani City, Northern Iraq. *Journal of Engineering*. https://doi.org/10.31026/j.eng.2022.04.02
Salih, S. R., & Shafiqu, Q. M. S. (2024). Effect of Treating Expansive Soil with Lime. *Al-Nahrain Journal for Engineering Sciences*. https://doi.org/10.29194/njes.27020226
Sambre, T., Endait, M., & Patil, S. (2024). Sustainable soil stabilization of expansive soil subgrades through lime-fly ash admixture. *Discover Civil Engineering, 1*. https://doi.org/10.1007/s44290-024-00063-1
Sbahieh, S., Mckay, G., Nurdiawati, A., & Al-Ghamdi, S. G. (2025). The Sustainability of Partial and Total Replacement of Ordinary Portland Cement: A Deep Dive into Different Concrete Mixtures Through Life Cycle Assessment. *Journal of Building Engineering*. https://doi.org/10.1016/j.jobe.2025.112830
Seed, H. B., Woodward Jr, R. J., & Lundgren, R. (1962). Prediction of swelling potential for compacted clays. *Journal of the soil mechanics and foundations division*, *88*(3), 53-87.
Seed, H. B., Woodward, R. J., & Lundgren, R. (1964). Fundamental aspects of the Atterberg limits. *Journal of the Soil Mechanics and Foundations Division*, *90*(6), 75-106. https://ascelibrary.org/doi/abs/10.1061/JSFEAQ.0000685
Selvakumar, S., Soundara, B., Raj, N. *et al.* Microstructural investigation on the expansive soils for sustainable stabilization purposes. *Discov. Soil* **1**, 8 (2024). https://doi.org/10.1007/s44378-024-00009-0
Sengul, T., Akray, N., & Vitoşoğlu, Y. (2023). Investigating the effects of stabilization carried out using fly ash and polypropylene fiber on the properties of highway clay soils. *Construction and Building Materials*. https://doi.org/10.1016/j.conbuildmat.2023.132590
Seyrek, E. (2018). Engineering behavior of clay soils stabilized with Class C and class F fly ashes. *Science and Engineering of Composite Materials, 25*, 273 - 287. https://doi.org/10.1515/secm-2016-0084
Shafqat, K., Khalid, U. & Rehman, Z.u. Coupling effect of cyclic wet-dry environment and compaction state on desiccation cracking and mechanical behavior of low and high plastic clays. *Bull Eng Geol Environ* **84**, 66 (2025). https://doi.org/10.1007/s10064-024-04049-2
Shao, L., Ding, Z., Wang, S., Pan, K., & Hu, C. (2023). Effect of Organic Matter Components on the Mechanical Properties of Cemented Soil. *Materials, 16*. https://doi.org/10.3390/ma16175889
Shi, X., Yang, P., Li, L., Geng, X., Liu, X., & Zhao, J. (2024). Strength and microscopic pore structure characterization of cement-fly ash stabilized organic soil under freeze-thaw cycles. *Construction and Building Materials*. https://doi.org/10.1016/j.conbuildmat.2024.135635
Shibi, T., & Kamei, T. (2014). Effect of freeze–thaw cycles on the strength and physical properties of cement-stabilised soil containing recycled bassanite and coal ash. *Cold Regions Science and Technology, 106*, 36-45. https://doi.org/10.1016/j.coldregions.2014.06.005
Shirkhanloo, S., Najafi, M., Kaushal, V., & Rajabi, M. (2021). A Comparative Study on the Effect of Class C and Class F Fly Ashes on Geotechnical Properties of High-Plasticity Clay. *CivilEng*. https://doi.org/10.3390/civileng2040054
Shirmohammadi, S., Jahromi, G. S., Payan, M., & Senetakis, K. (2021). Effect of Lime Stabilization and Partial Clinoptilolite Zeolite Replacement on the Behavior of a Silt-Sized Low-Plasticity Soil Subjected to Freezing–Thawing Cycles. *Coatings*. https://doi.org/10.3390/coatings11080994
Simoni, M., Wilkes, M., Brown, S. F., Provis, J., Kinoshita, H., & Hanein, T. (2022). Decarbonising the lime industry: State-of-the-art. *Renewable and Sustainable Energy Reviews*. https://doi.org/10.1016/j.rser.2022.112765
Sivapullaiah, P., Prashanth, J., & Sridharan, A. (1998). EFFECT OF DELAY BETWEEN MIXING AND COMPACTION ON STRENGTH AND COMPACTION PARAMETERS OF FLY ASH.
Skempton, A. W. (1953). The colloidal activity of clays. *Selected papers on soil mechanics*, *1*, 57-61.
Soğancı, A., Yıldız, M., & Üniversitesi, S. (2012). Effect of freezing and thawing on strength and permeability of lime-stabilized clays. *Scientia Iranica, 19*, 1013-1017. https://doi.org/10.1016/j.scient.2012.06.003
Solanki, P., & Hauk-Jegen, B. (2016). Freeze-Thaw Durability of Soil Stabilized with Class C Fly Ash and Cement Kiln Dust. https://doi.org/10.18552/2016/scmt4d145
Solanki, P., Khoury, N., & Zaman, M. (2009). Engineering Properties and Moisture Susceptibility of Silty Clay Stabilized with Lime, Class C Fly Ash, and Cement Kiln Dust. *Journal of Materials in Civil Engineering, 21*, 749-757. https://doi.org/10.1061/(asce)0899-1561(2009)21:12(749)
Solanki, P., Zaman, M., & Khalife, R. (2013). Effect of Freeze-Thaw Cycles on Performance of Stabilized Subgrade. 566-580. https://doi.org/10.1061/9780784412770.038
Soltani, A., Taheri, A., Khatibi, M., & Estabragh, A. R. (2017). Swelling Potential of a Stabilized Expansive Soil: A Comparative Experimental Study. *Geotechnical and Geological Engineering, 35*, 1717-1744. https://doi.org/10.1007/s10706-017-0204-1

Sorsa, Alemineh. "Engineering Properties of Cement Stabilized Expansive Clay Soil." *Civil and Environmental Engineering*, vol. 18, 2022, pp. 332 - 339, https://doi.org/10.2478/cee-2022-0031.
Sreekrishnavilasam, A., Rahardja, S., Kmetz, R. J., & Santagata, M. (2007). Soil treatment using fresh and landfilled cement kiln dust. *Construction and Building Materials, 21*, 318-327. https://doi.org/10.1016/j.conbuildmat.2005.08.015
Tang, C. S., Cheng, Q., Leng, T., Shi, B., Zeng, H., & Inyang, H. I. (2020). Effects of wetting-drying cycles and desiccation cracks on mechanical behavior of an unsaturated soil. *Catena*, *194*, 104721. https://doi.org/10.1016/j.catena.2020.104721
Terán-Cuadrado, G., Tahir, F., Nurdiawati, A., Almarshoud, M., & Al-Ghamdi, S. G. (2024). Current and Potential Materials for the Low-Carbon Cement Production: Life Cycle Assessment Perspective. *Journal of Building Engineering*. https://doi.org/10.1016/j.jobe.2024.110528
Terzaghi, K. (1925). Principles of soil mechanics: III. Determination of permeability of clay. *Engineering News Record*, *95*(21), 832-836.
Terzaghi, K. (1943). Liner-plate tunnels on the Chicago (Il) subway. *Transactions of the American Society of Civil Engineers*, *108*(1), 970-1007.
Tremblay, H., Duchesne, J., Locat, J., & Leroueil, S. (2002). Influence of the nature of organic compounds on fine soil stabilization with cement. *Canadian Geotechnical Journal, 39*, 535-546. https://doi.org/10.1139/t02-002
Turan, C., Javadi, A., & Vinai, R. (2022). Effects of Class C and Class F Fly Ash on Mechanical and Microstructural Behavior of Clay Soil—A Comparative Study. *Materials, 15*. https://doi.org/10.3390/ma15051845
Turan, C., Javadi, A., Vinai, R., Shariatmadari, N., & Farmani, R. (2020). Use of Class C fly ash for stabilization of fine-grained soils. *E3S Web of Conferences*. https://doi.org/10.1051/e3sconf/202019506001
Turrakheil, K. S., Shah, S. S. A., & Naveed, M. (2025). A Comparison of Cement and Guar Gum Stabilisation of Oxford Clay Under Controlled Wetting and Drying Cycles. *Applied Sciences*. https://doi.org/10.3390/app15126913
Umar, I., Tarauni, Z. A., Bello, A. B., Lin, H., Hassan, J. I., & Cao, R.-H. (2025). Performance Prediction and Optimization of High-Plasticity Clay Lime–Cement Stabilization Based on Principal Component Analysis and Principal Component Regression. *Applied Sciences*. https://doi.org/10.3390/app15137150
Utkarsh & Jain, P. K. (2024). Enhancing the properties of swelling soils with lime, fly ash, and expanded polystyrene -A review. *Heliyon, 10*. https://doi.org/10.1016/j.heliyon.2024.e32908
Vukićević, M., Marjanović, M., Pujević, V., & Jocković, S. (2019). The alternatives to traditional materials for subsoil stabilization and embankments. *Materials*, *12*(18), 3018. https://doi.org/10.3390/ma12183018
Wang, Y., Burris, L., Hooton, R., Shearer, C. R., & Suraneni, P. (2021). Effects of unconventional fly ashes on cementitious paste properties. *Cement and Concrete Composites*. https://doi.org/10.1016/j.cemconcomp.2021.104291
Widjaja, B., & Chriswandi, C. (2020, December). New relationship between linear shrinkage and shrinkage limit for expansive soils. In *IOP Conference Series: Materials Science and Engineering* (Vol. 1007, No. 1, p. 012187). IOP Publishing https://iopscience.iop.org/article/10.1088/1757-899X/1007/1/012187/meta
Witte, A., & Garg, N. (2024). Particle shape, crystallinity, and degree of polymerization of fly ash via combined SEM-EDS and Raman spectroscopy. *Cement and Concrete Research*. https://doi.org/10.1016/j.cemconres.2024.107612
Wonglakorn, N., Thumrongvut, J., Pruemphonchai, K., Tiyasangthong, S., Tabyang, W., Osinski, P., Van Duc, B., & Suksiripattanapong, C. (2025). Engineering and Microstructure Properties of Soft Clay Improved with Ordinary Portland Cement and Polymers. *Civil Engineering Journal*. https://doi.org/10.28991/cej-2025-011-04-022
Wu, E., Wang, Q., Ke, L., & Zhang, G.-G. (2023). Study on Carbon Emission Characteristics and Emission Reduction Measures of Lime Production—A Case of Enterprise in the Yangtze River Basin. *Sustainability*. https://doi.org/10.3390/su151310185
Wu, Y., Qiao, X., Yu, X., Yu, J., & Deng, Y. (2020). Study on Properties of Expansive Soil Improved by Steel Slag Powder and Cement under Freeze-Thaw Cycles. *KSCE Journal of Civil Engineering, 25*, 417 - 428. https://doi.org/10.1007/s12205-020-0341-6
Yan, Q., Peng, B., Li, W., Wang, B., Zuo, J., Lv, G., & Wang, T. (2025). Low-carbon stabilization of expansive soils using cement kiln dust and calcium carbide slag: mechanisms and performance. *Frontiers in Earth Science*. https://doi.org/10.3389/feart.2025.1554812
Yangsukkasem, N., Suebsuk, J., Kampala, A., Siriphan, A., Somna, R., Jiammeepreecha, W., & Chindaprasirt, P. (2024). Durability against cyclic wetting-drying of cement-stabilized loess subgrade for railway in tropical semi-arid regions. *Construction and Building Materials*. https://doi.org/10.1016/j.conbuildmat.2024.139123
Yoobanpot, N., Jamsawang, P., & Horpibulsuk, S. (2017). Strength behavior and microstructural characteristics of soft clay stabilized with cement kiln dust and fly ash residue. *Applied Clay Science, 141*, 146-156. https://doi.org/10.1016/j.clay.2017.02.028
Zapata, C. E., Houston, S. L., Houston, W. N., & Dye, H. (2006). Expansion index and its relationship with other index properties. In *Unsaturated Soils 2006* (pp. 2133-2137). https://doi.org/10.1061/40802(189)180

Zemouli, S., Gouider, N., Fatma, Z. M., & Wissem, I. (2024). Cement kiln dust and polypropylene fiber in expansive clay improvement. *STUDIES IN ENGINEERING AND EXACT SCIENCES*. https://doi.org/10.54021/seesv5n1-089

Zha, F., Liu, C., Kang, B., Xu, L., Yang, C., Chu, C., ... & Liu, Z. (2021). Effect of Carbonation on the Leachability of Solidified/Stabilized Lead-Contaminated Expansive Soil. *Advances in Civil Engineering*, *2021*(1), 8880818.https://doi.org/10.1155/2021/8880818.

Zha, F., Liu, S.-Y., Du, Y.-J., & Cui, K. (2008). Behavior of expansive soils stabilized with fly ash. *Natural Hazards, 47*, 509-523. https://doi.org/10.1007/s11069-008-9236-4

Zhang, H., Yang, J., Xu, Y., Wang, L., Lan, S., Luo, J., & Chang, Z. (2022). Experimental and Numerical Investigation on Failure Mechanism of Expansive Soil Subgrade Slope. *SSRN Electronic Journal*. https://doi.org/10.2139/ssrn.4295697

Zhang, R., Long, M.-X., & Zheng, J.-L. (2019). Comparison of Environmental Impacts of Two Alternative Stabilization Techniques on Expansive Soil Slopes. *Advances in Civil Engineering*. https://doi.org/10.1155/2019/9454929

Zhang, Y., Johnson, A. E., & White, D. (2019). Freeze-thaw performance of cement and fly ash stabilized loess. *Transportation Geotechnics*. https://doi.org/10.1016/j.trgeo.2019.100279

Zhang, Y., Li, L., & Hu, B. (2026). Enhancing Frost Durability of Cement-Stabilized Silty Clay: Experimental Evaluation and Prediction Model Development. *Buildings*. https://doi.org/10.3390/buildings16030484

Zhao, R., Zhang, L., Fan, G., Chen, Y., Huang, G., Zhang, H., Zhu, J., & Guan, X. (2021). Probing the exact form and doping preference of magnesium in ordinary Portland cement clinker phases: A study from experiments and DFT simulations. *Cement and Concrete Research, 144*, 106420. https://doi.org/10.1016/j.cemconres.2021.106420

Zhao, Y., Zhang, H., Wang, G., Yang, Y., & Miao, O. (2024). Development Characteristics and Mechanism of Crack in Expansive Soil under Wet–Dry Cycling. *Applied Sciences*. https://doi.org/10.3390/app14156499

Zhong, Y., Cai, G.-H., Wang, S., Qin, H., Zhang, C., & Li, J. (2022). Influence of Organic Content on the Mechanical Properties of Organic-Rich Soils Stabilized with CaO-GGBS Binder and PC. *Water*. https://doi.org/10.3390/w14193053

Zimar, Z., Robert, D., Giustozzi, F., Zhou, A., Setunge, S., & Kodikara, J. (2024). Use of industrial wastes for stabilizing expansive clays in pavement applications: durability and microlevel investigation. *Acta Geotechnica, 19*, 6259 - 6287. https://doi.org/10.1007/s11440-024-02298-9

Zimar, Z., Robert, D., Zhou, A., Giustozzi, F., Setunge, S., & Kodikara, J. (2022). Application of coal fly ash in pavement subgrade stabilisation: A review. *Journal of environmental management, 312*, 114926. https://doi.org/10.1016/j.jenvman.2022.114926